Enhancement of Cu (II), Zn (II), Ni (II) and humic acid adsorption in modified bentonite

Kanogwan Tohdee

A Thesis Submitted in Fulfillment of the Requirements for the Degree of Doctor of Philosophy in Chemical Engineering
Prince of Songkla University
2018

Enhancement of Cu (II), Zn (II), Ni (II) and Humic Acid Adsorption in Modified Bentonite

Kanogwan Tohdee

A Thesis Submitted in Partial Fulfillment of the Requirements for the Degree of Doctor of Philosophy in Chemical Engineering
Prince of Songkla University
2018

Thesis Title	Enhancement of Cu (II), Zn (II), Ni (II) and humic acid adsorption in modified bentonite
Author	Miss Kanogwan Tohdee
Major Program	Chemical Engineering

Major Advisor

.....
(Assoc. Prof. Dr. Lupong Kaewsichan)

Examining Committee:

…….....Chairperson
(Assoc. Prof. Dr. Nurak Grisdanurak)

…….....Committee
(Assoc. Prof. Dr. Supawan Tirawanichakul)

.....Committee
(Assoc. Prof. Dr. Ram Yamsaengsung)

.....Committee
(Assoc. Prof. Dr. Kanda Panthong)

….....Committee
(Assoc. Prof. Dr. Lupong Kaewsichan)

The Graduate School, Prince of Songkla University, has approved this thesis as fulfillment of the requirements for the Degree of Doctor of Philosophy in Chemical Engineering.

.....
(Prof. Dr. Damrongsak Faroongsarng)
Dean of Graduate School

This is to certify that the work here submitted is the result of the candidate's own investigations. Due acknowledgement has been made of any assistance received.

.....Signature
(Assoc. Prof. Dr. Lupong Kaewsichan)
Major Advisor

.....Signature
(Miss Kanogwan Tohdee)
Candidate

I hereby certify that this work has not been accepted in substance for any degree, and is not being currently submitted in candidature for any degree.

.....Signature
(Miss Kanogwan Tohdee)
Candidate

ชื่อวิทยานิพนธ์ การเพิ่มประสิทธิภาพการดูดซับของ Cu (II) Zn (II) Ni (II) และกรดฮิวมิกในเบนโทไนท์ที่ดัดแปลง
ผู้เขียน นางสาวกนกวรรณ โต๊ะดี
สาขาวิชา วิศวกรรมเคมี
ปีการศึกษา 2561

บทคัดย่อ

มลพิษทางสิ่งแวดล้อมเป็นที่ยอมรับว่าเป็นปัญหาหลักทั่วโลก ความเป็นพิษของมลพิษเหล่านั้นอาจทำให้เกิดปัญหาร้ายแรงต่อสิ่งมีชีวิต ดังนั้นการกำจัดมลพิษทั้งจำพวก สารอนินทรีย์และสารอินทรีย์เป็นความท้าทายของนักวิจัยทั้งหลายทั่วโลกในช่วงทศวรรษที่ผ่านมา การศึกษาครั้งนี้มีวัตถุประสงค์เพื่อเพิ่มความสามารถในการดูดซับสารโลหะและสารอินทรีย์ของเบนโทไนท์โดยการปรับปรุงพื้นผิว ด้วยวิธีการเติมสารลดแรงตึงผิวชนิดประจุบวก (cationic surfactant Benzyl hexadecyl dimethyl ammonium chloride, BCDMACl) ได้ประสบความสำเร็จ ดินเบนโท-ไนท์ธรรมชาติและดินเบนโทไนท์ที่ได้มีการปรับปรุงแล้วได้ถูกตรวจสอบลักษณะเฉพาะโดยวิธี FTIR spectroscopy, XRF, BET และการทดสอบการบวมตัวของดิน (swelling test) BCDMACl ประกอบด้วย micelles ที่สามารถแทรกซึมเข้าไปใน interlayers ของดินและป้องกันไม่ให้ดินเหนียวเกิดการบวมตัว การดูดซับโลหะหนักประกอบด้วย Cu (II) Zn (II) และ Ni (II) และกรดฮิวมิกจาก aqueous solution ได้ถูกศึกษาโดยการทำ batch experiment โดยพิจารณา ความเป็นกรด-เบสของสารละลาย (pH solution) เวลา (contact time) ความเข้มข้นของสาร (concentration) และความแข็งแรงของพันธะไอออนิก (ionic strength) ความเข้มข้นของโลหะและกรดฮิวมิกในสารละลายได้ทำการตรวจวัดโดยวิธี Atomic Absorption Spectroscopy (AAS) และ UV-Visible ตามลำดับ

ผลการทดลองแสดงให้เห็นว่าสมการ pseudo-second-order rate ให้ผลดีที่สุดของ (R^2 ใกล้เคียง 1) ซึ่งแสดงให้เห็นว่าเป็นการดูดซับทางเคมี ข้อมูลการดูดซับจากการทดลองถูกนำเข้าแบบจำลองโมเดลของ Langmuir, Freundlich, Temkin และ Dubinin-Radushkevich ซึ่งแบบจำลอง Langmuir ให้ผลดีที่สุด โดยที่ R^2 และ APE มีค่าเท่ากับ 0.960-0.998 และ 2.35-9.43% ตามลำดับ

สำหรับทุกกรณี นอกจากนี้ แบบจำลองโมเดลแบบสามพารามิเตอร์ (three-parameter isotherm) ทั้งหมดยังสนับสนุนแบบจำลอง Langmuir เบนโทไนท์ที่ถูกปรับปรุงมีความสามารถในการดูดซับได้ดี (q_{max} = 50.76, 35.21 และ 25.06 และ 86.21 mg / g สำหรับโลหะหนัก [Cu (II), Zn (II), Ni (II)] และกรดฮิวมิก ตามลำดับ ซึ่งเป็นปริมาณ 1.7-2.5 เท่าเมื่อเทียบกับเบนโทไนท์ธรรมชาติ ผลการดูดซับในระบบ multi-component ยังแสดงให้เห็นว่าโลหะแต่ละชนิดที่มีการแข่งขัน ซึ่งทำให้ปริมาณของโลหะที่ดูดซับมีค่าลดลงประมาณ 35.41-47.41% สำหรับทุกกรณี

Thesis Title Enhancement of Cu (II), Zn (II), Ni (II) and humic acid adsorption in modified bentonite

Author Miss Kanogwan Tohdee

Major Program Chemical Engineering

Academic Year 2018

ABSTRACT

Environmental pollutants are recognized as a main problem around the world. Their toxicity can cause serious problems to living beings. Therefore, the removal of toxic inorganic and organic materials has been the great challenges of several researchers worldwide over the last decade. This study sought to enhance the metal and organic substance adsorption capacity of bentonite by improving its surfaces. Surface modification by the cationic surfactant (Benzyl hexadecyl dimethyl ammonium chloride, BCDMACl) was successful in this respect. Natural and modified bentonite were characterized by FTIR spectroscopy, XRF, BET, and swelling test. A major characteristic of BCDMACl is forming micelles that can intercalate into interlayers of clay and prevent swelling. The adsorption of heavy metals [Cu (II), Zn (II) and Ni (II)] and humic acid from aqueous solutions was studied in batch experiments, varying several effects; pH solution, contact time, concentrations of substances, and ionic strength. Concentration of the metals and humic acid in solution was detected by Atomic Absorption Spectroscopy (AAS) and UV-Visible, respectively.

Kinetic results showed that the pseudo-second-order rate equation provided the best fit to observed adsorption kinetics (R^2 almost equaled to 1), indicated as chemical adsorption. The adsorption data were fitted with Langmuir, Freundlich, Temkin, and Dubinin-Radushkevich isotherm models, of which the Langmuir isotherm provided the best fit with experimental data, R^2 and APE ranged 0.960-0.998 and 2.35-9.43%, respectively for all cases. Moreover, all the three-parameter models fits supported the two-parameter Langmuir model, regarding these

fundamental assumptions underlying it. The modified bentonite had significantly improved adsorption capacities (q_{max} = 50.76, 35.21 and 25.06; and 86.21 mg/g for heavy metals [Cu (II), Zn (II), Ni (II)] and humic acid, respectively); about 1.7-2.5 fold improvements over natural bentonite. Competitive adsorption result indicated that each metal competed together (antagonism), adsorption of all metals decreases totally which adsorption equilibrium reduction (ΔY) ranged 35.41-47.41 % for all cases.

ACKNOWLEDGMENTS

I would like to appreciate the people for their help and support during my research. My thanks and gratitude goes to my principal advisor Assoc. Prof. Dr. Lupong Kaewsichan. He gave an opportunity, motivation, and stimulation throughout my work. I sincerely thank all committee members Assoc. Prof. Dr. Nurak Grisdanurak, Supawan Tirawanichakul, Ram Yamseangsung and Kanda Panthong, for their support and invaluable comments on my research. Also, I would like to acknowledge the financial support of Ph.D. scholarship, Prince of Songkla University.

My further gratitude goes to my family: my father and mother, for their love, encouragement, supporting, patience and attention throughout my life. Importantly, I especially want to thank to my husband Dr. Surat Semmad and my lovely son for help in everything. I am truly blessed to have you as my family.

Finally, I would like to forward all my appreciation to almighty ALLAH who guided those people who supported and helped me through my research.

CONTENTS

CONTENTS (Continue)

CONTENTS (Continue)

LIST OF FIGURES

LIST OF FIGURES (Continue)

LIST OF FIGURES (Continue)

LIST OF TABLES

CHAPTER 1

INTRODUCTION

1.1 Background

Water is one of the necessities for human consumption and uses. Safe water becomes more scarce as a result of anthropogenic contamination of the water resources (Jackson et al., 2001). The water demands around the world have significantly raised with 15% of the world population growth (WHO, 2000). WHO also found that 2.2 million people of an annual mortality caused by contaminated water consumption. Such contamination, either natural or anthropogenic, can affect to river or groundwater. Groundwater represents the most important water for human consumption. Groundwater contamination occurs due to geochemical phenomena which caused to accumulated chemical substance during the natural cycle of water into the bed rock. People around the world are being begged sustainable use of water for present and future generations. Therefore, a majority of technological improvements are unveiled to repair/recycle the industrial wastewater and contaminated water before it is left to the natural water resources.

1.2 Heavy metals pollution in water and their effects

Water pollution by heavy metals is harmful to most animal species. Most of such pollutions are released in water resources, from chemical industries including electric batteries, mining, and manufacture of glass. According to a list by the United States Environmental Protection Agency (USEPA, 2009), Cu (II) and Zn (II) are potentially harmful to human health. Moreover, The World Health Organization (WHO) suggests that maximum allowed concentrations of these heavy metals in drinking water should not exceed 1.0 mg/L and 5.0 mg/L (WHO, 2003; WHO, 2004), respectively. An increase in the amount of Cu (II) can cause health problems such as liver and kidney failure, Wilson's disease, gastrointestinal disturbance, and insomnia to human. Zn (II) can create some severe effects such as depression, lethargy,

neurologic signs, and increased thirst (Kurniawan et al., 2006a; Kurniawan et al., 2006b). These problems are particularly serious concerns because these heavy metals can be accumulated by a living organism: even low levels of exposure can be harmful if prolonged. Another metal, Ni (II) is known as one of many carcinogenic metals which are occupational and environmental pollutant. Chronic exposure has been resulted with high risk of lung cancer, neurological deficits, developed deficits in childhood, and high blood pressure (Chervona et al., 2012). The removal and control of heavy metal ions from wastewater/contaminated water are now a subject of major challenge of several researcher around the globe. Hence, it is important to control the metal level in wastewaters before it disposal into the water resources.

1.3 Humic substance in water and their effects

Humic substances are mostly present in natural soils. Generally, they are categorized as three different groups; fulvic acids (FA), humic acids (HA), and humin, based on their solubility under several conditions in aqueous solutions. In treatment processes of drinking water, humic substances can react with chlorine and produce some products form disinfection such as trihalomethanes. This can cause potentially adverse health impacts (Karnik et al., 2005; Wan Ngah et al., 2008). The major type of humic substances is humic acid which occurs from a degradation of the microbial. Humic acid can blind several pollutants including heavy metals, and transport them through water treatment facilities (Li et al., 2011). Thus, humic substance removal from water is become necessary which many methods of the removal have been developed such as chemical coagulation, precipitation, adsorption, and advanced oxidation.

1.4 Removal of heavy metals and organic matters from water

Several methods have been developed to remove heavy metals and organic matters from wastewater and contaminated soil, including physicochemical methods (e.g., chemical precipitation, coagulation and flocculation, electrochemical treatments, ion exchange, membrane filtration, and electrodialysis) and biological methods (Gunatilake, 2015). Physicochemical adsorption is considered as suitable methods due

to inexpensiveness and easy to adapt (Bhattacharya et al., 2006). Recently, clay minerals become an alternative adsorbent because their properties are more suitable for adsorption processes. Natural bentonite is an essential adsorbent which was recently used to adsorb heavy metals and organic substances (e.g. Anna et al., 2015; Iskander et al., 2011; Ghomri F. et al., 2013). To enhance the adsorption efficiency of the bentonite, a surface modification can be available with cationic surfactants, such as hexadecyltrimethylammonium bromide (HDTMA-Br), cetyl pyridinium bromide (CPB), and benzyl hexadecyl dimethyl ammonium chloride (BCDMACl) (Chutia et al., 2009; Jin et al., 2008; Yusof and Malek, 2009). These methods have been proved that the surface modification can be improved the adsorption ability of clay.

1.5 Aims and objectives

The aim of this study was to prepare a modified bentonite (a new adsorbent) by surface modification technique, and to evaluate their efficacy for the removal of heavy metals (Cu (II), Zn (II), and Ni (II)) and humic acid from aqueous solution.

1.5.1 To perform the surface modification of bentonite using a cationic surfactant named benzyl hexadecyl dimethyl ammonium chloride (BCDMACl).

1.5.2 To investigate and compare the characteristics of natural and modified bentonite by several methods such as XRF, FTIR, BET, and CEC.

1.5.3 To investigate several influent factors to adsorption processes of heavy metals (Cu (II), Zn (II), and Ni (II)) and humic acid.

1.5.4 To study a performance of BCDMACl modified bentonite through the removal of heavy metals (Cu (II), Zn (II), and Ni (II)) and humic acid from aqueous solution by determining the adsorption capacity, applying kinetic models and some commonly used adsorption isotherms through non-linear modeling.

1.5.5 To investigate the competitive adsorption of heavy metals mixed together onto both natural and BCDMACl modified bentonite.

This research is expected that this work would strengthen the information available on a use of bentonite clay and its modification for removal of heavy metals from wastewater, and enhance the knowledge of adsorption behavior.

1.6 Scope of this study

This study focus on the adsorption of heavy metals and humic acid in aqueous by conducting only laboratory batch experiments and focusing on adsorption kinetics and isotherms. All experiments were conducted at chemical engineering laboratory, Faculty of engineering, Prince of Songkla University.

CHAPTER 2

BACKGROUND

2.1 Clay minerals

2.1.1 Structure of clay minerals

Clay minerals (i.e. particle size is less than 2 μm) are main constituents of several soils, refers to hydrous aluminium silicates with magnesium substituting either partly or wholly for the aluminium in some minerals. Some cations (alkali and alkaline earth metals) also show as an essential chemical constituents in many soils (Grim, 1962). The atomic structure of clay minerals can be classified as two main kinds of cell geometry unit as follows

a) Tetrahedral unit

Structure of tetrahedral unit is built from silica tetrahedral (Si^{4+}) which is the foundation of silicate structures. This structure consists of one Si^{4+} at the center balancing with four O^{2-} at the vertexes of tetrahedron (Fig. 2.1). These tetrahedral unit arranged an interlocking array connected with the same plane by sharing oxygen anions to form a hexagonal network, usually called a tetrahedral sheet (Schultz, 1989). This hexagonal network is indefinitely repeated to form the tetrahedral sheet of $Si_4O_6(OH)_6$ composition (Grim, 1962).

b) Octahedral unit

Generally, aluminum and magnesium are a coordinating cation, and surrounded by six oxygens or hydroxyls. Its arrangement of these atoms results in an octahedron formation, so that the horizontal-plane linkage of each octahedra involved to a octahedral sheet (Fig. 1). The structure of gibbsite $A1(OH)_3$ and brucite $Mg(OH)_2$ are an example of clay minerals which their structure is similar to the octahedral sheets. In case of gibbsite structure, only two-thirds of hydroxyl positions are balanced the structure charges. This clay structure is therefore classified as

dioctahedrals. In other case, brucite structure, all hydroxyl positions are balanced the charge of the structure, which is thus classified as *trioctahedrals* (Grim, 1962).

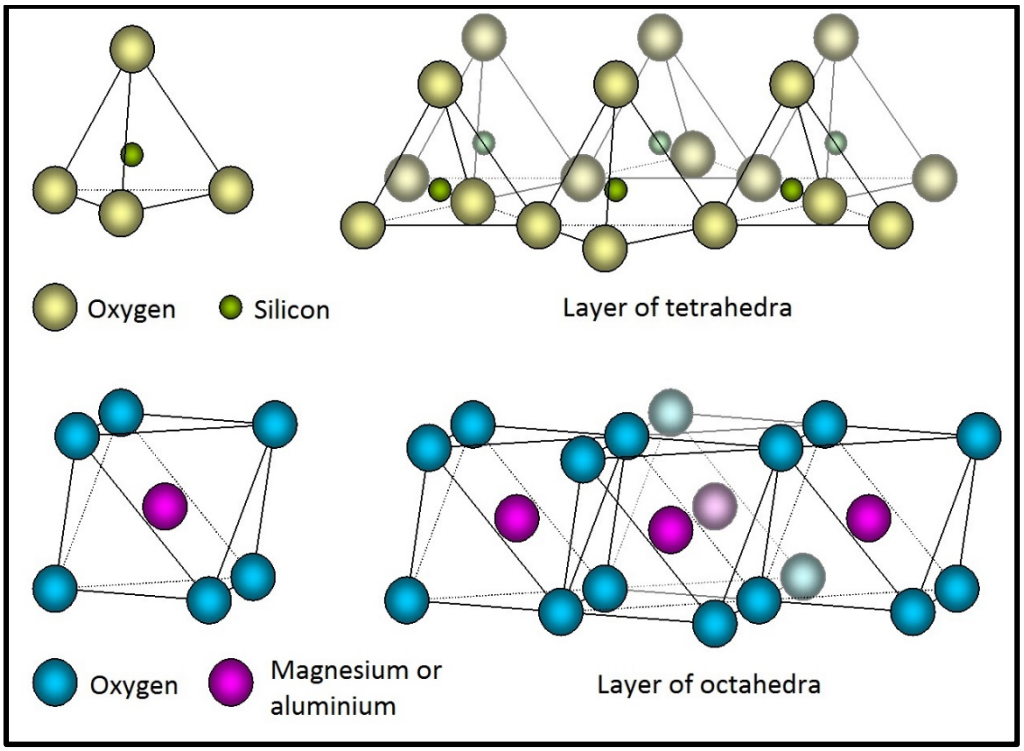

Figure 2.1 Structure of clay mineral unit; tetrahedral and octahedral (https://gsoil.wordpress.com/tag/clay/).

2.1.2 Isomorphous substitution

An arrangement of clay structure presents a formation of silicate clay minerals. It is a fact that the composition of the clay minerals varies as a result of ion substitution in their structure. The substitution of Si^{4+}, Al^{3+} and Mg^{2+} with another comparable cations under similar size of ionic radii can occur to tetrahedral and octahedral sheets. This process is referred to isomorphous substitution which one cation in clay structure was replaced with another ion resulting the charge in clay minerals presents a permanently negative and positive charges. For example, the clay structure with negative charge is built from Al^{3+} replacing with Si^{4+} in the tetrahedron sheet. In other case, alternatively, the replacement of Fe^{2+} (lower valence cation) by Fe^{3+} (higher valence cation) may result to gain one positive charge. However, some

clays exhibit both positive and negative charges, so that the electron gain and loss within mineral structure are balanced to determine the net charge of the minerals.

2.1.3 Clay mineral classification

Groups of clay minerals are commonly referred to two main types (e.g. 1:1 and 2:1 formation), depending on the arrangement of tetrahedral and octahedral sheets as layers in their structure.

a) 1:1 Clay Minerals

This layer mineral consists of one tetrahedral and one octahedral sheet in structural unit which van der Waals bonding between the basal oxygens of the tetrahedral sheet and the hydroxyls of the octahedral sheet. Each layers are tightly hold by hydrogen bonding between the tetrahedral oxygens and octahedral hydroxyl ion. Kaolinite, the most common mineral in 1:1 type of clay mineral which the general structure exhibits Si^{4+} tetrahedral and Al^{3+} octahedral coordination (dioctahedral clay mineral), illustrated in Fig. 2.2. The arrangement of this structure allows to fix a lattice structure which kaolinite prevents water adsorbed into the interlayer, resulting swelling are unallowable. Also, it is ensure that the kaolinite cannot undergo isomorphic substitution adsorption (Brigatti et al., 2006). So that soils composed kaolinite show poor adsorption of cations.

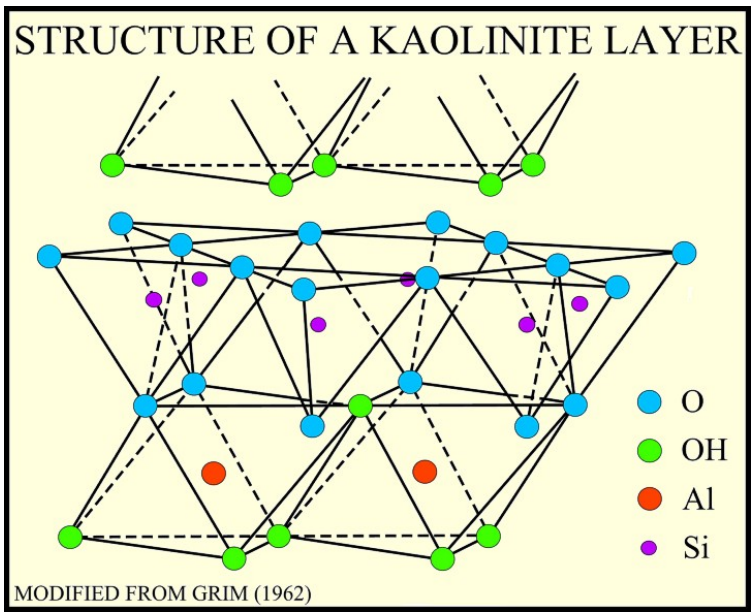

Figure 2.2 Structure of kaolinite.

b) 2:1 Clay Minerals

The octahedral sheet is sandwiched by two tetrahedral sheets, which unshared vertex of each tetrahedral sheet forms to each side of the octahedral sheet, producing a type of three-sheet mineral called 2:1 clay minerals. Cations of interlayer may coordinate with hydroxyls, and present individual cations. Montmorillonite is the most common mineral in this 2:1 type which presents the substitution of Mg^{2+} for Al^{3+} in octahedral sheets. The layers exhibit weak cation-to-oxygen linkages and are held by van der Waals bonding. Figure 2.3 displays the structure of montmorillonite, the water, other polar molecules and exchangeable cations can enter to the interlayer which other cation can be adsorbed for offsetting the isomorphous substitution (Sparks, 2002.). Bentonite clay, originating from weathering of volcanic ash, mostly consists of montmorillonite and amounts of quartz and feldspar. Generally, the bentonite clay forms by a combination of the montmorillonite mineral with different cations (e.g. sodium, potassium or calcium) under different substitutions of the silicate structure (Brigatti et al., 2006).

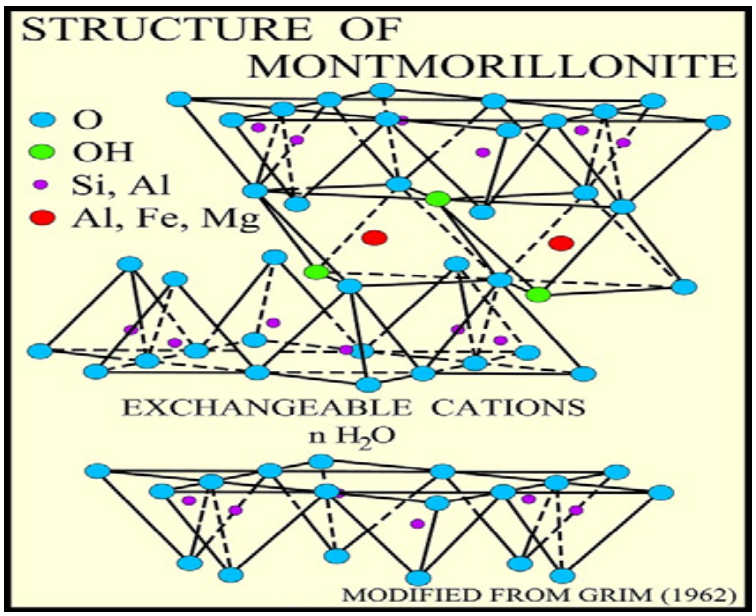

Figure 2.3 Structure of montmorillonite.

2.1.4 Surface charge of soils

Surface properties of soils especially in clay minerals often play a major rule in their chemistry. The surface charge is one of important properties, depending on an organic and inorganic components which have an amphoteric character, and greatly present in the nature. Both components are a main source of negative and positive charge.

Negative charge

The negative charge can be subdivided as two type of charge, a constant charge and pH-dependent charge. The constant charge (i.e. this is often called a permanent charge) results from the shortcoming of soil structure due to isomorphous substitution (Sparks, 2002) or vacancies of site, in crystalline minerals and non-crystalline hydrous oxides of Si, Al and Fe (Gast, 1977), does not depend on pH. An example of clay mineral for this constant charge are montmorillonite and chlorite (2:1 mineral formation) which their physical and chemical properties are governed a location of isomorphous substitution in the mineral structure. Other, pH-dependent charge, this charge has an influence from protonation and deprotonation of surface

functional groups existing on the minerals. The 1:1 clay mineral is generally an example of this charge, such as kaolinite.

2.1.5 Surface functional groups

In adsorption processes, surface functional groups in soil play an important role. The surface functional group was defined to a chemically reactive molecular per unit bound into soil structure. Either organic, such as carboxyl and carbonyl, or inorganic molecular can be the surface functional groups. In case of inorganic, the main functional groups are the siloxane surface groups. These functional groups associate with oxygen atoms bounded to the silica tetrahedral layer, and hydroxyl groups occurred as the edges of inorganic minerals (e.g. kaolinite and metal oxides, oxyhydroxides and hydroxides). Figure 2.4 depicted possible bounding of the functional groups at the interface of soils.

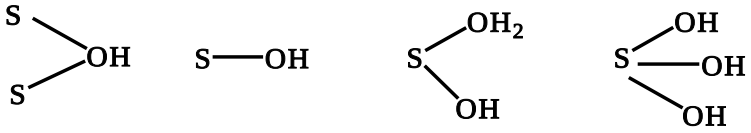

Figure 2.4 Surface functional group in soil.

Protonation and deprotonation of the surface functional groups can occur by adsorption of H^+ and OH^- respectively, and can undergo under metal binding, ligand exchange, and ternary surface complexation. The simplest reaction equilibrium of these processes are presented below (Schindler et al., 1987; Stumm, 1992; Stumm, 1996):

Acid-Base Equilibria

$$\equiv S\text{—}OH + H^+ \rightleftharpoons \equiv S\text{—}OH_2^+ \quad \textbf{(protonation)}$$

$$\equiv S\text{—}OH \rightleftharpoons \equiv S\text{—}O^- + H^+ \quad \textbf{(deprotonation)}$$

Metal binding

$$S\text{—}OH + M^{z+} \rightleftharpoons S\text{—}OM^{(z-1)+} + H^{+}$$

$$2S\text{—}OH + M^{z+} \rightleftharpoons (S\text{-}O)_2M^{(z-2)+} + 2H^{+}$$

$$S\text{—}OH + M^{z+} + H_2O \rightleftharpoons S\text{-}OMOH^{(z-2)+} + 2H^{+}$$

Ligand Exchange

$$S\text{—}OH + L \rightleftharpoons S\text{—}L + OH^{-}$$

$$2S\text{—}OH + L \rightleftharpoons S2\text{-}L + 2OH^{-}$$

Ternary Surface Complex Formation

$$S\text{—}OH + L^{-} + M^{z+} \rightleftharpoons S\text{-}L\text{-}M^{z+} + OH^{-}$$

$$S\text{—}OH + L^{-} + M^{z+} \rightleftharpoons S\text{-}OM\text{-}L^{(z-2)+} + H^{+}$$

2.1.6 Surface complexation

Surface complexation refer to the interaction between the surface functional groups with molecules in the solution which can create a molecular entity. Figure 2.5 depicts the surface complexations which can be classified as two types of surface complexes, outer-sphere and inner-sphere. The surface complexes between siloxane ditrigonal cavities and metal cations which occur on the edges of clay minerals as illustrated in Fig. 2.5. Outer-sphere complex is formed when a water molecule presents between the surface functional group and the bound ion. Other case, there is non-presented water molecule referred to an inner-sphere complex

Outer-sphere complex involves electrostatic interactions and is thus weak bond, the binding type is covalent or ionic. This is usually a rapid process and reversible. So that, the adsorption only occurs on the surfaces that are an opposite charge to the adsorbate. In contrast, the inner-sphere complexation is slower than that of outer-sphere complexation (i.e. this process is irreversible). Adsorption *via* inner-sphere complexation can occur on the surfaces regardless of the original charge. However, it is important to note that both complexations can occur simultaneously.

Ionic strength effects are an indirect evidence indicating outer-sphere or inner-sphere complex is formed. For example, metal adsorption process is ionic strength dependent, outer-sphere complex is assumed to form. In contrast, independent of ionic strength on adsorption process is assumed to form inner-sphere complex.

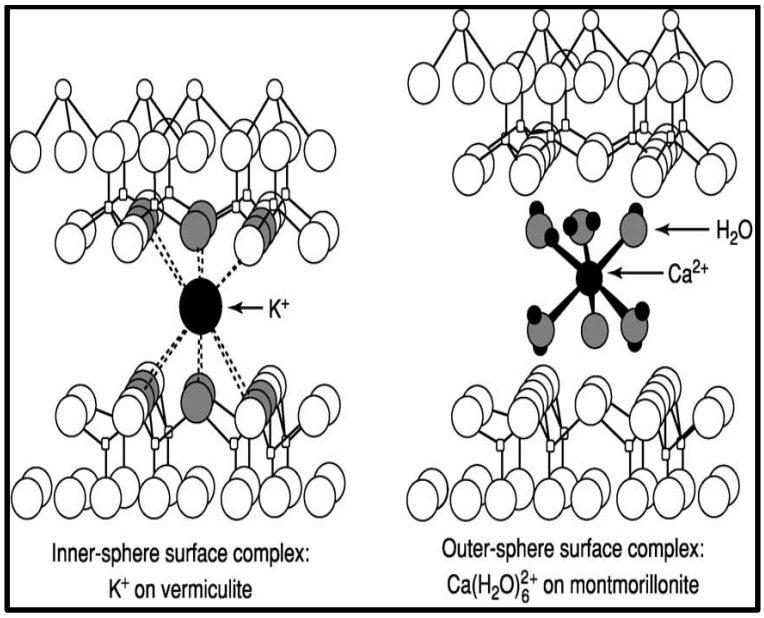

Figure 2.5 Formation of sphere complexes (Sparks, 2005).

2.1.7 Cation exchange capacity (CEC)

Cation exchange capacity (CEC) is defined as the capacity of a soil for ion exchange between the soil and the solution. An amount of cations which the clay minerals can accommodate on their negatively charged of surface, the quantity of CEC is expressed as milliequivalent (meq) per 100 g or $cmol_c/kg$.

CEC values for clay minerals depend on the amount of impurities in the clay and the pH of clay at which the CEC value was measured. For example, the CEC of kaolinite clay is range 2-15 meq/100g (very low) because the degree of isomorphous substitution is small, while a high CEC value of montmorrilonite is range 80-150 meq /100 g due to a large isomorphous substitution, and the existance of all expanded interlayers promoted ion exchange. Other important clay, Illite has a low CEC value, ranged 20-30 meq/100 g, due to the inaccessibility of the exchangeable potassium ion in its interlayer.

2.2 Natural Organic Matter in Soils

2.2.1 Composition of NOM

Humic substances can be extracted from organic matter which can be virtually characterized as yellow to black color, high molecular weight. The humic substances are categorized into three main groups based on their soluble ability in aqueous media as (Hayes and Swift, 1978) humic acid, fulvic acid and humin. Humic acid has insoluble under strongly acidic phases (< pH 2) while fulvic acid is soluble under both acid and alkaline conditions (> pH 2). Humin is also insoluble under both acid and alkaline phases.

Elemental composition of humic and fulvic acid, and a nature of functional groups exist in natural organic matter are tabulated in table 2.1 and 2.2. The main elemental composition of humic substances are carbon and oxygen which can sum to more than 86 % of total elements. The main functional groups are carboxyl and phenolic hydroxyl groups which the carboxyl is the most common group. Also, alcoholic, quinonic, and ketonic groups are the minor groups present in humic substances.

Table 2.1 Elemental composition of soil humic substances.

Element	Humic acids (%)	Fulvic acids (%)
Carbon	53.8-58.7	40.7-50.6
Hydrogen	3.2-6.2	3.8-7.0
Oxygen	32.8-38.3	39.7-49.8
Nitrogen	0.8-4.3	0.9-3.3
Sulphur	0.1-1.5	0.1-3.6

Table 2.2 Functional groups in NOM.

Element	Functional groups
Acidic	Carboxyl, Enol, Phenolic OH, Quinone
Neutral	Alcoholic OH, Ether, Ketone, Aldehyde, Ester
Basic	Amines, Amides

2.2.2 Structure of humic substances

Many proposed structures of humic substances have been characterized by the same functional groups and the existence of aromatic and aliphatic structure (Sparks, 2002). The macrostructure of humic substances is of most importance which can affect to several conditions such as the chemical of organic matter, stability of organomineral aggregates and transport of pollutants in soils under several factors (e.g. pH, electrolyte concentration, ionic strength, and acid concentrations) (Hayes and Swift, 1978; Chen and Schnitzer, 1976). Figure 2.6 show proposed model structure for humic acid, was developed by Schulten and Schnitzer (1993).

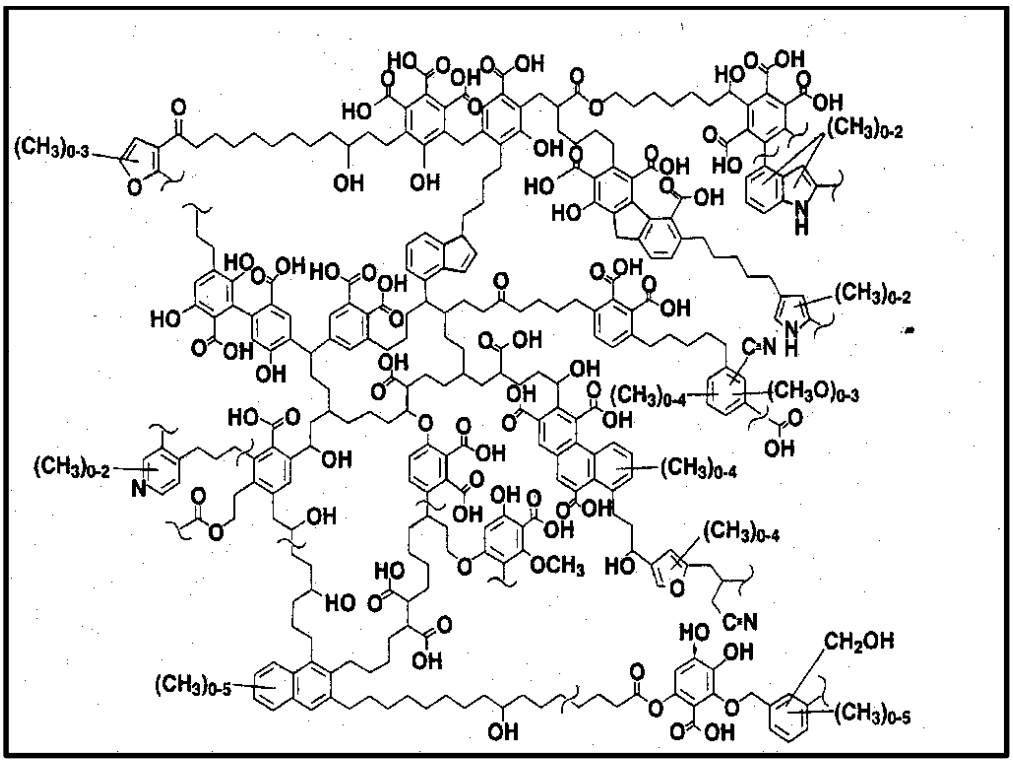

Figure 2.6 A Proposed structure for humic acid (Schulten and Schnitzer, 1993; Sparks, 2002).

2.3 Adsorption

2.3.1 Basic of adsorption

Adsorption is a widely used process in practice for removing substances from fluid phases. General definition of adsorption is an adhesion of chemical species from a fluid phase (adsorbate) on the surface of a liquid or a solid (adsorbent). However,

the adsorption does not include both surface precipitation and polymerization (monomer molecules formed to polymer). These processes (e.g. adsorption, precipitation, and polymerization) are in term of sorption which involved in several mechanisms concerning both physical and chemical processes. In water treatment, molecules or ions are removed from the aqueous solution or wastewater by adsorption onto solid surfaces of adsorbent.

In adsorption theory, the basic terms shown in Figure 2.7 are used. The solid material that provides the surface for adsorption is referred to as adsorbent. By changing the properties of the liquid phase, adsorbed molecules can be released from the adsorbent surface and reversed into the liquid phase. This process is referred to desorption.

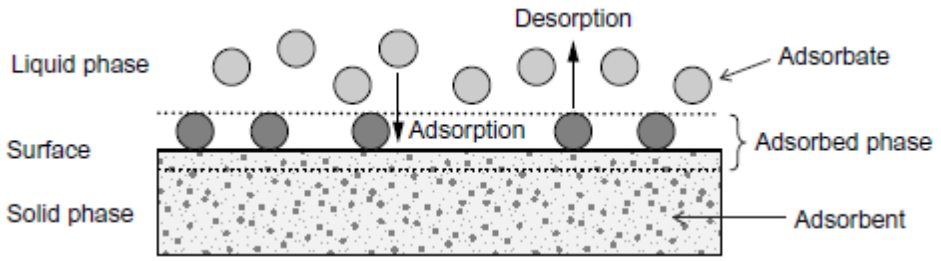

Figure 2.7 Conceptual model of adsorption.

2.3.2 Modeling adsorption kinetic

Many factors are important component controlling the adsorption kinetics. These factors may include (1) mass transfer (solute) from the solution to the boundary interface surrounding the particle (bulk diffusion), (2) diffusion from the interface to the adsorbent surface (external diffusion), (3) diffusion from the adsorbent surface to the intra-particular sites (intra-particular diffusion) and (4) solute adsorption by several processes such as complexation, physicochemical adsorption and ion exchange. Bulk diffusion process can be ignored when sufficient agitation is allowable, avoiding particle and solute gradients. This can be assumed that the kinetic rate is not limited by mass transfer from the bulk liquid to the particle external surface, resulting external diffusion might govern the adsorption process. The adsorption kinetic is time-dependent process which is a good way to describe the adsorption behavior of heavy metals (e.g. copper, zinc and nickel etc.) by adsorbent

produced from biological sources. Amount of adsorbate adsorbed on a solid surface at time (q_t, in mg of ion/g of adsorbent) can be determined from the following mass-balance equations:

$$q_t = \frac{(C_i - C_t) \times V}{m} \tag{2.1}$$

$$\% \text{ Removal} = \frac{(C_i - C_e) \times 100}{C_i} \tag{2.2}$$

where C_i, C_e and C_t are the concentrations of adsorbate at initial, equilibrium and given time (mg/L), respectively, V is volume of the aqueous solution (L), and m is mass of the adsorbent (g).

a) Pseudo-first-order model

The adsorption kinetics can be accessed by using the differential rate equation fitting to the experimental data. A general form of rate expression of pseudo-first-order model proposed by Lagergren (Lagergren, 1898) is expressed as follows:

$$\frac{dq_t}{dt} = k_1(q_e - q_t) \tag{2.3}$$

where q_t is the adsorbate adsorbed at the given contact time (mg/g), and k_1 is the rate constant of the pseudo-first order (1/ min) . Integration of Eq. (2.3) with initial condition q_t = 0 at t = 0 and simplifies to 'Lagergren' first-order equation (Lagergren, 1898)

$$\ln(q_e - q_t) = \ln q_e - k_1 t \tag{2.4}$$

Eq. 2.4 can also be expressed as:

$$\log(q_e - q_t) = \log q_e - k_1 \frac{t}{2.303} \tag{2.5}$$

Equation 2.5 is a linear form of pseudo-first-order model, relationship between $\log(q_e - q_t)$ and t. The model parameters can be calculated from slope and intercept.

b) Pseudo-second-order model

The pseudo-second-order equation is the most widely used rate equation for the sorption of a solute from a liquid phase. The experimental data can also be tested for pseudosecond- order adsorption. The commonly represented pseudo-second-order adsorption equation is:

The pseudo-second-order model is commonly used when the adsorption/desorption balance controls the overall sorption kinetics. The model was developed by Blanchard (Blanchard et al., 1984) is expressed as follows:

$$\frac{dq_t}{dt} = k_2(q_e - q_t)^2 \tag{2.6}$$

where k_2 is the rate constant of the pseudo-second order $(\mathrm{g/mg/min})$. Integration of Eq. (2.6) with suitable boundary conditions gives linearly related t/q_t and t, and the rate constant k_2 can be calculated from the slope.

2.3.3 Modelling adsorption isotherms

Breakthrough curve of adsorption can be obtained by solving uptake rate equation and isotherm equation (partial differential equations). Although several methods have been modified to determine the isotherm, the most widely used one is the conventional static method in a closed system. Due to the complexity of the structure of adsorbent and the interaction between each corpuscle, isotherms can present diverse shapes as four types shown in fig. 2.8. There are three principles to formulate an isotherm: thermodynamic equilibrium between phases and species, dynamic equilibrium between adsorption and desorption and adsorption potential theory (Malek and Farooq, 1996).

According to Giles et al, 1960, adsorption isotherm can be classified as four different isotherms; types S, L, H and C shown in Fig. 2.8. Thermodynamic equilibrium between phases and species, and adsorption potential theory were used to formulate equilibrium isotherms as different characteristics. It is clear that there are noting adsorption model to fit well with all cases because of the complexity of adsorption systems. However, one of those has to determine the best suitable isotherm

associating with specific experiments. Herein, the discussion of adsorption isotherm is given the details below.

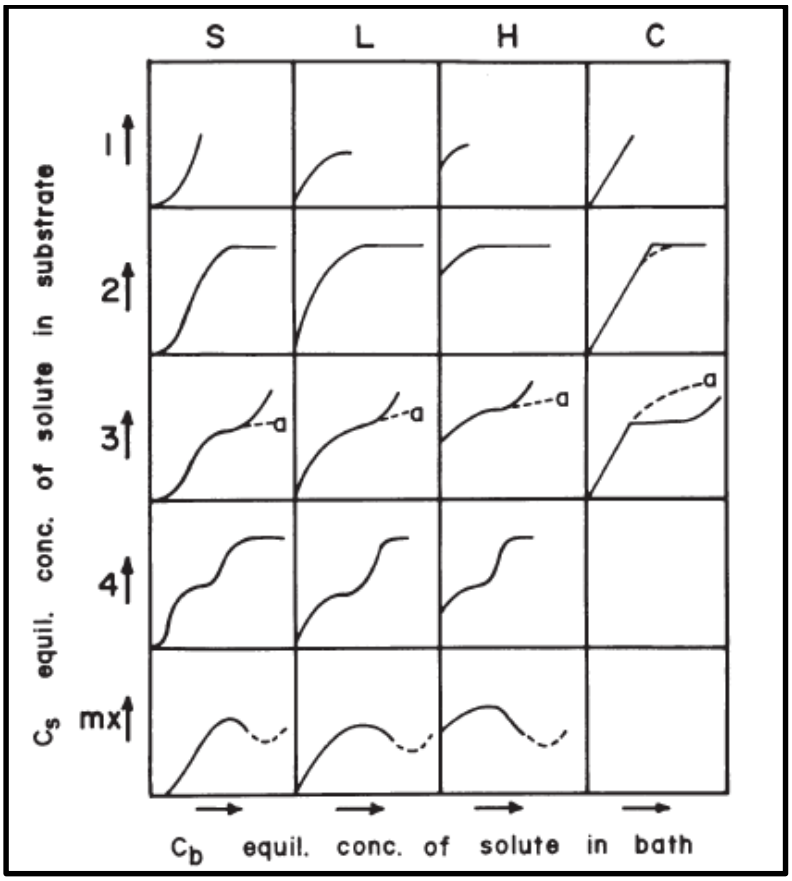

Figure 2.8 Adsorption isotherm categorized by Giles et al, 1960.

a) Two-parameter isotherms

Langmuir isotherm

The Langmuir model is based on the major assumptions that the adsorption is of monolayer adsorption type (chemical adsorption) and the surfaces of adsorbent pellets (or the adsorption sites) are homogeneous. The Langmuir model can be written as follows:

$$q_e = \frac{q_m b C_e}{1 + bC_e} \tag{2.7}$$

where q_e is the equilibrium adsorptive capacity, q_m is the maximum adsorptive capacity, C_e is the concentration of adsorbate in the liquid phase at equilibrium, and

b is the Langmuir constant obtaining from experiment. Certainly, Langmuir model can be rewritten as a linear form shown in equation 2.8.

$$\frac{1}{q_e} = \frac{1}{q_m b C_e} + \frac{1}{q_m} \tag{2.8}$$

$$b = k_a / k_d \tag{2.9}$$

where k_a is adsorption rate coefficient of the Langmuir kinetic model, and k_d is the desorption rate coefficient (Azizian, 2004). Because of its simple form and well-fitting performance, the Langmuir isotherm has become one of the most popular models in adsorption studies.

Freundlich isotherm

Freundlich isotherm model is also used to adsorption study. Comparing with the Langmuir isotherm, the Freundlich isotherm does not have much limitation. The model can deal with both homogeneous and heterogeneous surfaces, and both physical and chemical adsorption. Specifically, the adsorption behavior of organic compounds and reactive matters can frequently succeed by this model. The Freundlich isotherm is expressed as

$$q_e = K C_e^{1/n} \tag{2.10}$$

where K and n are the parameters to be determined. Though the Freundlich isotherm is one of the earliest empirical correlation. According to (Haghseresht and Lu, 1998), the surface heterogeneity and type of adsorption can be roughly estimated by the Freundlich parameters. The Freundlich isotherm can be rewritten as a linear form shown in equation 2.11.

$$\ln q_e = \ln K + \frac{1}{n} \ln C_e \tag{2.11}$$

Dubinin-Radushkevich isotherm

Dubinin-Radushkevich model is more general than the Langmuir model. It does not assume a homogenous adsorbent, and this model is used to assess the nature

of adsorption processes (Matouq et al., 2015). The Dubinin-Radushkevich model is as follows (Dubinin, 1965):

$$q_e = q_m \exp\left(-K_{DR}\varepsilon^2\right) \tag{2.12}$$

$$q_e = q_m \exp\left(-K_{DR}\left[RT\ln\left(1+\frac{1}{C_e}\right)\right]^2\right) \tag{2.13}$$

where K_{DR} is the Dubinin-Radushkevich constant related to the free energy of adsorption (mol^2/J^2), and ε^2 is a Polanyi potential (J^2/mol^2). Rearranging Eq. (2.12) gives a linear relationship between $\ln q_e$ and ε^2 and the model parameters can again be calculated from the slope and the intercept. Moreover, the roles of chemisorption and physical adsorption can be assessed from Eq. (2.13). An E_s value between 8 and 16 kJ/mol indicates chemisorption. On the other hand, the E_s value below that range indicates that physical adsorption is dominant.

$$E_s = \frac{1}{\sqrt{2K_{DR}}} \tag{2.14}$$

Temkin isotherm

The Temkin model (Temkin and Pyzhev, 1940) is an early one which develops from the adsorption of hydrogen onto platinum electrodes within acidic solutions. Temkin model is one of two-parameter isotherms, and contains a factor taking into account the absorbent-adsorbate interactions. Generally, the Temkin model assumes that (1) the heat of all molecules in a layer would decrease linearly with increasing adsorbent coverage, and (2) the adsorption is characterized by uniform distribution of binding energies. The Temkin isotherm is generally applied in the following equation:

$$q_e = B_T \ln\left(A_T C_e\right) \tag{2.15}$$

$$q_e = \frac{RT}{b_T}\ln(K_T) + \frac{RT}{b_T}\ln(C_e) \tag{2.16}$$

where B_T is the Temkin isotherm energy constant $B_T = RT/b_T$, b_T is constant value related to the heat of adsorption (J/mol), R is the constant of ideal gas (8.314 J/molK), A_T is the Temkin isotherm constant (L/g). Equation 2.16 gives a linear relationship between q_e and $\ln C_e$, and the model parameters can again be calculated from the slope and the intercept.

b) Three-parameter isotherms

Redlich-Peterson isotherm

The Redlich-Peterson isotherm (Redlich and Peterson, 1959) is a hybrid isotherm which combined features both Langmuir and Freundlich isotherms (Witek-Krowiak et al., 2011). This model is linearly dependent on concentration which can be used with multiple adsorption system (e.g. homogeneous or heterogeneous systems) over a wide range of concentration (Bulgariu and Bulgariu, 2012). So that, the mechanism of this model is not completely valid as ideal monolayer adsorption (Redlich and Peterson, 1959). The Redlich-Peterson model is one of three-parameter isotherms, which combines the elements of the Langmuir and Freundlich isotherms in a single equation given below:

$$q_e = \frac{AC_e}{1 + BC_e^g} \tag{2.17}$$

where A is the model constant of Redlich-Peterson (L/g), B is also the model constant having unit of $(L/mg)^g$, and g is an exponent value ranged from 0 and 1. At high concentrations of the adsorbate, Eq. (2.17) reduces to the Freundlich equation. For g equal to 1, Eq. (2.17) transforms to the Langmuir equation and when $g = 0$, Eq. (2.17) become to Henry's law equation.

Sips isotherm

The Sips isotherm is three-parameter isotherm which combines the Langmuir and Freundlich isotherms for predicting the heterogeneous adsorption systems. The Sips equation is similar to the Freundlich equation, but there is a limit at sufficiently high concentration (Sips, 1948) which avoiding the limitation of higher adsorbate

concentration. Moreover, this model reduces to the Freundlich isotherm at low concentration while high concentration presents the adsorption capacity of a monolayer similar to the Langmuir isotherm. The Sip isotherm equation is given as;

$$q_e = \frac{q_{mS} K_s C_e^{mS}}{1 + K_s C_e^{mS}} \tag{2.18}$$

where q_{mS} the maximum adsorption capacity of Sips model (mg/g), K_S the Sips constant $(L/mg)^m$, and mS is the Sips model exponent.

Toth isotherm

The Toth isotherm is another three-parameter isotherm which modified to improve the Langmuir isotherm fittings, to reduce the error of model prediction. This model is useful for describing the adsorption systems of heterogeneous and satisfies both the low and high boundaries of concentration. The Toth equation express as follows (Toth, 2000):

$$q_e = \frac{q_{mT} C_e}{\left(1/K_T + C_e^{mT}\right)^{1/mT}} \tag{2.19}$$

where q_{mT} the a maximum adsorption capacity of Toth model (mg/g), K_T the Toth model constant, and mT is the Toth model exponent, related to surface heterogeneity when it is less than the unity. In contrast, the model suggests that the adsorption process occurs on a homogenous surface when it equals to the unity.

CHAPTER 3

EXPERIMENTAL INVESTIGATION

This chapter describes the details of the materials and reagents, also including an overview of the methods used for preparing the adsorbents (natural bentonite and modified bentonite), stock solution of metal Cu (II), Zn (II) and Ni (II) and organic substance (humic acid), the characterization of adsorbents, experimental conditions, experimental procedures. An additional description of each method used for experiments of each adsorbent is also shown in relevant sections of a chapter.

3.1 Adsorbent

3.1.1 Natural bentonite

A commercial grade natural bentonite (clay mineral) was used in this study. The material was passed through a 200 mesh laboratory sieve and dry at 80 ˚C, 24 h before use in experiments.

3.1.2 Modified bentonite

To modify bentonite, surface modification technique was employed to use with natural bentonite. A cationic surfactant (benzyl hexadecyl dimethyl ammonium chloride, BCDMACl) obtained from Sigma Aldrich, was used to modify bentonite in this study. BCDMACl micelles consists of two main parts (hydrophilic head and hydrophobic tail), with ammonium cation [R′-$(CH_3)_2N^+R$] being the head and a long chain forming the tail (see Fig. 3.1). The ammonium cation of BCDMACl micelles intercalated into the interlayers and replaced exchangeable cations (Ca^{2+} and Na^+ in interlayer) and Mg^{2+} for Al^{3+} in the central octahedral layer.

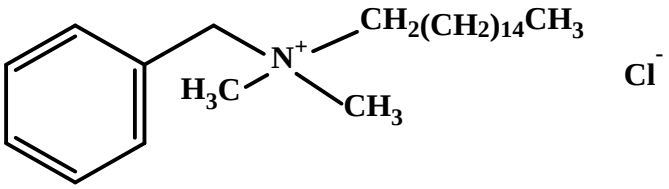

Figure 3.1 Structure of BCDMACl.

Modification step of cationic modified bentonite can be seen in Fig. 3.2. The modified bentonite (MB) was prepared from natural bentonite (NB) specimens by adding the NB into 1M sodium acetate buffer solution at pH 5, and allowing to react for 18 h. Potassium chloride solution (1 M at pH 7) was then added and allowed to react for 18 h. After that, the solid phase was separated and left in 0.2 M cesium chloride solution for 6 h. The solid-phase was again separated and left in cesium chloride solution for 10 min (Diaz-Nava et al., 2012). The solids (preprocessed bentonite) were then mixed into 8.40 mmol/L of BCDMACl. The mixture was shaken for 48 h at 303 K. Finally, the clay sample was separated from the solution using a centrifuge at 2500 rpm (770 relative centrifugal force) for 10 min and rinsed with distilled water for various times to eliminate excess surfactant. The solid sample was then dried at 343 K for 24 h.

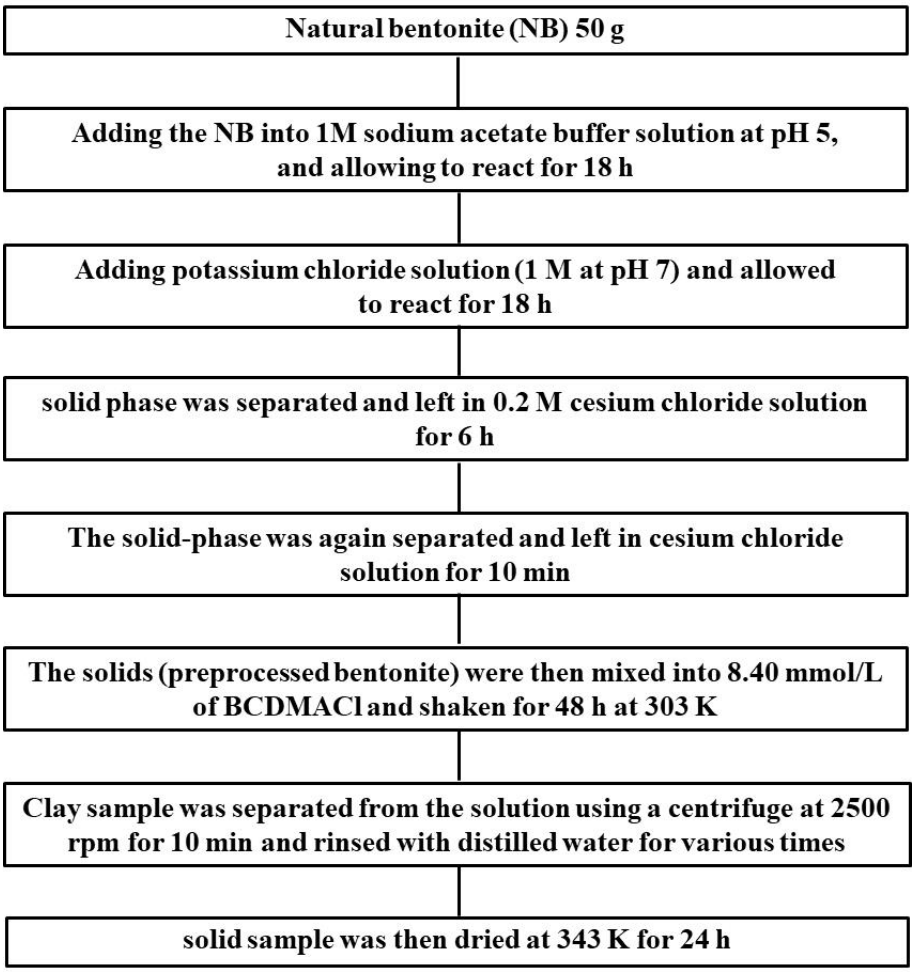

Figure 3.2 Flow chart of modified bentonite preparation by cationic surfactant.

3.2 Chemicals

All chemicals used in this study were analytical grade. Heavy metal salts $CuSO_4 \cdot 5H_2O$, $Zn(NO_3)_2$ and $NiSO_4 \cdot 6H_2O$ purchased from Ajax Finechem, and Loba Chemie, respectively, were used to prepare the stock solutions of Cu (II), Zn (II) and Ni (II). A solid humic acid (HA) purchased from Aldrich Chemistry. Figure 3.3 show a general structure of HA. A cationic surfactant (BCDMACl), obtained from Sigma Aldrich, was used to modify bentonite in this study as described above.

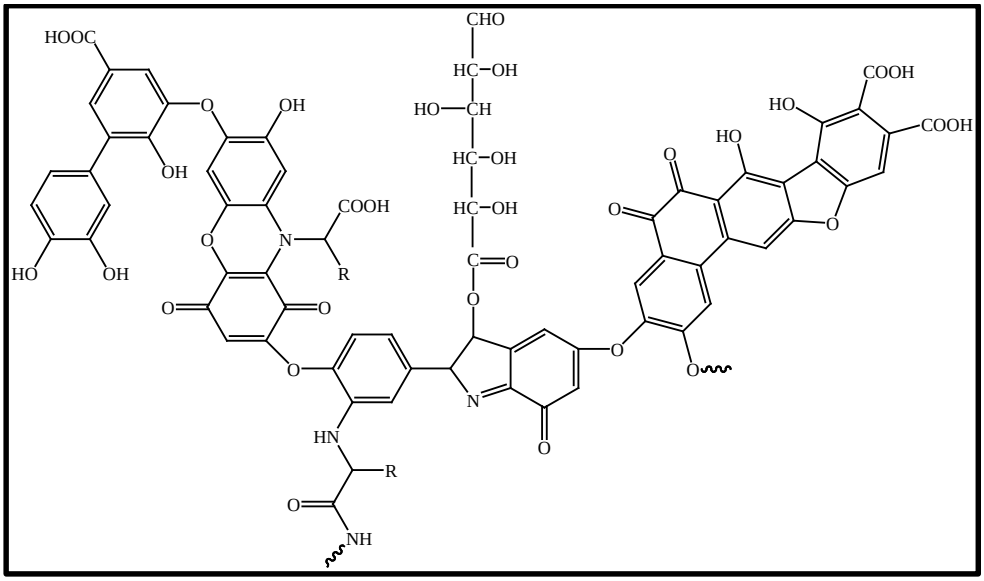

Figure 3.3 Structure of humic acid.

3.2.1 Cu (II) stock solution

A stock solution (1000 mg/L) of Cu (II) was prepared by dissolving 3.929 g of $CuSO_4 \cdot 5H_2O$ in 1 L distilled water. Working solution was prepared by diluting stock solution with distilled water.

3.2.2 Zn (II) stock solution

Stock solution of Zn (II) was prepared by dissolving 2.896 g of $Zn(NO_3)_2$ in 1 L distilled water to achieve a concentration of 1000 mg/L. Used water samples for all experiments were prepared by diluting the stock solution to the pre-determined concentration.

3.2.3 Ni (II) stock solution

The stock solution (1,000 mg/L) of Ni (II) were prepared by dissolving 4.479 g of $NiSO_4 \cdot 6H_2O$ in 1 L distilled water. The working solutions were diluted from the above stock solution and were used throughout the experiments.

3.2.4 Humic acid stock sulotion

Humic acid was prepared by dissolving 0.50 g of humic acid (solid) in 0.1 N NaOH. The working solutions were diluted from the above stock solution and were used throughout the experiment.

3.3 Characterization of adsorbents

3.3.1 Chemical properties

a) Fourier transform infrared

Fourier transform infrared (FTIR) technique is based on the excitation of molecular vibrations by light absorption. It is widely used in the determination of structure and identification of both organic and inorganic compounds. It is also used in the identification of functional groups present in a given sample. The FTIR spectrum represents the molecular absorption and transmission, creating a molecular fingerprint of the sample. This leads FTIR spectroscopy useful for several types of analyses including identification of an unknown material.

In this work used the FTIR spectra for detection functional group of the natural and the modified bentonite were recorded from KBr pellets with a Fourier Transform Infrared Spectrometer, VERTEX 70, Bruker, Germany, provided by Scientific Equipment Center (SEC), Prince of Songkla University.

Figure 3.4 Fourier Transform Infrared Spectrometer (FTIR), VERTEX 70.

b) X-ray fluorescence

The principle of XRF is individual atoms emitting X-ray photons of a characteristic energy. Identification and quantity measurement can be done by counting the number of photons emitted from the sample. This identification of elements is under certain conditions of the characteristic radiation emitted from the inner electronic shells of the atoms, the X-ray method is therefore reliability.

Natural and modified bentonites were characterized with an X-ray fluorescence spectrometer, PW2400, PHILIPS, Netherlands, provided by Scientific Equipment Center (SEC), Prince of Songkla University.

c) Cation exchange capacity

Cation exchange capacity (CEC) is important properties which indicated among cation capacity in soil. Cation exchange occurs due to the negative charges of clay. The CEC value can be calculated by summation of exchangeable cation (Ca, Mg, Na and K) and exchangeable Al. The neutral 1.00 M ammonium acetate (NH_4OAc) extraction is the most widely applied method to estimate the soluble and rapidly exchangeable pools of alkali and alkaline elements in soils. Procedure of this method and determination are follows:

Analytical procedure

1. Cation replacement
    1.1 Weight 5 g of air-dried soil sample adding into centrifuge tube.
    1.2 Add 30 mL of 1 M NH_4OAc and shaking 30 min.
    1.3 Centrifuge at 2500 rpm, 10 min and separating only solution by number 5 of filter paper.
    1.4 Duplicate 2 times from order 1.2-1.3, instead of centrifuging by shaking with hand 1 min. Filtering and adjusting solution volume by 1 M NH_4OAc reach to 100 mL.
2. Washing ammonium
    2.1 Add 30 mL of 80% w/w ethanol into soil sample tube (order 1.4) and shaking 1 min.
    2.2 Centrifuge the sample, similar to order 1.3 and collect only soil sample.
    2.3 Follow the procedure from order 2.1-2.2, duplicating 3 times.
3. Expelling adsorbed ammonium
    3.1 Add 30 mL of 10% w/v NaCl into 2.3, shaking 1 min.
    3.2 Follow 1.3 and collect only the solution to volumetric flask without filtration.
    3.3 Duplicate 3.1-3.2, 2 times and adjusting solution volume with NaCl to 100 mL.
4. Distillation of ammonium
    4.1 Pipet 20 mL of the solution from 3.3, adding 10 mL of magnesium oxide.
    4.2 Distill ammonium in 5 mL boric acid into 125 mL flask until the volume reach to 30 mL using VAPODEST® - C. Gerhardt GmbH & Co. KG (Fig. 3.5).
    4.3 Titrate with 0.01 M H_2SO_4.
    4.4 Distill NaCl (blank) similar the procedure from 4.1-4.3.

Determination

$$CEC(cmol_c / kg) = 200AB \quad (3.1)$$

where A is The known concentration of H_2SO_4 (mL) and B is different volume between titrated and blank volume (mL).

Figure 3.5 Apparatus for distillation system.

3.3.2 Physical properties

a) BET surface area

This technique was developed in 1938 by three inventors: S. Brunauer, P. H. Emmet and E. Teller (BET). This is the first method for measuring the specific surface area of fine and porous material. Based on adsorption of N_2 on a surface, the BET surface area can be determined as the amount of gas adsorbed at a given pressure. In experiment of the BET, the specimen is placed in a vacuum chamber at low and constant temperature, and subjected to a wide range of pressures, to generate adsorption and desorption isotherms. A total surface area of the material sample can

be determined by using an adsorption model with known occupied area of the sample by one molecule of adsorbate.

The BET surface areas and porosity of natural and modified bentonite were determined using BET-technique, ASAP2460, Micromeritics, USA, provided by Scientific Equipment Center (SEC), Prince of Songkla University.

Figure 3.6 BET ASAP2460.

b) Swelling

The swelling test can imply the swelling characteristics of clay, particularly sodium bentonite, in term of swell index. The swell index can be indicated bentonite quality which a high swell is considered to be a good quality. This method was contained in testing standard (ASTM-D5890). The testing procedure can be done by two simple steps following:

1. Add a 2 g of total dried bentonite clay into 100 ml of graduated cylinder by 0.1 g increments, this step could be done in 10 min followed, the entire 2g sample has been added to the cylinder.

2. The sample was then covered from the disturbance for a period of 16-24 hours, at which time the level of the settled and swollen clay is recorded to the nearest 0.5 mL.

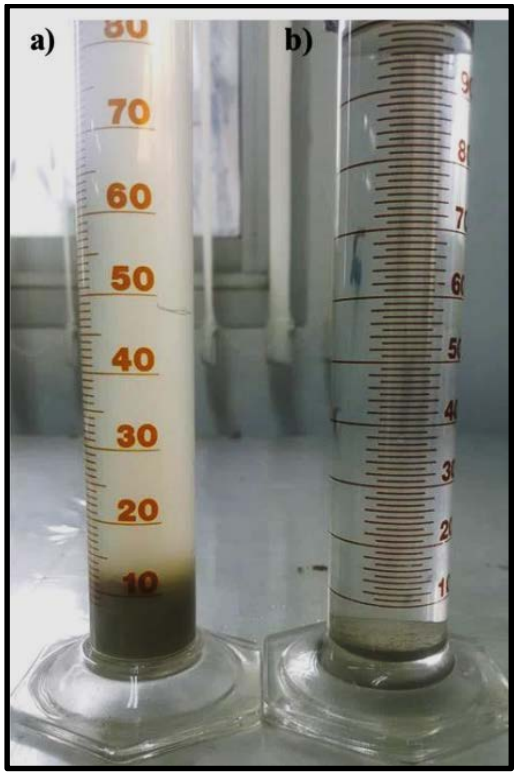

Figure 3.7 Swelling experiment of clay; a) natural bentonite, b) modified bentonite.

3.3 Adsorption study

3.3.1 Adsorption kinetics

Kinetic removal for adsorption of metals (Cu (II), Zn (II), and Ni (II)) and humic acid onto natural and modified bentonite were performed in 50 mL of metal and humic substance at 150 rpm at room temperature. Four concentrations (50.0, 100.0, 150.0 and 200.0 mg/L) were selected for kinetics adsorptions. Powdered natural and modified bentonite (0.5 g) were thoroughly mixed with 50 mL of metals and humic substance, and were agitated for selected time (5-80 min). After these processes, collected water was filtered by micro filter 0.45 micron and was collected to determine retaining concentration of metals and humic acid. The adsorbed metals from adsorbent phase (q_t, mg/g) were calculated by the following expression:

$$q_t = \frac{(C_0 - C_t) \times V}{m} \quad (3.2)$$

where: C_0 and C_t are the initial concentration and concentrations at time in the eluent (mg/l), 'V' is the eluent volume (L) and m is the mass of the adsorbent (g).

3.3.2 Adsorption isotherm

Batch adsorption experiments were performed at room temperature (25 °C) on a rotary shaker at 150 rpm containing 50 mL of metal ion solutions and 0.5 g of natural and modified bentonite adsorbents, the contact time was ranged from 5-80 min. After agitation, the suspensions were centrifuged at 2500 rpm for 10 min and the supernatant was kept for all metals (Cu (II), Zn (II), Ni (II)) and humic acid analyses (see section 3.3.4). Various conditions, including the contact time, the pH, the initial concentration and the ionic strength, were tested. In case of multi-solution system (Cu-Zn-Ni), ratio 1:1:1 of all metals was used. All experiments were carried out in duplicates and the data obtained were used for analysis. The amount of heavy metals and humic acid adsorbed on a solid surface at equilibrium (q_e, in mg of ion/ g of adsorbent) can be determined from the following mass-balance equations (Eq. 2.2).

3.3.3 Experimental condition

a) Effect of solution pH

The optimum pH for adsorption of Cu (II), Zn (II), Ni (II) and Humic acid by the adsorbents were determined experimentally. Metal standard Cu (II), Zn (II), Ni (II) and humic acid solutions in the range 50-800 mg/L were then prepared by diluting appropriately the stock solutions, and 0.1 M NaOH or HCl was used to adjust the final pH range 3-11of the metal solutions. On testing an aliquot of a prepared solution (50.0 mL) was placed in a 250 mL conical flask and 0.5 g of adsorbent was added to it before placing in an incubator shaker at 150 rpm and 293 K (controlled temperature). The samples were separated by 0.45 micron filter, heavy metal and humic acid concentrations were analyzed by using atomic adsorption spectrometer and UV-visible spectroscopy system (λ = 400 nm), respectively. The optimum pH for each

metal's adsorption was adopted from maximum metal adsorption by the adsorbents for the next experiments.

b) Effect of contact time

The effect of contact time (5-80 min) on adsorption of metals Cu (II), Zn (II), Ni (II) and humic acid onto adsorbents were studied at the optimum initial metals concentration (50.0-200.0 mg/L) and 0.5 g of adsorbent dose. The experimental procedure was the same as in the effect of adsorbent. The optimum contact time was implemented in this study for the next experiments.

c) Effect of initial concentration

The effect of initial metal and organic substance concentration Cu (II), Zn (II), Ni (II) and humic acid were examined with optimum pH, contact time for 50.0-800.0 mg/L metals and organic substance concentration in 50.0 mL water. After filtering the water samples were analyzed for residual concentrations of metals and organic substance. The optimum concentrations of metals and organic substance were taken on in this study during other experiments.

d) Effect of ionic strength

The effect of electrolyte was studied using $NaNO_3$ and NaCl in three concentrations (0.01, 0.05 and 0.1 M) for metal (Cu (II), Zn (II) and Ni (II)) and organic substance (HA), respectively. The various weights required for the preparation of each concentration of electrolyte were added to the weights of metal ion salts required to prepare the various concentrations of the metal ion. These were mixed and made up to standard mark using distilled water. Subsequently, 50.0 mL of these solutions were added to 0.5 g of adsorbents. They were subsequently centrifuged for 10 min at 2500 rpm. The supernatants collected for metal ions (Cu (II), Zn (II) and Ni (II)) and organic substance (HA) analysis. The amounts of the metal ion and organic substance were analyzed by AAS and UV-visible, respectively.

3.3.4 Determination of metals and humic acid concentration in the aqueous solutions

The concentrations of metal Cu (II), Zn (II), and Ni (II) were measured by using atomic absorption spectrophotometry (AAS, Fig. 3.8), using AANALYST 100 SPECTROMETER, Perkin-Elmer, Norwalk CT/USA. The calibration curve of all metals were prepared from their standard solutions.

Figure 3.8 Atomic Absorption Spectrophotometer (AAS), AANALYST 100 SPECTROMETER.

A retention of humic acid concentrations in the aqueous solutions was determined by using an UV-visible Spectroscopy system Lambda 400 nm (Fig. 3.9), UV 8453, Hewlett Packard, at pH 3. Standard calibration curve was obtained by varying the solutions of humic acid in the concentration range between 10.0 to 50.0 mg/L.

Figure 3.9 UV-visible Spectroscopy, UV 8453.

CHAPTER 4

RESULTS AND DISCUSSIONS

4.1 Characteristic of natural and modified bentonite

The characteristic of adsorbent play a major role in the adsorption study of tested substance. In this study, major adsorbents used are natural (NB) and modified bentonite (MB). Both NB and MB were prepared and their properties were examined by several techniques (e.g. FTIR, XRF, BET) including CEC and swelling test for supporting their properties. The details of adsorbent characteristics are explained below.

4.1.1 Structure of natural and modified bentonite

Bentonite is a clay mineral containing montmorillonite. As shown in Fig. 4.1, montmorillonite structure has three mineral layers periodically, with two tetrahedral layers (silica sheets) sandwiching a central octahedral layer (alumina sheet). NB shows a net negative charge due to isomorphic replacement of Al^{3+} with Mg^{2+} in the central octahedral layer. The negative charge is balanced by exchangeable cations in the lattice structure, such as Ca^{2+} and Na^{+} located in the interlayer, which can enhance the adsorption of cationic pollutants (Hu et al., 2006; Tahir and Rauf, 2006).

To modify bentonite, a cationic surfactant (BCDMACl) was added to natural bentonite. BCDMACl micelles consists of two main parts (hydrophilic head and hydrophobic tail), with ammonium cation [R'-$(CH_3)_2N^+R$] being the head and a long chain forming the tail (see Fig. 4.2). The ammonium cation of BCDMACl micelles intercalated into the interlayers and replaced exchangeable cations (Ca^{2+} and Na^{+} in interlayer) and Mg^{2+} for Al^{3+} in the central octahedral layer, as shown in Fig. 4.1 (Li., 1999).

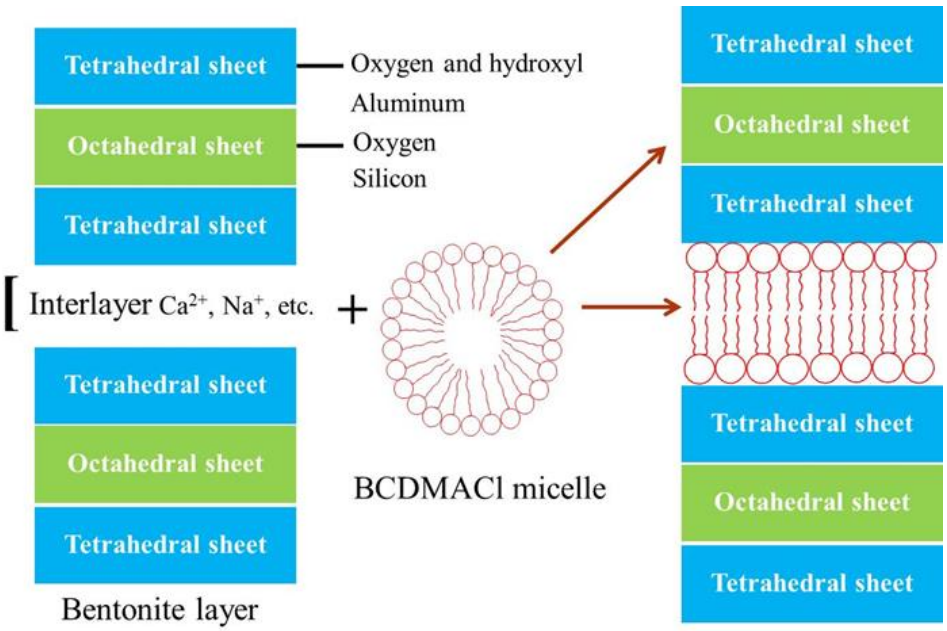

Figure 4.1 Schematic illustration of surfactant modified bentonite.

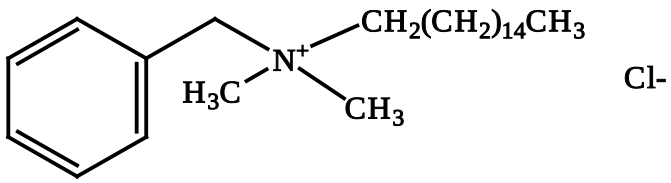

Figure 4.2 Chemical structure of cationic surfactant (BCDMACl).

4.1.2 FTIR analysis results

The FTIR spectra of natural bentonite (NB) and modified bentonite (MB) are shown in Fig. 4.3. FTIR spectra of NB and MB were recorded over the range 4,000-400 cm^{-1} and are reported in Fig. 4.3. The broad band at 3,452 cm^{-1} was assigned to OH stretching vibrations for NB and MB, whereas water present in the bentonite displayed the peak at 1,638 cm^{-1}, which is assigned to OH bending vibrations. The NB shows the Al-Al-OH stretching band at 3,620 cm^{-1}. At 917 and 852 cm^{-1} the bands can be assigned to Al-Al-OH and Al-Fe-OH bending vibrations, respectively (Farmer, 1974). The Si-O stretching was observed at band 1042-1045, and the band at 521 cm^{-1} was assigned to Si-O bending vibrations. The doublet at 852 and 797 cm^{-1} indicated the presence of quartz in the bentonite (Dutta and Singh, 2015). Generally, all the bands described above are typical in NB spectra. For MB, there was a slight

shift of those bands due to modification by cationic surfactants. Appearance of the pair of bands at 2,923 and 2,852 cm^{-1} confirmed that the cationic surfactant was present in the modified bentonite. These bands were assigned to symmetric and asymmetric C-H stretching vibrations of methyl and methylene groups, which were absent from spectra of NB (Dutta and Singh, 2015).

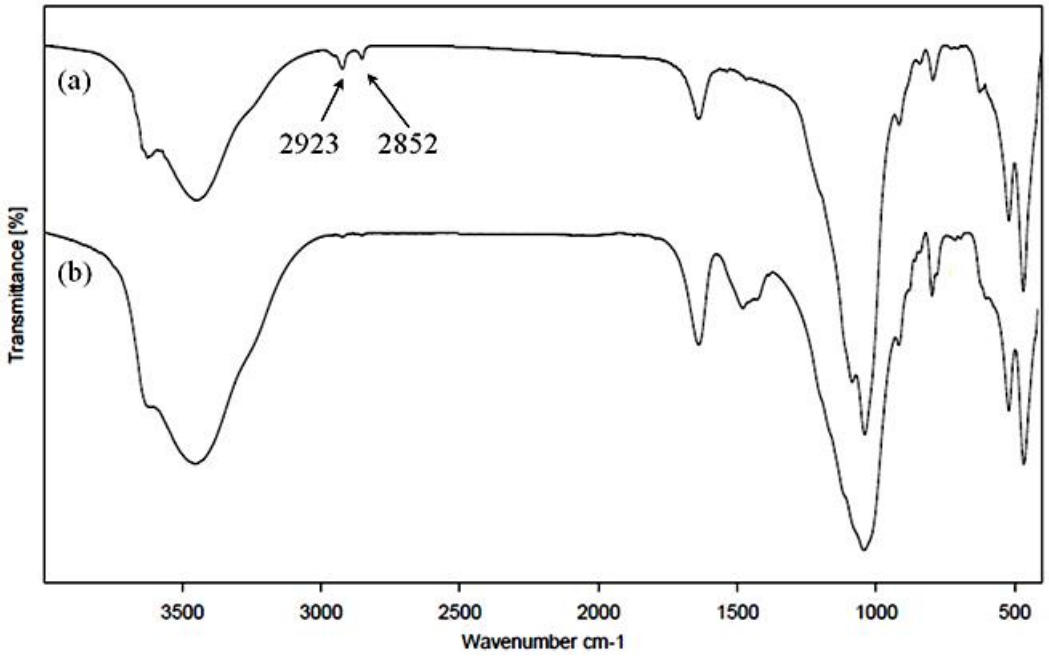

Figure 4.3 The FTIR spectra of (a) the modified bentonite (MB) and (b) natural bentonite (NB).

4.1.3 XRF analysis results

Table 4.1 shows a comparison of the chemical constituents in NB and MB, from the XRF results. The NB and MB had alumina and silica as the major species, at 13.81% and 59.73% and at 12.91% and 59.04% by weight, respectively. It was found that Cs and Cl were present in MB at 3.86 and 0.31%, respectively. This implies that the intercalation of BCDMACl was successful by ion exchange. Furthermore, the results indicate obvious decreases in the cations of the interlayer (Ca^{2+} and Na^{+}) and of the octahedral layer (Mg^{2+} for Al^{3+}), on forming MB from NB. This corroborates cation exchange and replacement as mechanisms acting during the modification (Li, 1999).

Table 4.1 Chemical constituents and physical properties of NB and MB.

Constituents	**NB**	**MB**
Chemical constituents (% by weight)		
Na_2O	2.72	0.48
MgO	2.38	1.81
Al_2O_3	13.81	12.91
SiO_2	59.73	59.04
P_2O_5	0.10	0.14
SO_3	0.31	0.28
K_2O	1.10	5.22
CaO	3.18	2.18
TiO_2	0.36	0.37
Fe_2O_3	3.00	3.57
SrO	0.06	0.04
ZrO_2	0.03	0.04
BaO	0.15	0.22
Cs_2O	-	3.86
Cl	-	0.31
Structural parameters		
BET surface area (m^2/g)	44.60	15.57
Pore volume (cm^3/g)	0.054	0.035
Pore size (nm)	4.81	9.10
CEC ($cmol_c/kg$)	75.95	68.70
Free swelling* (mL/2 g)	10.33	0.00 (no swelling)

*Following ASTM D5890-06 (2006)

4.1.4 CEC and textural characteristics

As a consequence of the modification, cation exchange capacity (CEC) was reduced from 75.95 (NB) to 68.70 $cmol_c/kg$ (MB), as shown in Table 4.1. The cation from the surfactant was intercalated in the clay and pushed other cations into solution, thereby significantly decreasing CEC (Akpomie et al., 2016). After bentonite was

modified by BCDMACl, the BET results indicate significantly reduced specific surface, from 44.60 to 15.57 m^2/g, caused by the alkyl chains screening adsorbent pores (Gładysz-Płaska et al., 2012). The surfactant could also adsorb to the micropores and the inner surfaces of the particles, decreasing the specific surface of MB (Ma et al., 2010). Moreover, the average pore diameter increased from 4.81 to 9.10 nm, which suggests elimination of the smallest pores in the adsorbent (Gładysz-Płaska et al., 2012).

The BET surface area and the pore size are not the only determinants affecting the adsorption of heavy metals. The surface functional groups are key characteristics of an adsorbent which metal ions can be adsorbed by interactions with the surface functional group of the adsorbent (Worch, 2012). Eventually, swelling tests following ASTM D5890-06 (ASTM D5890-06, 2006) confirmed that no swelling occurred in the cationic surfactant modified bentonite, while the natural bentonite had 10.33 mL/2g which the swelling is almost completed during preparation process.

4.2 Adsorption of heavy metal Cu (II) and Zn (II) onto natural and modified bentonite

The modification of bentonite has been successfully achieved using cationic surfactant BCDMACl. Both NB and MB were primarily used to examine their applicability in heavy metal adsorption. Cu (II) and Zn (II) were then choose as the representative metals. A series of batch experiments were performed to determine the adsorption capacities of NB and MB, during removal of Cu (II) and Zn (II) from aqueous solutions. Several factors affecting were experimentally investigated to clarify adsorbent performance, such as pH solution, initial concentration, and ionic strength.

4.2.1 Adsorption kinetics

In order to study the adsorption kinetics, both pseudo-first and pseudo-second order of kinetic models were fit to the experimental data. Linear fits were used with the transformed models, instead of nonlinear regression. The results revealed that the pseudo-first-order model did not reliably match with the experimental data related to

coefficient of determination (R^2) ranges 0.164-0.923. In contrast, the adsorption kinetics of Cu (II) and Zn (II) were well described by the pseudo-second-order model, see Fig. 4.4, and the identified model parameters are listed in Table 4.2.

A comparison of q_e from the experiment ($q_{e,\exp}$) and from the model ($q_{e,cal}$) revealed the good fit with R^2 better than 0.990. This indicates that the pseudo-second-order model was appropriate for the adsorption kinetics in this study. Figure 4.5 shows a plot of the pseudo-second-order model without linearizing transform, while the parameters were obtained with the transform (see Table 4.2). The equilibrium was practically reached by 10 min. To ensure equilibration, 80 min equilibration time was used when determining the adsorption isotherms of the next section.

Table 4.2 Kinetic model parameters of Cu (II) and Zn (II) onto NB and MB.

Adsorbents	Metal	C_i (mg/L)	$q_{e,\exp}$ (mg/g)	Pseudo-first-order model			Pseudo-second-order model		
				k_1 (1/min)	$q_{e,cal}$ (mg/g)	R^2	k_2 (g/mg/min)	$q_{e,cal}$ (mg/g)	R^2
NB	Cu (II)	50.0	4.60	0.016	36.71	0.462	2.94	4.60	1.000
		100.0	9.01	0.046	20.35	0.888	2.93	9.01	1.000
		150.0	13.18	0.026	9.79	0.309	1.22	13.19	1.000
		200.0	16.40	0.050	2.57	0.665	0.43	16.42	1.000
	Zn (II)	50.0	4.75	0.020	13.78	0.923	2.13	4.76	1.000
		100.0	9.06	0.026	11.55	0.698	1.13	9.06	1.000
		150.0	12.75	0.051	17.62	0.861	2.79	12.76	1.000
		200.0	15.15	0.115	2.92	0.799	0.65	15.17	1.000
MB	Cu (II)	50.0	4.72	0.039	21.69	0.738	2.72	4.72	1.000
		100.0	9.30	0.103	16.12	0.468	1.72	9.30	1.000
		150.0	14.07	0.007	2.79	0.922	0.17	14.08	1.000
		200.0	18.95	0.004	1.04	0.164	0.06	19.01	0.999
	Zn (II)	50.0	4.95	0.076	5.82	0.835	1.19	4.96	1.000
		100.0	9.81	0.064	15.77	0.631	1.01	9.82	1.000
		150.0	14.79	0.045	31.05	0.315	0.89	14.81	1.000
		200.0	19.78	0.108	6.22	0.721	0.53	19.80	1.000

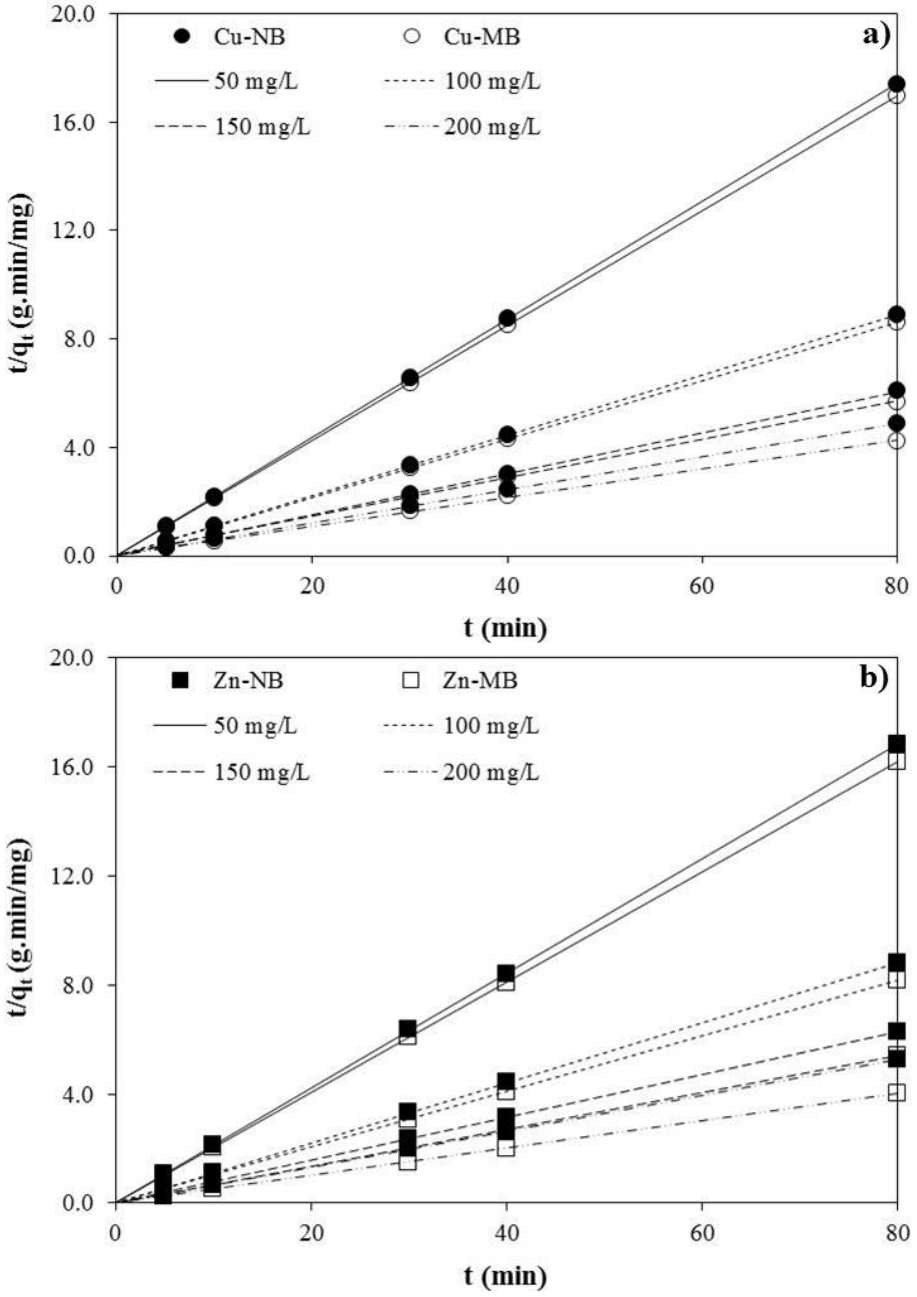

Figure 4.4 Pseudo-second-order model of Cu (II) (a) and Zn (II) (b) on to NB and MB, linear plot.

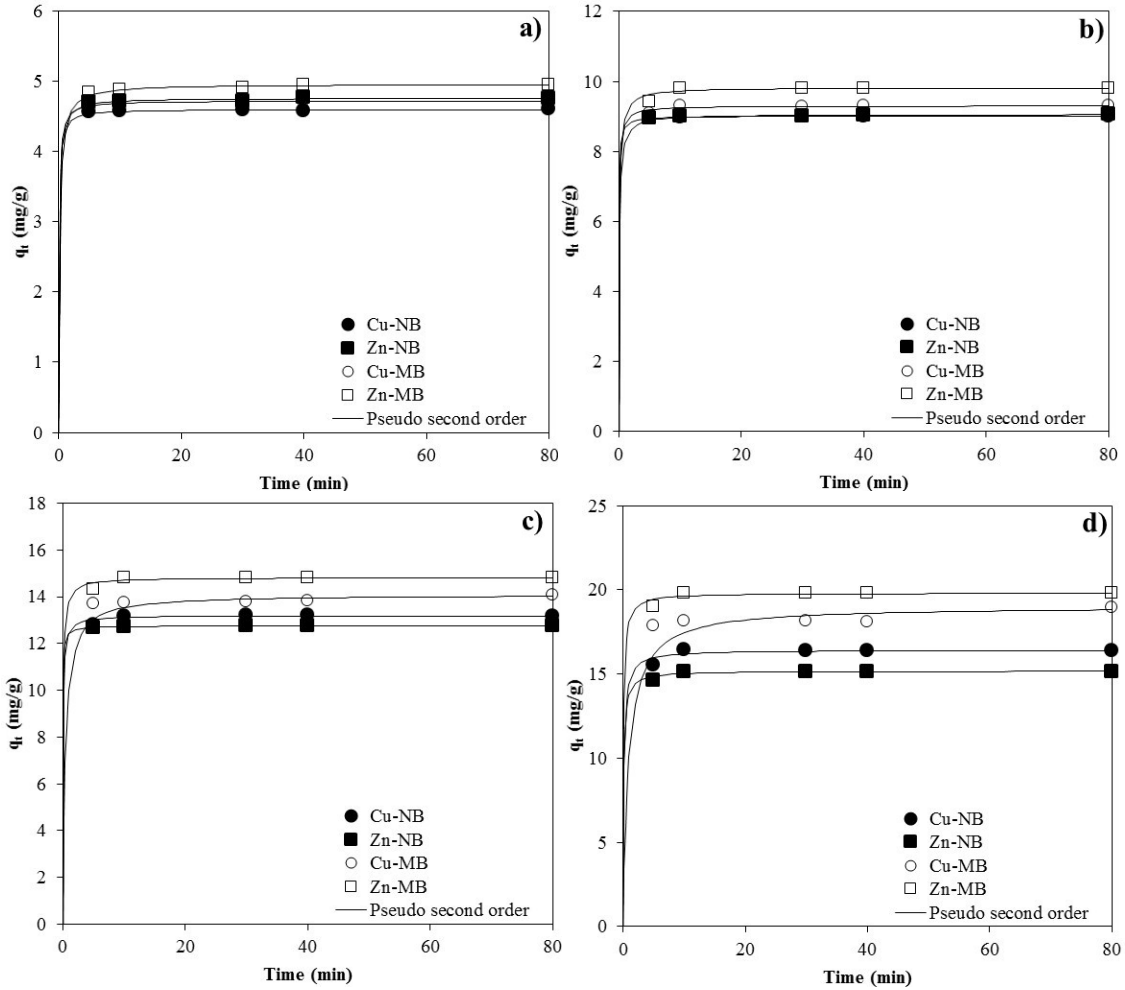

Figure 4.5 Pseudo-second-order model of Cu (II) and Zn (II) onto NB and MB, non-linear plot at initial metal concentration 50.0 (a) 100.0 (b) 150.0 (c) and 200.0 (d) mg/L, NB and MB dosage 0.5 g, and pH 5.

4.2.2 Factors affecting adsorption capacity

(a) Effect of initial solution pH

Solution pH is an important factor which can affect the adsorption process. The removals of metal Cu (II) and Zn (II) were observed by batch experiments at various pH of metal solutions range 3-11. Figure 4.6 illustrated the metal removal as a function of solution pH. There were increases in the removals of Cu (II) and Zn (II) with increasing the pH solutions over the range of 3-5. However, it was remarkable that the removals of both ions almost reached a maximal capacity of metal concentration at the solution pH 7-11 (more than 95%). This was due to the reason that a chemical precipitation became a dominant process on metal removal at this range which mainly formed the solid state of $Cu(OH)_2$ and $Zn(OH)_2$. This condition was not solely considered as the adsorption because the metal precipitation may lead to a misinterpretation of adsorption capacity. This result had a similar trend with adsorption study on several metal ions which has been reported by numerous studies (Abollino et al., 2008; Chen et al., 2008; Arias and Sen, 2009). Therefore, the optimum pH in this study should be 5-6 for adsorption study of both Cu (II) and Zn (II).

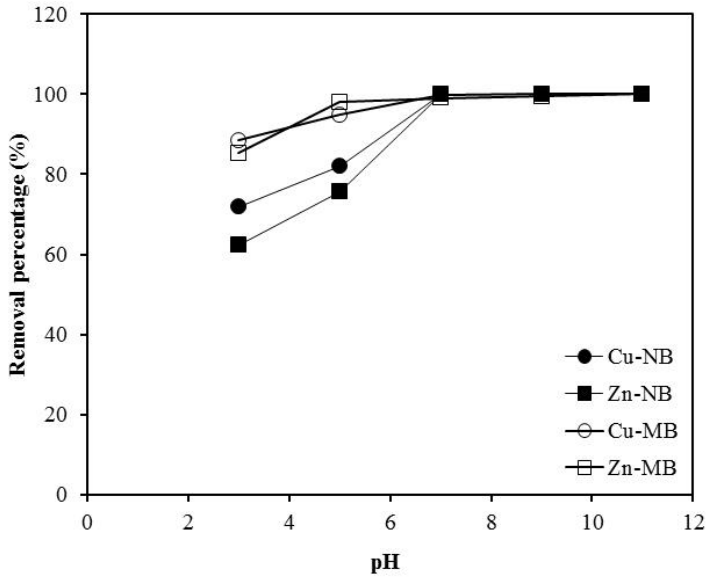

Figure 4.6 Effect of solution pH of Cu (II) and Zn (II) onto NB and MB, initial metal concentration 200.0 mg/L, NB and MB dosage 0.5 g, and contact time 80 min.

(b) Effect of contact time

Contact time is one of the most important factors affecting adsorption efficiency. The adsorption efficiency can be experimentally optimized for optimal pH, adsorbent dose and concentration of adsorbate. Therefore, a series of a batch experiments varying contact time was performed, and the metal ion concentrations were determined by Atomic Absorption Spectrophotometry (AAS).

The adsorption capacities of Cu (II) and Zn (II) by the different adsorbents were determined as the removal percentages of Cu (II) and Zn (II) and are presented as time profiles in Fig. 4.7. The removal of metal ions by adsorption onto both NB and MB was in the ranges 77.50-94.75 % (±0.50-2.81%) and 72.97-98.93 % (± 0.17-1.51%) for Cu (II) and Zn (II), respectively, with initial concentrations varying from 50.0 to 200.0 mg/L. NB maximally removed 82.05 % and 75.74 % of Cu (II) and Zn (II), respectively, from 200.0 mg/L initial concentration. The maximal removal was higher on using MB, reaching up to 94.75 % and 98.90 % of Cu (II) and Zn (II), respectively. Generally, the removal rapidly increased initially for about 10 min, and thereafter either increased only slightly or remained constant. The high equilibrium fractions of ions removed indicate that the dosages of NB and MB were sufficient for adsorption over the range of initial concentrations tested.

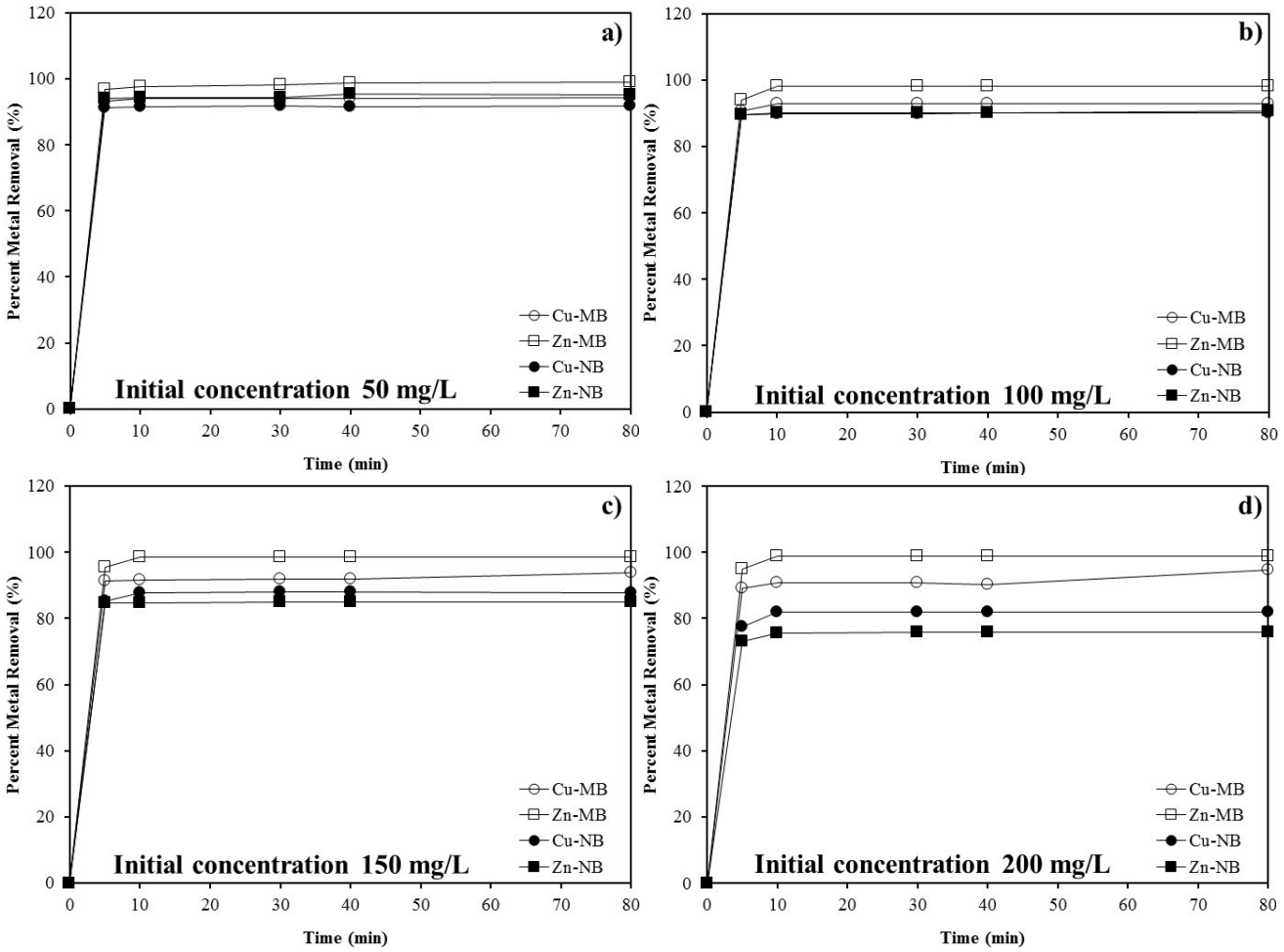

Figure 4.7 Effect of contact time on the removal of Cu (II) and Zn (II) by NB and MB, initial metal concentration 50.0 (a), 100.0 (b), 150.0 (c), and 200.0 (d) mg/L, NB and MB dosage 0.5 g, and pH 5.

(c) Effects of metal ion concentration

Figure 4.8 illustrates the relationship of metal ion concentration to the removals of Cu (II) and Zn (II) at equilibrium. The overall response shapes are similar across all cases, but MB was clearly better adsorbent than NB at high concentration of the heavy metals. The maximal improvement in removal by adsorption on comparing MB to NB was by 40.93 and 43.88 % for Cu (II) and Zn (II), respectively.

The experimental results indicate near complete removal or cleanup of 100.0-150.0 mg/L concentrations with NB, and the higher 250.0-300.0 mg/L range with MB. These are higher concentration ranges than previously reported for natural bentonite by Veli and Alyuz (Veli and Alyuz, 2007). The results clearly confirm that cationic surfactant treatment enhanced the adsorption capacity of natural clay.

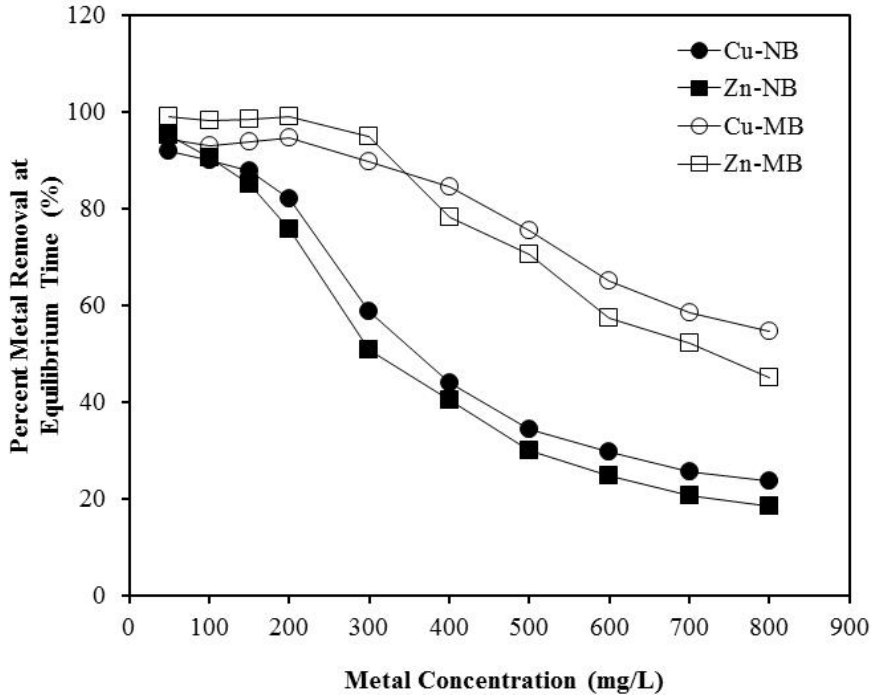

Figure 4.8 Effect of initial metal concentration on the removal of Cu (II) and Zn (II) by NB and MB, clay dosage 0.5 g, pH 5 and contact time 80 min.

4.2.3 Adsorption isotherms

The adsorption of Cu (II) and Zn (II) onto NB and MB was assessed against various equilibrium isotherm models, namely the Langmuir, Freundlich and Dubinin-Radushkevich models. The experimental results were applied to those models as the linear plot illustrating in Figs. 4.9-4.11. The identified parameters obtained from the linear plot are tabulated in Table 4.3, along with the coefficient of determination (R^2) to indicate the goodness of fit (larger values are better).

It is found that the experimental data were best fit by the Langmuir isotherm among the models tested, suggesting homogenous adsorption sites on the surfaces and monolayer formation (Blanchard et al., 1984; Langmuir, 1918). This result indicated that the Langmuir isotherm can be described the adsorption mechanism in this study although the mean free energy of adsorption (E_s) in the Dubinin-Radushkevich model was below 6-18 kJ/mol indicating physical adsorption of Cu (II) and Zn (II). Moreover, as shown in Table 4.4, three-parameter isotherms supported that the results can be described with Langmuir by g , m_S, and m_T from Redlich-Peterson, Sips, and Toth model approached to the unity.

The model-based responses of q_e to C_e of all the adsorption isotherms are shown in Fig. 4.12. The Langmuir isotherm model was the best fit over the experiments for all metal and adsorbents compared to other isotherm models. The maximal adsorption $q_{\max}$ was estimated from the fitted Langmuir models to be 19.76 and 15.46 mg/g for Cu (II) and Zn (II) on NB, while MB had $q_{\max}$ improved by 2.0-2.5 fold with up to 50.76 and 35.21 mg/g adsorptions of Cu (II) and Zn (II), respectively. This is considerable because the cationic surfactant treatment of bentonite in this study modified it to MB by changing the functional groups of natural bentonite and increasing both the anionic adsorptive capacity and the cation affinity of the clay (Adebowale et al., 2006; Li and Gallus, 2005), thereby improving the adsorption of heavy metals.

Table 4.3 Adsorption isotherm two-parameters of Cu (II) and Zn (II) onto NB and MB.

Adsorbate-Adsorbent	Langmuir model				Freundlich model				Dubinin-Radushkevich model				
	K (L/mg)	q_{max} (mg/g)	R^2	APE (%)	K_f (mg/g)	n	R^2	APE (%)	K (mol^2/J^2)	q_{max} (mg/g)	E_s (kJ/mol)	R^2	APE (%)
Cu-NB	0.077	19.76	0.987	6.79	5.363	4.684	0.741	17.42	5.0E-06	17.66	0.316	0.896	10.16
Cu-MB	0.037	50.76	0.984	5.41	5.026	2.486	0.713	14.41	4.0E-06	29.62	0.354	0.872	35.62
Zn-NB	0.177	15.46	0.993	6.22	5.887	5.988	0.868	18.80	2.0E-06	14.25	0.500	0.728	11.45
Zn-MB	0.303	35.21	0.962	9.42	10.170	4.203	0.799	19.74	3.0E-07	28.11	1.291	0.762	28.32

Table 4.4 Adsorption isotherm three-parameters of Cu (II) and Zn (II) onto NB and MB.

Adsorbate-Adsorbent	Redlich-Peterson model				Sips model				Toth model			
	B $(L/mg)^g$	g	A (L/g)	APE (%)	q_{mS} (mg/g)	K_S $(L/mg)^m$	m_S	APE (%)	q_{mT} (mg/g)	K_T	m_T	APE (%)
Cu-NB	0.110	1.000	2.044	6.30	18.62	0.110	1.000	6.30	18.62	0.110	1.000	6.30
Cu-MB	0.032	1.000	0.857	3.63	27.36	0.036	0.959	3.14	27.22	0.036	0.971	3.48
Zn-NB	0.179	1.000	2.785	4.20	15.52	0.179	1.000	4.20	15.52	0.179	1.000	4.20
Zn-MB	0.470	0.965	13.741	10.13	35.58	0.354	0.900	10.60	35.94	0.505	0.813	10.49

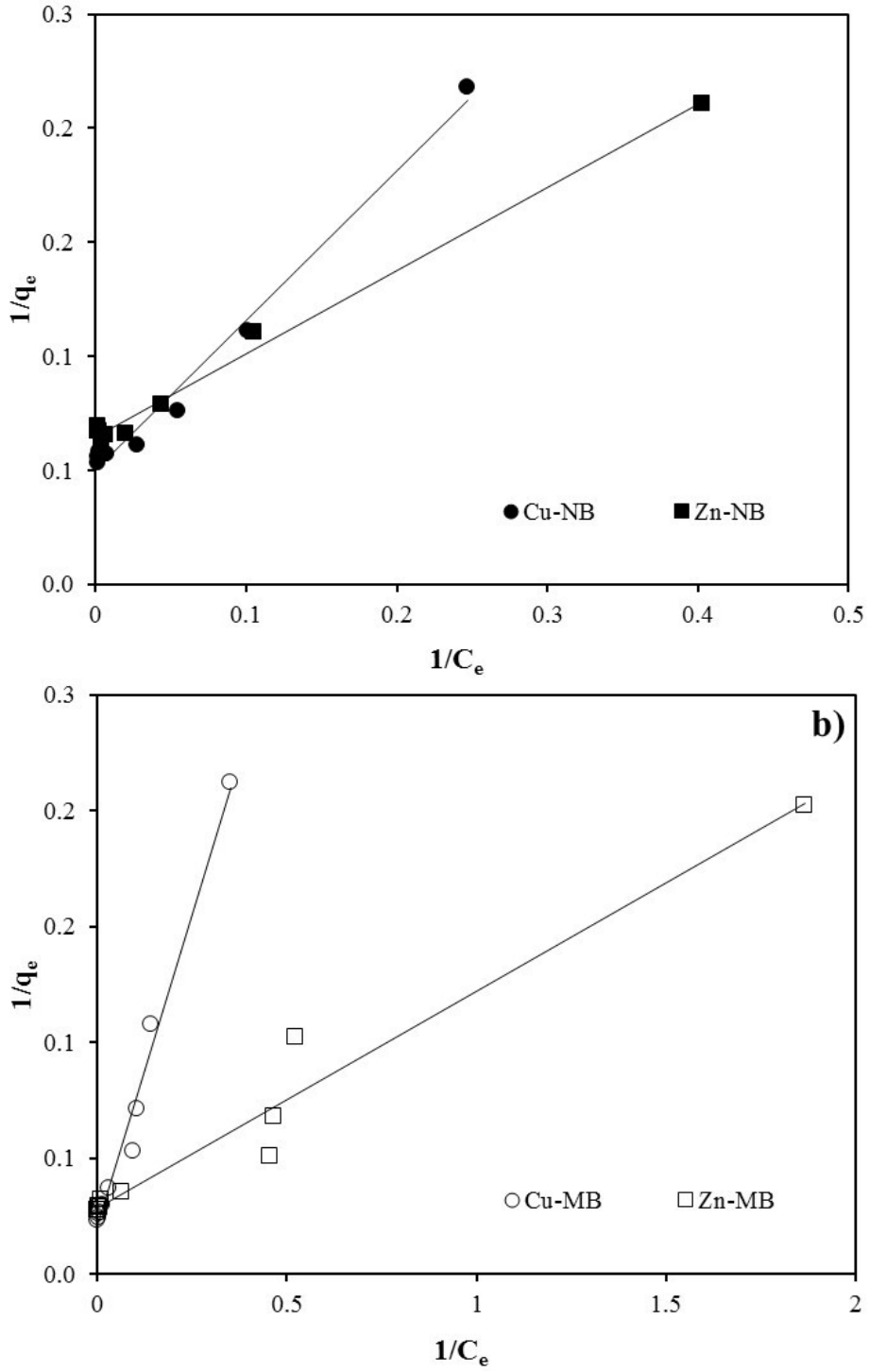

Figure 4.9 Linear plot of Langmuir isotherm for adsorption of Cu (II) and Zn (II) onto NB (a) and MB (b).

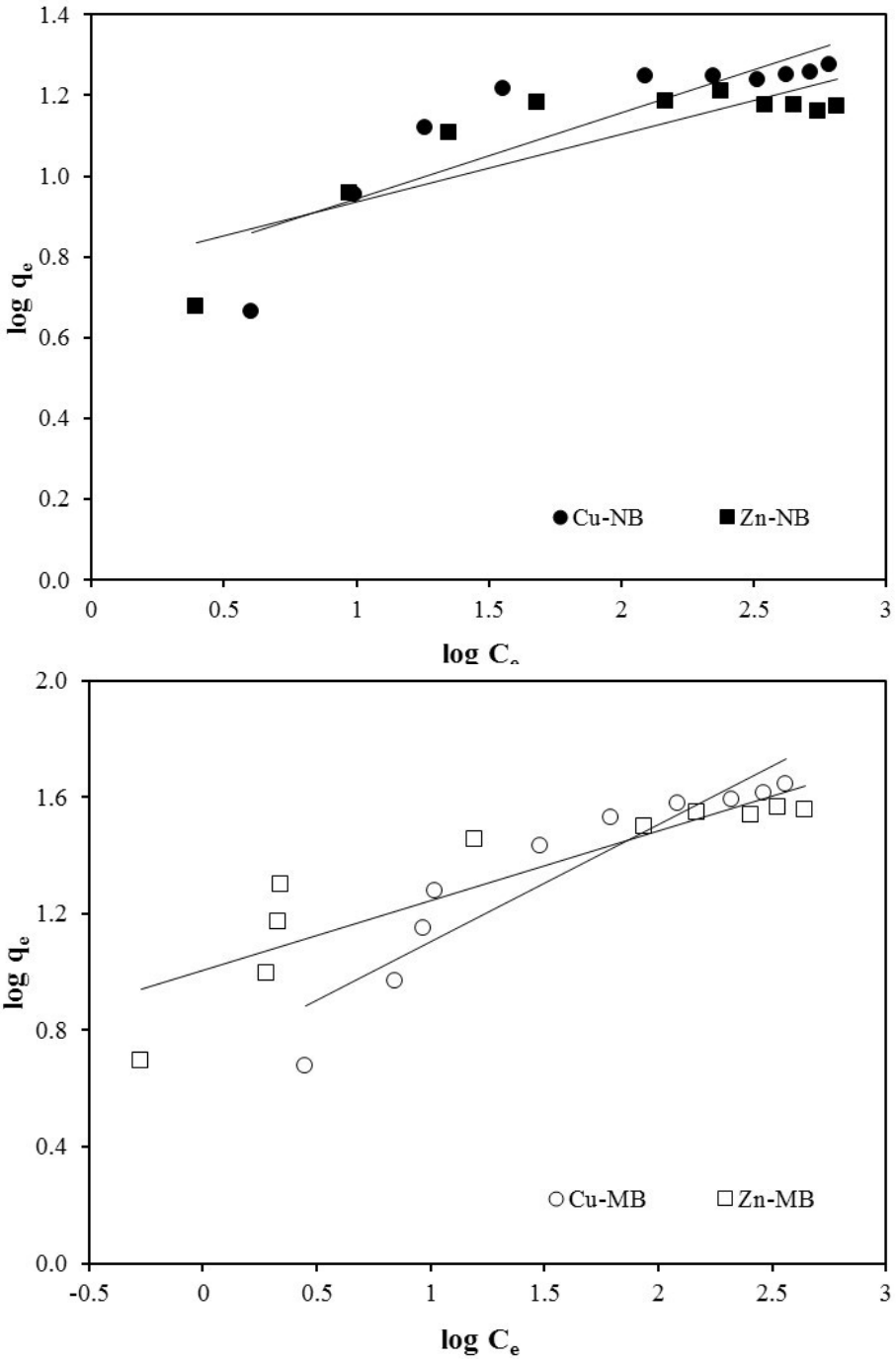

Figure 4.10 Linear plot of Freundlich isotherm for adsorption of Cu (II) and Zn (II) onto NB (a) and MB (b).

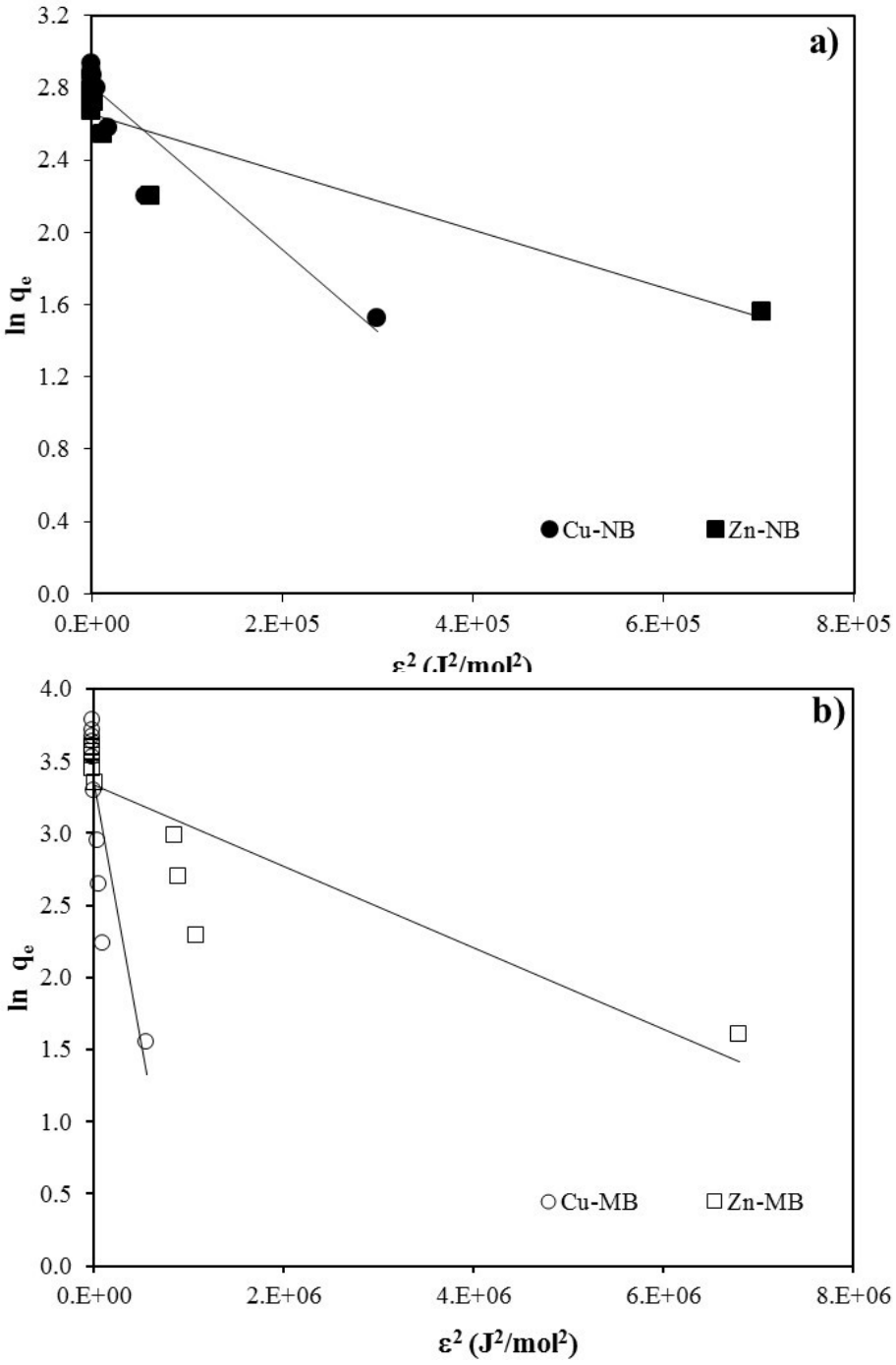

Figure 4.11 Linear plot of Dubinin-Radushkevich isotherm for adsorption of Cu (II) and Zn (II) onto NB (a) and MB (b).

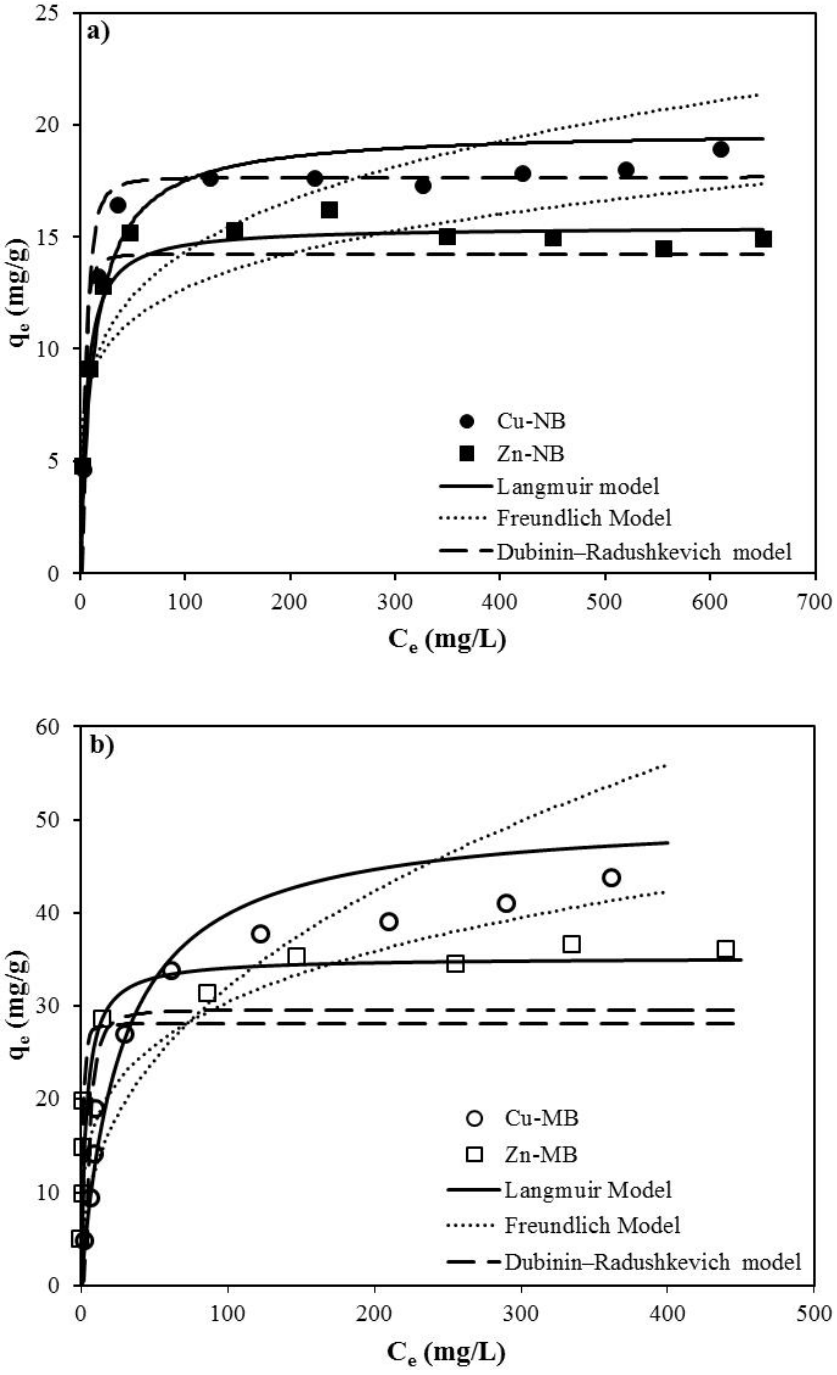

Figure 4.12 non-linear curves of various adsorption isotherms with experimental data, a) NB, and b) MB.

It can be seen from Fig. 4.12 that the experimental adsorption isotherms of this study were L-type (Giles et al., 1974) in all cases, indicating high affinity of sorbent and solute. Amount of the metal ions adsorbed on the adsorbents was increased with

increasing an equilibrium concentration (C_e). In addition, there was insignificant difference between NB and MB in q_e at low initial concentrations (C_i 50.0-150.0 mg/ L), while at higher initial metal ion concentrations the NB became saturated earlier than MB. An initial slope of the breakthrough graph, the q_e was suddenly increased with increasing C_i while there was gradually risen when C_i was more than 150.0 and 200.0 mg/L for NB and MB, respectively. This result confirmed the fact that, a large number of surface coverage sites can be available for the adsorption at the lower concentration. However, the adsorption at higher initial concentration is difficult to occur due to a repulsive forces between the metal molecules adsorbed on the adsorbent and those in the bulk phase (Anna et al., 2015; Srivastava et al., 2008).

The maximum adsorption capacities ($q_{\max}$) estimated from Langmuir model for modified bentonite are compared to relevant prior studies in Table 4.5. The middling performance of MB in this study, however, is associated with simple and attractive pre-processing to prepare/modify the adsorbent. This comparison obviously concluded that the modification of natural bentonite using cationic surfactant clearly improved physical and chemical properties of its capacity as an adsorbent which were effectively used to enhance the adsorption efficiency of heavy metals, by over 2-fold relative to untreated bentonite.

Table 4.5 A comparison of maximum adsorption capacity (q_{max}) for Langmuir model of previous studies in literature.

Metal	Adsorbents	q_{max} (mg/g)	Reference
Zn (II)	Zeolite	3.45	Alvarez-Ayuso et al., 2003
	Coal fly ash prepared zeolite 4A	30.80	Hui et al., 2005
	Na-modified zeolite	49.69	Stefanovic et al., 2007
	NH_4-zeolon P4A clinoptilolite	111.90	Bujnova et al., 2004
	Chitosan/cellulose	19.81	Sun et al., 2009
	Sugar beet pulp	17.78	Chen et al., 2009
	Activated alumina	13.69	Bhattacharya et al.,2006
	Modified bentonite	35.21	This study
Cu (II)	Chitosan/cellulose	26.50	Sun et al., 2009
	Carbon nanotubes CNTs/CA	84.88	Yanhui et al., 2010
	Modified clay	83.3	Vengris et al., 2001
	Spent activated clay	13.20	Weng et al., 2007
	Natural zeolite	8.96	Erdem et al., 2004
	Crosslinked chitosan-coated bentonite beads	9.43	Dalida et al., 2011
	Sulphate-modified bentonite	158.73	Olu-Owolabi et al., 2011
	Modified bentonite	50.76	This study

4.3 Adsorption of heavy metal Ni (II) and humic acid onto natural and modified bentonite

The adsorption efficiency of adsorbent NB and MB was continuously studied with another substances. Ni (II) and humic acid (HA) were also used as the representation of heavy metal and organic compound, respectively. A series of batch experiments were simultaneously conducted to determine the adsorption capacities of NB and MB through the removal of both Ni (II) and HA. Similar to section 4.2, several effects were experimentally investigated to repeatedly clarify adsorbent performance, such as pH solution, initial concentration, and ionic strength.

4.3.1 FTIR spectra studies of Ni (II) and HA adsorbed onto modified bentonite samples

Adsorption mechanisms of Ni (II) and HA onto MB can be understood by considering three main influences to adsorption processes, surface area, pore size and surface functional group of adsorbent. Table 4.1 (section 4.1) shown the characteristics of MB which indicated that they were not only played significant role dealing adsorption (Tohdee et al., 2018). The surface functional group of MB is an important factor to adsorption which can be detected by FTIR. Figure 4.13 shows the results of the FTIR spectra (range 4,000-400 cm^{-1}) of MB before and after adsorption of Ni (II) and HA.

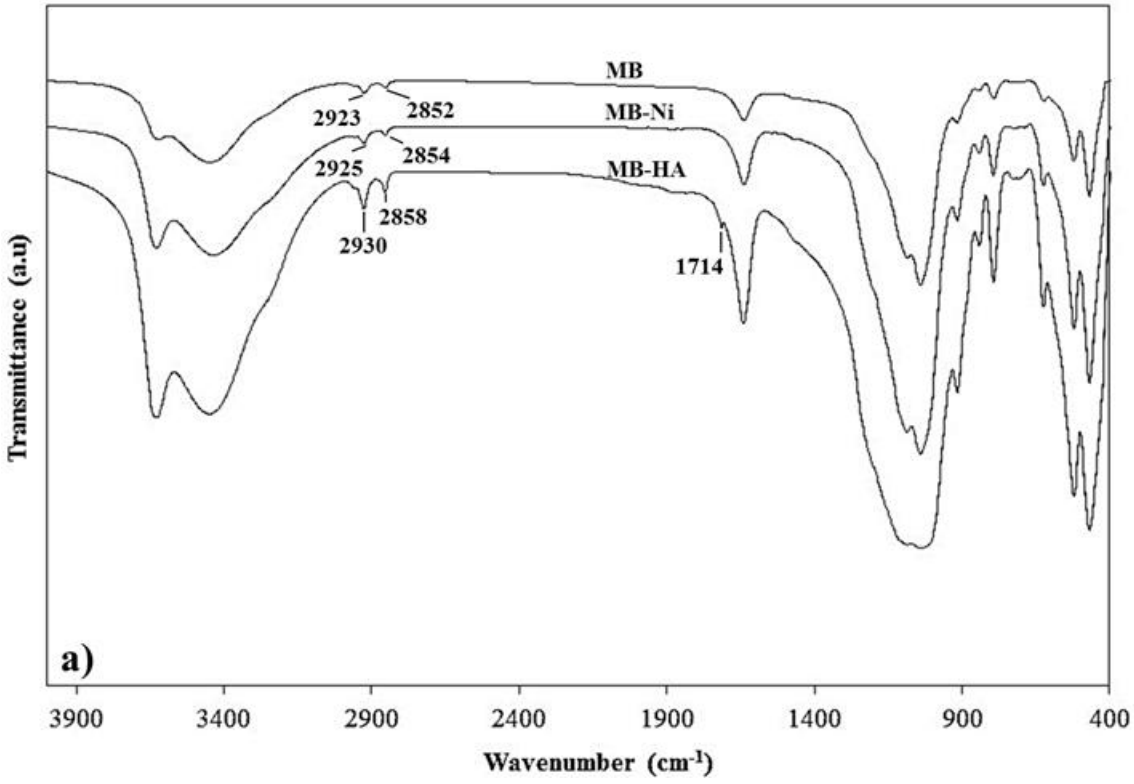

Figure 4.13 FTIR spectra of MB before and after adsorption of Ni (II) and HA (a), extended ranges of wavenumber presented specific functional group of Ni (II) (b) and HA (c) onto MB.

Note: Ni-MB and HA-MB are Ni (II) and HA adsorbed onto the modified bentonite.

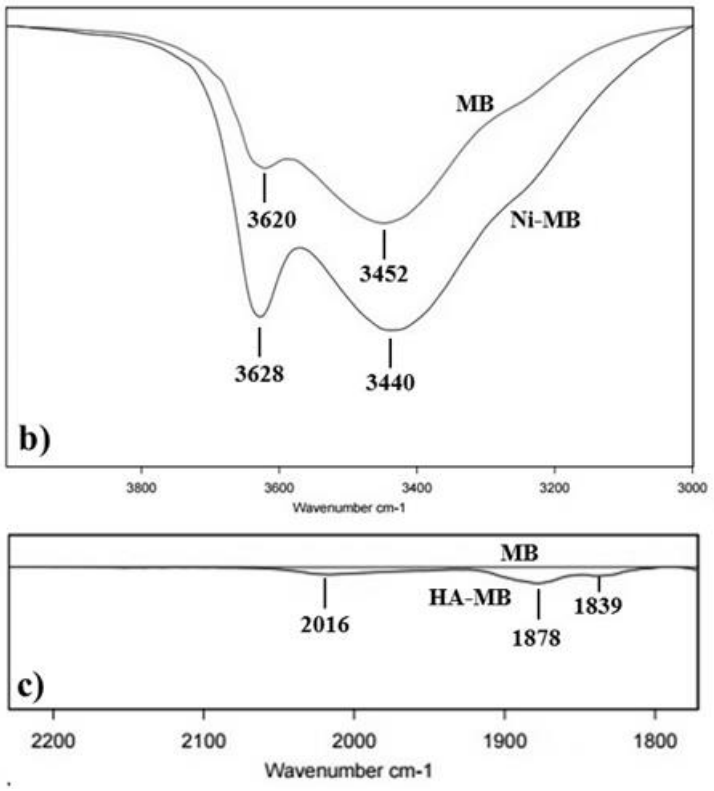

Figure 4.13 (continued) FTIR spectra of MB before and after adsorption of Ni (II) and HA (a), extended ranges of wavenumber presented specific functional group of Ni (II) (b) and HA (c) onto MB. Note: Ni-MB and HA-MB are Ni (II) and HA adsorbed onto the modified bentonite.

Before adsorption, the broad band OH stretching vibration was indicated at 3452 cm-1 for MB, whereas OH bending vibration presents at 1638 cm-1 which indicated the presence of water in bentonite. The Al-Al-OH stretching band shows at 3620 cm-1 while Al-Al-OH and Al-Fe-OH bending vibrations occur at 917 and 852 cm-1, respectively (Worch, 2012). The band 1042-1045 and 521 cm^{-1} were assigned to the Si-O stretching and bending vibrations, respectively (Tohdee et al., 2018).

After adsorption of Ni (II) and HA onto MB, there was a shift of Al-OH stretching vibrations from 3620 to 3628 and 3629 cm-1 for both Ni (II) and HA, respectively. There were shifts of OH stretching vibration from 3452 and 1638 cm-1to 3440 and 1641 cm-1 which indicated that the negative charge of OH group bound with positively charged-metal ions to the active site surface of MB (Farmer, 1974). In case of HA adsorption, the C-H stretching vibrations of methyl and methylene groups shifted from 2923 and 2852 to 2930 and 2858 cm-1 (Dawodua et al., 2014) An appearance of aromatic broad bands was indicated at 2016, 2878 and 1839 cm-1. Other important functional group of HA, the C=O stretching frequency occurred at 1714 cm-1 (Helal et al., 2011). Therefore, this spectrum clearly depicts an involvement of the important functional groups (i.e. the main characteristic of soil humic substances) during the adsorption of HA.

4.3.2 Adsorption kinetic

Both pseudo-first and pseudo-second order of kinetics were employed to fit with experimental data for studying the adsorption reaction kinetics. The results show that pseudo-second order can be well described the adsorption kinetics with a coefficient of determination (R^2) more than 0.990 as listed in (Table 4.6). In contrast, the pseudo-first-order model was fairly responded with the data which R^2 ranged 0.640-0.960. Kinetic model parameters obtained from a linear form of both pseudo-first and pseudo-second order were tabulated in Table 4.6. The results found that amount of adsorbed Ni (II) and HA from the experiment ($q_{e,\exp}$) and model ($q_{e,cal}$) were almost to be a same value for the pseudo-second order, linear plots were very good fit (Fig. 4.14). This is indicated that pseudo-second order can be undertaken to describe the reaction kinetics in this study.

Based on the parameters obtained from the linear plot, Fig. 4.15 depicts an increase of the amount of adsorbed Ni (II) and humic acid during the experiments. It is found that the chemical reaction runs to an equilibrium time at 10 and 40 min for Ni (II) and HA, respectively, and slightly increased or remained constant after that. However, to equilibrate an adsorption breakthrough curve, 80 min of testing time was used to determine adsorption parameters.

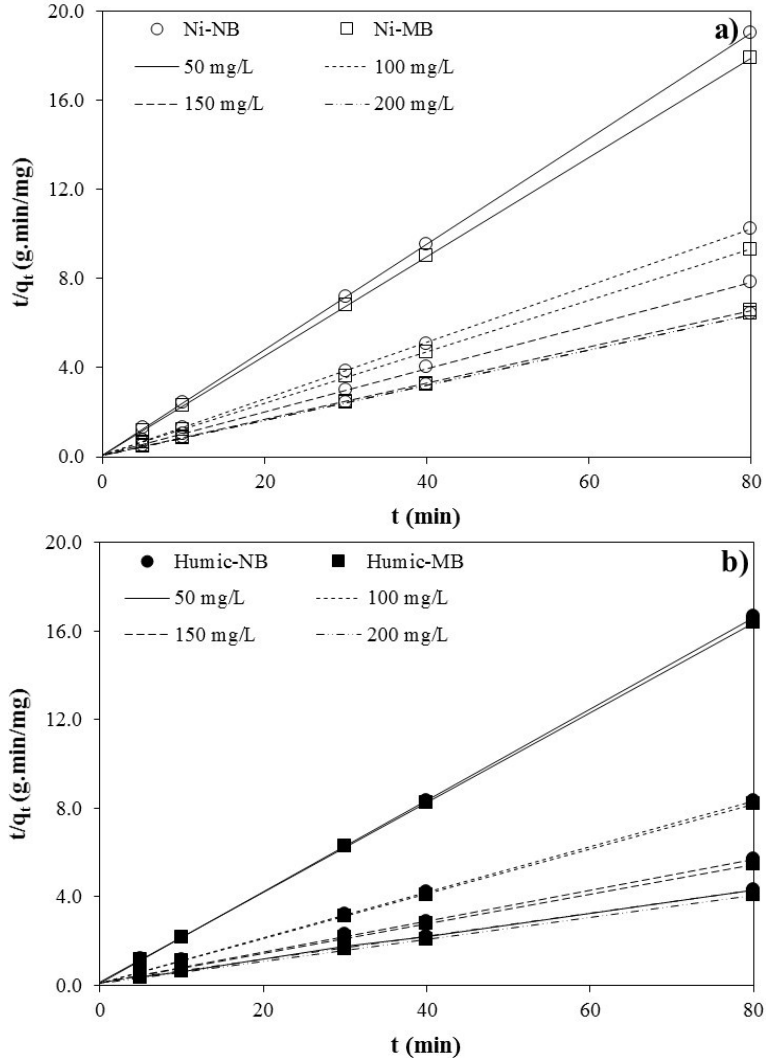

Figure 4.14 Pseudo-second-order model of Ni (II) (a) and humic acid (b) on to NB and MB, linear plot.

Table 4.6 Kinetic model parameters of Ni (II) and humic acid onto NB and MB.

Adsorbents	Metal	C_i (mg/L)	$q_{e,\exp}$ (mg/g)	Pseudo-second-order model			Pseudo-second-order model		
				k_1 (1/min)	$q_{e,cal}$ (mg/g)	R^2	k_2 (g/mg/min)	$q_{e,cal}$ (mg/g)	R^2
NB	Ni (II)	50.0	4.21	0.129	2.13	0.927	0.804	4.23	1.000
		100.0	7.89	0.029	1.82	0.651	0.282	7.89	0.999
		150.0	10.20	0.062	0.72	0.640	0.101	10.32	0.999
		200.0	12.50	0.064	0.72	0.843	0.095	12.66	0.999
	Humic acid	50.0	4.80	0.137	1.03	0.955	0.379	4.84	1.000
		100.0	9.59	0.079	0.44	0.959	0.089	9.74	1.000
		150.0	14.04	0.073	0.25	0.833	0.042	14.31	0.999
		200.0	18.50	0.065	0.14	0.921	0.021	19.05	0.999
MB	Ni (II)	50.0	4.48	0.044	5.84	0.802	0.771	4.49	1.000
		100.0	8.61	0.046	1.32	0.740	0.165	8.67	0.999
		150.0	12.25	0.045	1.11	0.841	0.156	12.32	0.999
		200.0	15.31	0.117	0.31	0.754	0.071	15.50	0.999
	Humic acid	50.0	4.89	0.067	1.51	0.965	0.277	4.93	1.000
		100.0	9.80	0.043	1.03	0.801	0.135	9.87	1.000
		150.0	14.59	0.083	0.24	0.917	0.051	14.84	1.000
		200.0	19.58	0.086	0.12	0.926	0.023	20.12	0.999

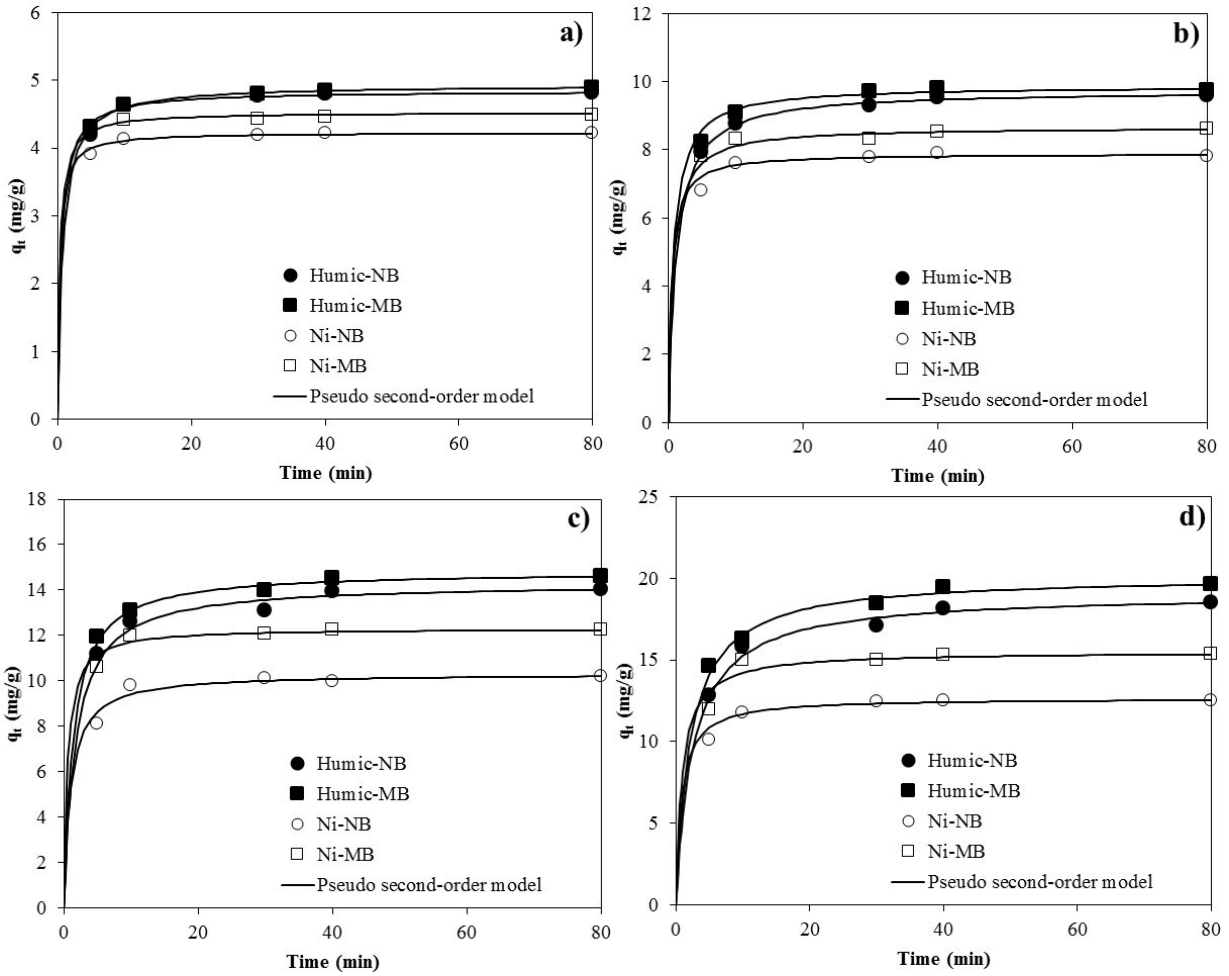

Figure 4.15 Pseudo-second order model of Ni (II) and HA onto NB and MB, nonlinear plot at initial metal concentration 50.0 (a) 100.0 (b) 150.0 (c) and 200.0 (d) mg/L, NB and MB dosage 0.5 g.

4.3.3 Factors affecting adsorption capacity

(a) Effect of initial solution pH

One of the most influent factors affecting adsorption processes is solution pH. Figure 4.16 demonstrated the pH-dependent adsorption ranged 3-11. The adsorption of Ni (II) from aqueous solution onto both NB and MB was strongly depended on solution pH. Removal of Ni (II) increased with increasing pH especially the value below 7. It is remarkable that the adsorption were slight increases in the pH range 5-6, the removal was up to 63.9% and 80% for NB and MB, respectively. Furthermore, pH above 7, a chemical precipitation became the main removal process instead of the adsorption due to forming as $Ni(OH)_2$ (Xu et al., 2008; Anna et al., 1015; Chang et al., 2008).

On the other hand, there were decreases of adsorption with increasing solution pH which a maximal adsorption of HA achieved at pH 3 associated to the removal down from 91.25% and 97.92% to 14.90% and 25.00% for NB and MB, respectively. The results in this study were similar trends with previous researchers reported by numerous studies (Anirudhan and Ramachandran, 2007; Salman et al., 2007).

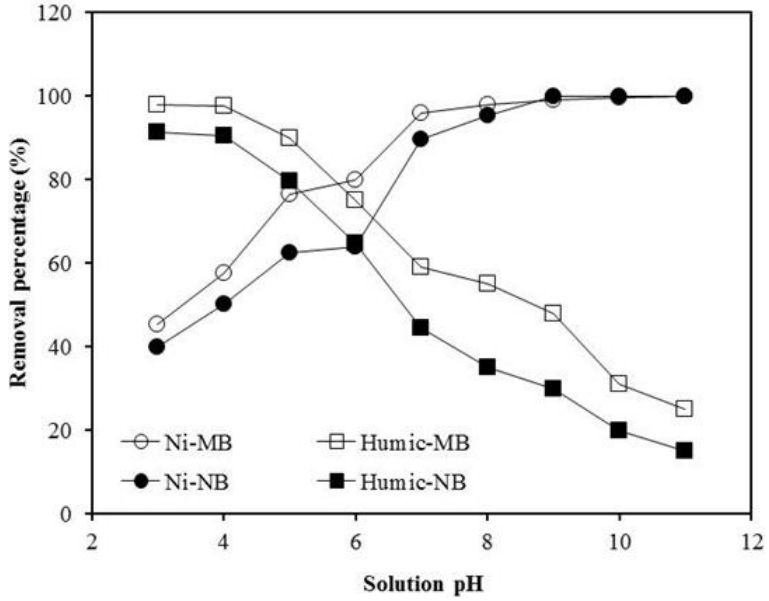

Figure 4.16 Effect of solution pH on adsorption of Ni (II) and HA; initial concentration 200.0 mg/L, dosage 10 g/L.

(b) Effect of contact time

Adsorption efficiency of adsorbents can be appropriately obtained with optimal contact time which was also recognized as one of the most important factors to adsorption processes. Figure 4.17 depicts the removal of both Ni (II) and HA at various contact times for both Ni (II) and HA onto different adsorbents. The maximal removal of the metal Ni (II) and the organic HA over the range of initial concentrations of 50.0-200.0 mg/L onto NB was 62.52% and 92.48%, respectively. In case of MB, there was an increase in the maximal removal reaching up to 76.56% and 97.92% of Ni (II) and HA, respectively. Furthermore, a minimal range of the removal was grown up to 9%. This evidence can be distinctively indicated that a capability of MB is efficient in this study. The equilibrium time of both Ni (II) and HA was an obvious difference as shown in Fig. 4.17. In general, the removal rate of both Ni (II) and HA was similar trends which increased approximately 10 min. Thereafter, only slightly or remained constant was occurred for NB. On the other hand, MB case, the removal of HA was gradually increased to 40 min. and remained constant after that which there was no further adsorption.

A dissimilar result of Ni (II) and HA adsorption is due to different reasons. The adsorption of metal Ni (II) is relatively fast at the initial stage because sufficient active sites are available for binding metal ions. Then, the adsorption is slower and reached an equilibrium which all metals have been covered at the binding sites owing to repulsion (Igberase and Osifo, 2015; Shanmugapriya et al., 2013). In case of HA, it is known that HA has large-size molecules so that the difficulty of the molecules to enter between bentonite layers has been made (El-Eswed and Khalili, 2006).

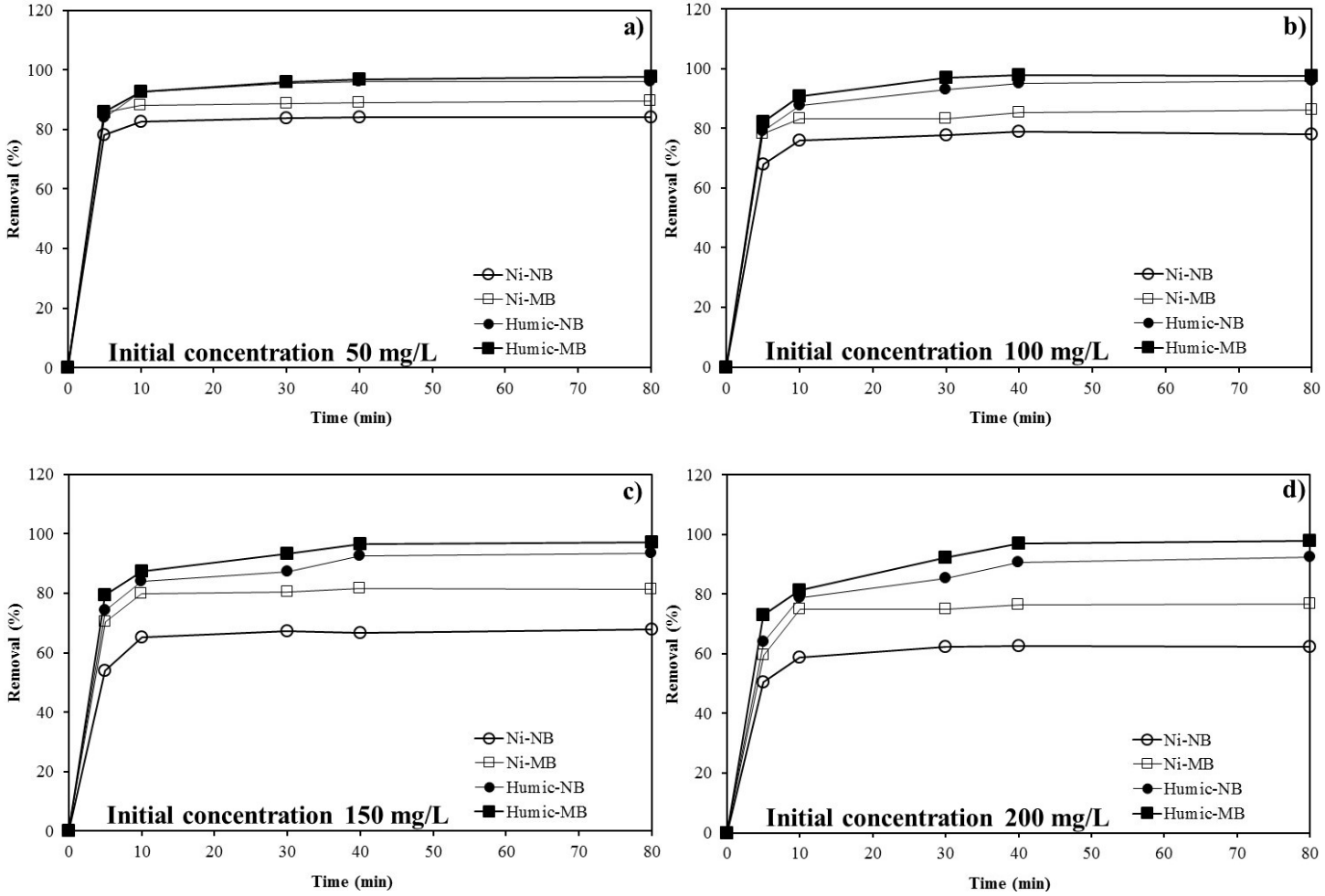

Figure 4.17 Effect of contact time; initial concentration 50.0-200.0 mg/L, dosage 10 g/L and, pH 5, 3 for Ni (II) and humic acid, respectively.

(c) Effects of metal and humic acid concentration

The effect of initial concentration of metal Ni (II) and HA illustrated in Fig. 4.18. A wide range of the concentration of 50.0-800.0 mg/L was examined to obtain adsorption efficiency of the adsorbents. The overall response shapes of removal curve present a similar line across all cases as decreasing with an increment of initial concentration. It is clear that MB was a better adsorbent than NB. The maximal enhancement by adsorption on a comparative efficiency between NB and MB was 25.0 and 34.1% for Ni (II) and HA, respectively. An optimal concentration can be unveiled when the adsorption efficiency rose up to a certain level in which adsorbent surfaces were saturation, no active sites can be available. The optimal concentration of HA was 100.0 and 200.0 mg/L on NB and MB, respectively. However, the removal curve shown in Fig 4.18 was disappearance of such optimal concentration over the range of initial concentration used in this study. It is possible that the Ni (II) adsorption is recognized as low affinity to several adsorbents reported by previous works (De-Pablo et al., 2011; Gupta and Bhattacharyya, 2008; Alvarez-Ayuso and Garcia-Sanchez, 2003).

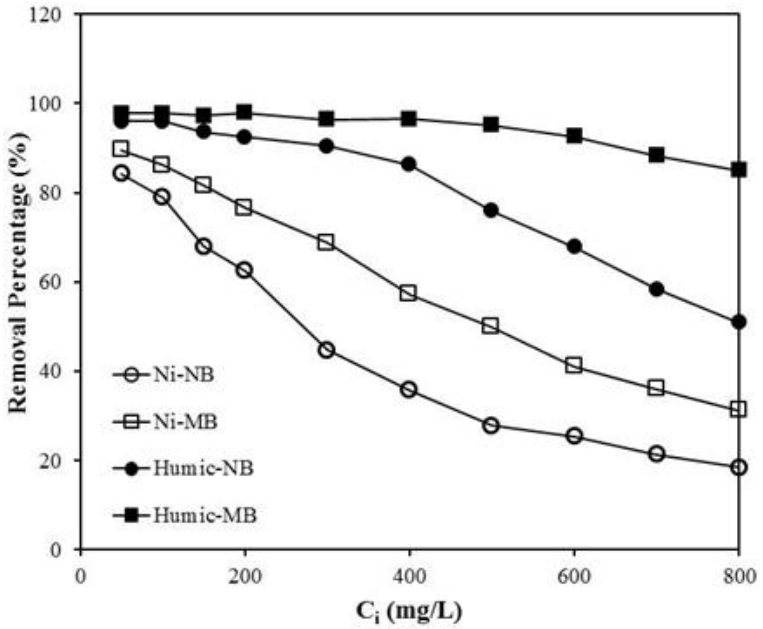

Figure 4.18 Effect of initial concentration on the adsorption efficiency.

(d) Effect of ionic strength

Beside solution pH and contact time, ionic strength is also the important factor that can affect adsorption uptake. The study of ionic strength was observed by conducting batch experiments at various concentration of NaCl and $NaNO_3$ ranged 0.01-0.1 M for Ni (II) and HA, respectively. McBride (1997) described that ions from inner-sphere and outer-sphere complexes show a different influence of ionic strength to adsorption process. Reduction of adsorption presents to the outer-sphere complexes under increasing ionic strength. In contrast, increasing ionic strength affects to increment of adsorption for the inner-sphere complexes.

Adsorption of Ni (II) decreased with increasing the concentration of $NaNO_3$ while the adsorption of HA increased with the presence of the NaCl concentration (Fig. 4.19), so that Ni (II) and HA form the outer and inner-sphere complexes, respectively. Maximal reduction of Ni (II) adsorption, due to ionic strength increase from 0 to 0.1 M, was 34.06% and 29.64% over the range 50.0-800.0 mg/L of initial concentration for NB and MB, respectively. The main hypothesis of this result is ion exchange with the hydrogen and sodium ions on the exchange sites (Pinskii et al., 2014; Echeverría et al., 2003). The ion exchange of Ni^{2+} with both –H and –Na is the main process of Ni (II) adsorption onto bentonite. Elementary reactions below depict the ion exchange which consists of two steps as shown in Eq. (9-10).

$$2 \equiv S - OH + Ni^{2+} \rightarrow \left(\equiv S - O\right)_2 Ni + 2H^+ \qquad (4.1)$$

$$2 \equiv S - ONa + Ni^{2+} \rightarrow \left(\equiv S - O\right)_2 Ni + 2Na^+ \qquad (4.2)$$

In case of HA, there were 18.64% and 4.84% of the maximal increase due to increasing ionic strength from 0.0 to 0.1 M of NaCl for NB and MB, respectively. Major reasons for this result may be explained by several mechanisms. Molecular volume of HA is miniaturized by a minimization of the repulsion which facilitates the adsorption. Also, compression caused by increasing ionic strength reduces the diffuse double layer of clay. Such compression encourages HA molecules and clay particle to approach each other. Moreover, the solubility of HA at high ionic strength is low,

which could support the mass transfer of HA to the solid phase of clay (Peng et al., 2005; Seki and Yurdakoç, 2006; Paul Chen and Wu, 2004).

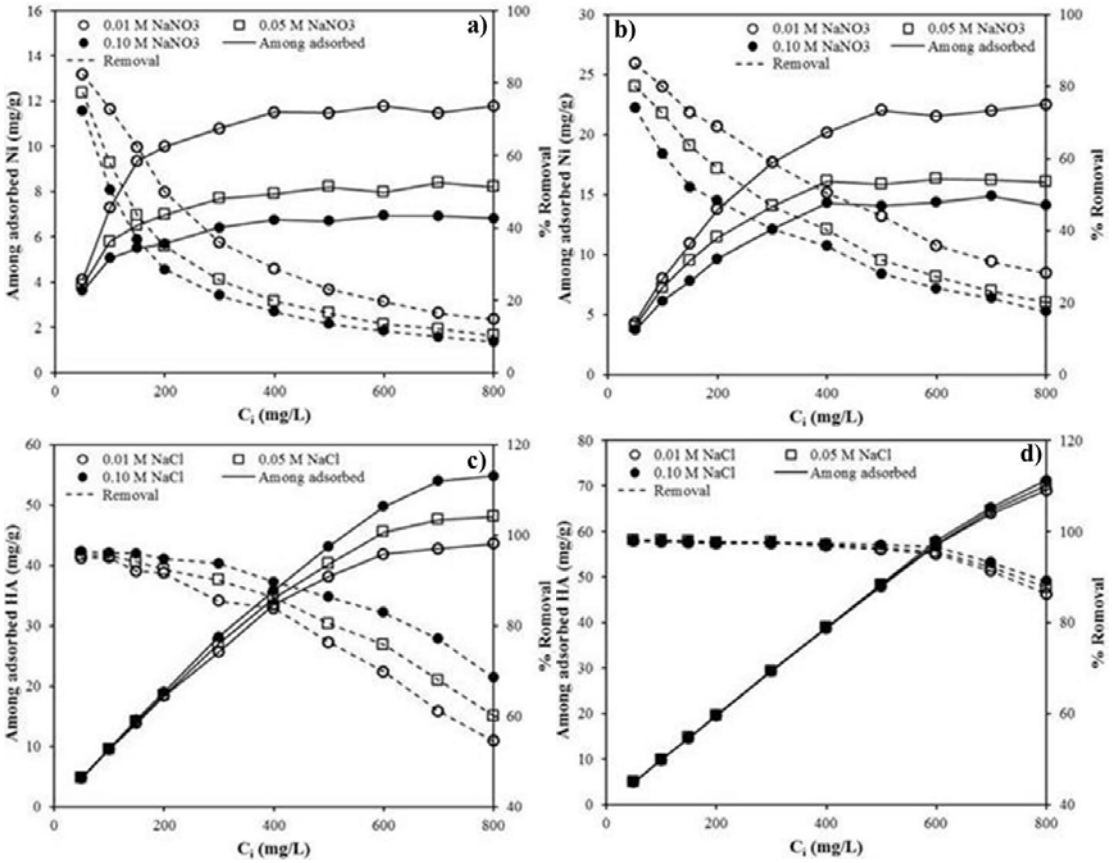

Figure 4.19 Effect of ionic strength on adsorption of Ni (II) and HA onto different adsorbents; a) Ni-NB, b) Ni-MB, c) HA-NB, and d) HA-MB.

4.3.4 Adsorption isotherms

The adsorption capacity of Ni (II) and HA onto NB and MB can be determined by accessing equilibrium isotherm models. A number of isotherm models including two-parameter models (e.g. Langmuir, Freundlich, and Temkin models) and three-parameter models (e.g. Redlich-Peterson, Sips, and Toth models) were employed. The experimental results were applied to those models which mean absolute percentage error (MAPE, Eq. (4.3)) (Bowerman et al., 2004) was used to quantitatively compare a reliability of the isotherm models.

$$MAPE(\%) = \frac{\sum_{i=1}^{N} \left| \left(q_{e,\exp} - q_{e,pre} \right) / q_{e,\exp} \right|}{N} \times 100 \qquad (4.3)$$

where $q_{e,\exp}$ and $q_{e,pre}$ are the experimental and predicted among adsorbed (mg/g), N is a number of data.

(a) Two-parameter models

The two-parameter isotherm models were initially considered which the results indicated that the Langmuir isotherm was the best fit (Fig. 4.20-4.22) with high coefficient of determination (R^2) ranged 0.989-0.998 and low MAPE ranged 2.35-9.43% for all cases (Table 4.7). This result implied that the adsorption of both Ni (II) and HA occurred as homogenous site and monolayer formation (Blanchard and Maunaye, 1984; Langmuir, 1918) and can be characterized as chemical adsorption. Figure 4.23 illustrates a non-linear curve of adsorption which model parameters obtained from a linear plot. Although the two-parameter model provided high R^2, the model cannot exactly be fitted with all experimental data.

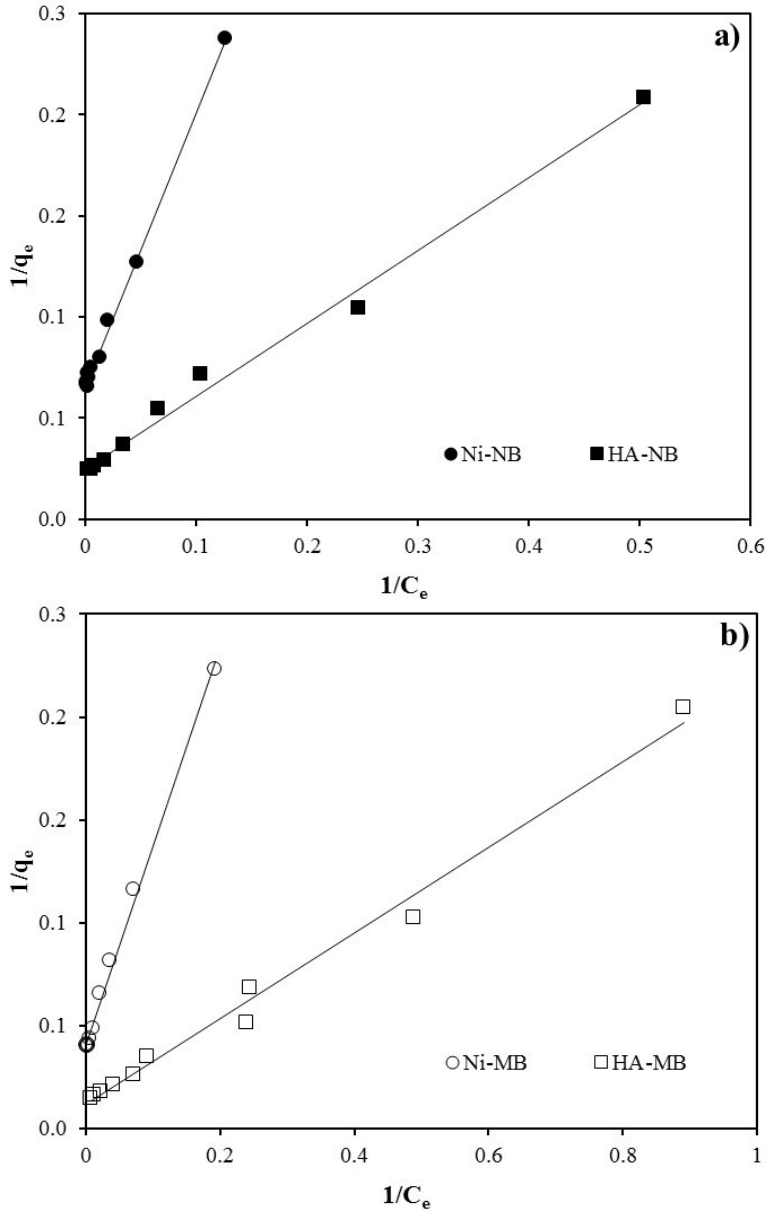

Figure 4.20 Linear plot of Langmuir isotherm for adsorption of Ni (II) and humic acid onto NB (a) and MB (b).

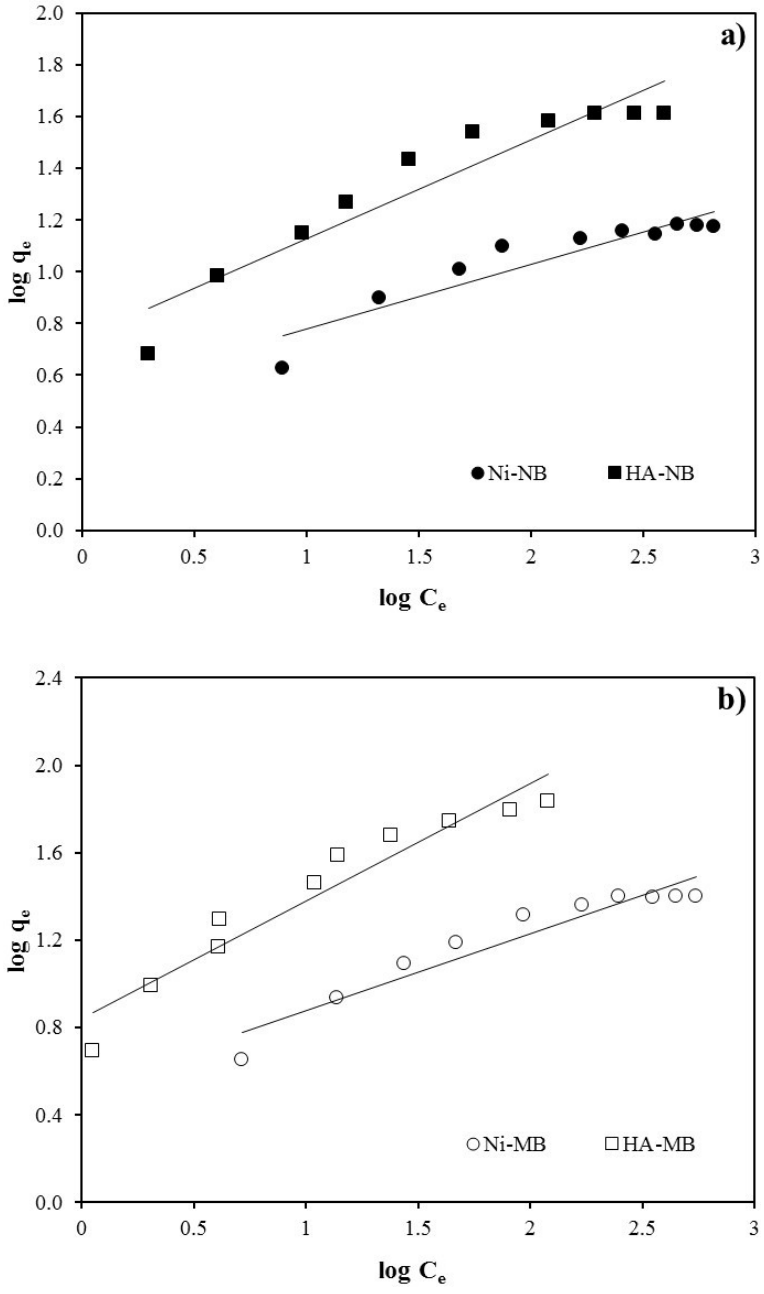

Figure 4.21 Linear plot of Freundlich isotherm for adsorption of Ni (II) and humic acid onto NB (a) and MB (b).

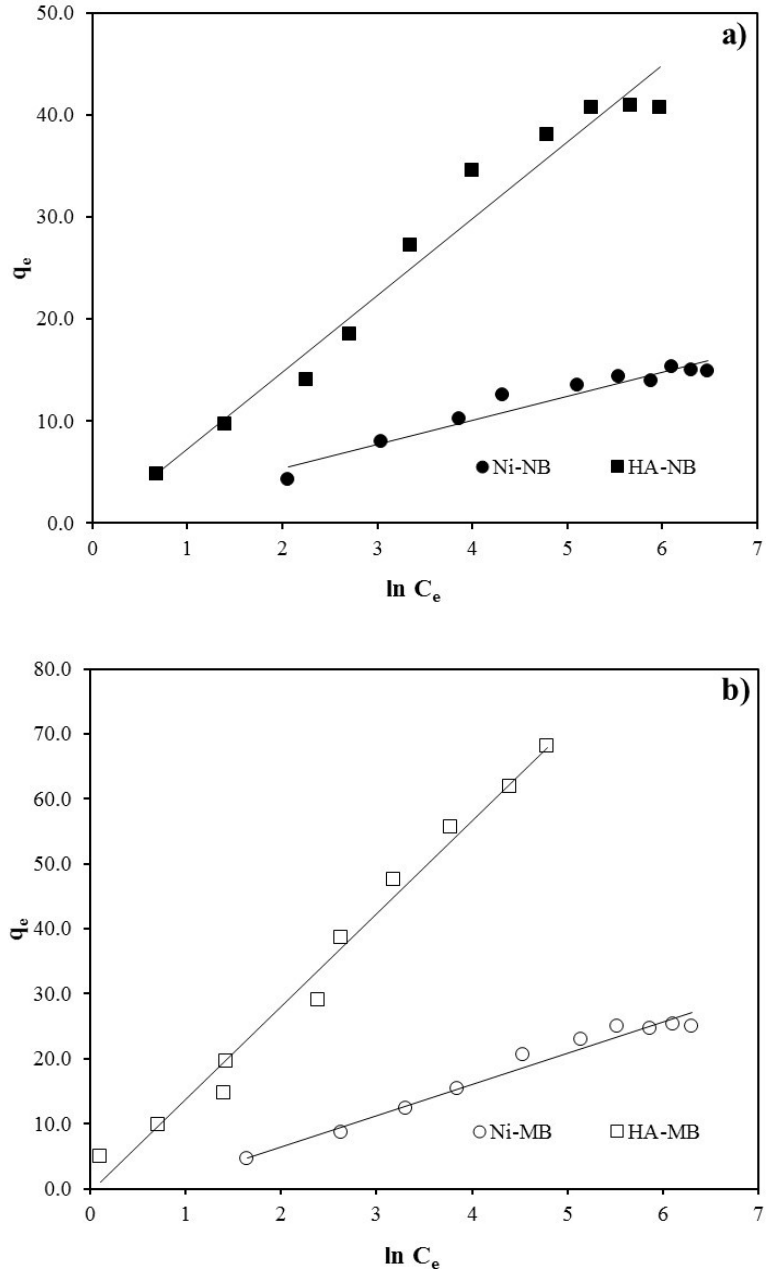

Figure 4.22 Linear plot of Temkin isotherm for adsorption of Ni (II) and humic acid onto NB (a) and MB (b).

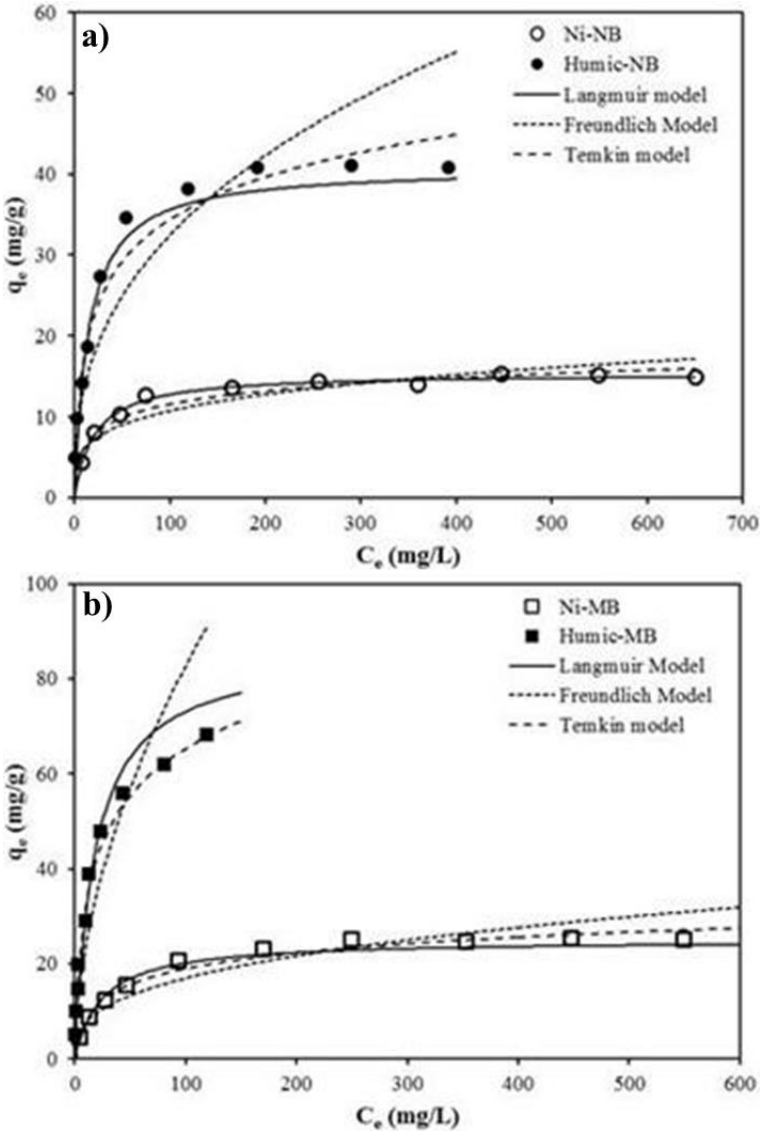

Figure 4.23 Non-linear curve of Ni (II) and HA adsorption onto (a) NB and (b) MB; two-parameter isotherms.

(b) Three-parameter models

The three-parameter models were then accessed with the same experimental data. Figure 4.24 shows a non-linear curve of both Ni (II) and HA adsorption. All three-parameter models give a good fit which MAPE ranged 2.44-6.91% (see Table 4.8) less than those obtained from two parameter-models isotherms. This comparison implied that a use of three-parameter isotherm may be a better consideration in this study. It is important to note that model parameters; g, m_S, and m_T from Redlich-

Peterson, Sips, and Toth model approached to the unity. The parameter g and m_S from Redlich-Peterson and Sips model are close to unity which is transformed to the Langmuir model, a special case of Redlich-Peterson model. Also, the parameter m_T from the Toth isotherm exponent indicated the adsorption process occurs on a homogenous surface. The implication of these values encouraged that the Langmuir model can describe the adsorption of Ni (II) and HA in this study.

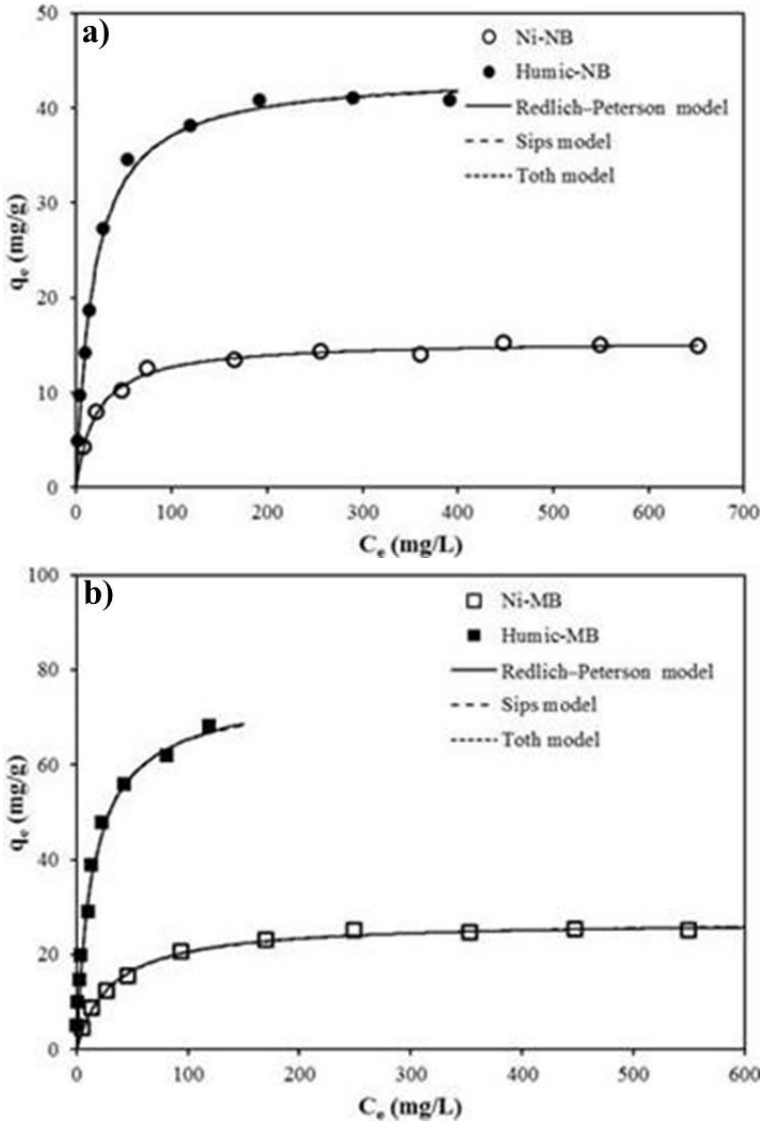

Figure 4.24 Non-linear curve of Ni (II) and HA adsorption onto (a) NB and (b) MB; three-parameter isotherms.

Table 4.7 Adsorption isotherm Two-parameters of Ni (II) and Humic acid onto NB and MB.

Adsorbate-Adsorbent	Langmuir model				Freundlich model				Temkin model			
	K (L/mg)	q_{max} (mg/g)	R^2	APE (%)	K_f (mg/g)	n	R^2	APE (%)	B_T (J/mol)	A_T (L/g)	R^2	APE (%)
Ni-NB	0.048	15.36	0.998	2.35	3.351	3.970	0.856	12.44	2.35	1.343	0.937	2.13
Ni-MB	0.041	25.06	0.995	5.41	3.360	0.915	0.915	14.41	4.79	0.522	0.972	5.67
Humic acid-NB	0.068	40.82	0.993	6.22	5.578	2.616	0.898	18.80	7.54	0.956	0.966	7.85
Humic acid-MB	0.056	86.21	0.989	9.43	6.963	0.925	0.925	19.74	14.32	0.955	0.984	14.72

Table 4.8 Adsorption isotherm Three-parameters of Ni (II) and Humic acid onto NB and MB.

Adsorbate-Adsorbent	Redlich-Peterson model				Sips model				Toth model			
	B (L/mg)^g	g	A (L/g)	APE (%)	q_{mS} (mg/g)	K_S (L/mg)^m	m_S	APE (%)	q_{mT} (mg/g)	K_T	m_T	APE (%)
Ni-NB	0.052	0.991	0.760	2.44	15.46	0.051	0.976	2.46	15.48	0.056	0.962	2.45
Ni-MB	0.032	1.000	0.857	3.63	27.37	0.036	0.959	3.14	27.22	0.036	0.971	3.47
Humic acid-NB	0.056	1.000	2.437	5.23	43.45	0.053	1.022	5.58	43.69	0.056	1.000	5.23
Humic acid-MB	0.079	0.979	5.348	6.83	75.39	0.071	0.980	6.91	75.90	0.080	0.955	6.85

4.3.5 Maximal adsorption capacity

According to the comparison of among models, three-parameter models were more reliability with experimental data, also supporting the Langmuir isotherm. All three-parameter models provide that maximal adsorption capacities ($q_{\max}$) of NB to adsorb Ni (II) and HA were 15.46-15.48 and 43.45-43.69 mg/g, respectively. NB was modified with the cationic surfactant to improve the adsorption capacities which improved 1.70 fold with up to 27.22-27.37 and 75.39-75.90 mg/g for Ni (II) and HA. This result was attractive because MB used in this study was prepared by the cationic surfactant. A major reason of these increments may be the fact that the micelles of BCDMACl intercalate to the bentonite surfaces, changing the functional group of NB cause to increase both anionic adsorptive capacity and the cation affinity of the clay (Adebowale et al., 2006; Li and Gallus, 2005), which improve the adsorption capacity of bentonite. In general, the cationic surfactant is composed of a hydrophilic and positive charge of head group and a hydrophobic tail (Chao and Chen 2012; Guan et al., 1997; Zhang et al., 1993) which has been proven by previous studies (Li et al., 2011; Zhan et al., 2010) as a good adsorption efficiency of HA in aqueous solution.

4.4 Competitive adsorption of heavy metal Cu (II) Zn (II) and Ni (II) under ternary system

Competitive adsorption of heavy metals, adsorption capacity ratio between multi-component system, q_i^{mix}, and single-component systems, q_i^o expressed as follows (Mohan and Singh, 2002):

$$\frac{q_i^{mix}}{q_i^o} \approx \frac{q_{im}^{mix}}{q_{im}^o} \tag{4.4}$$

where q_{im}^o, q_{im}^{mix} is maximum amount adsorbed in single- or multi-component system, respectively (mg/g). If $q_i^{mix}/q_i^o > 1$, ion i enhances the adsorption of other ions. If $q_i^{mix}/q_i^o = 1$, ion i has no effects on other ions. If $q_i^{mix}/q_i^o < 1$, ion i competes for adsorption sites of bentonite with other ions and its adsorption is suppressed by the presence of other ions. The competitive equilibrium coefficient expresses the competition ability of ions. The competitive equilibrium coefficient for component i,

a_{ie}, is the equilibrium ratio of adsorbed i to all adsorbed components. The competitive equilibrium coefficient for component i among n components may be written as

$$a_{ie} = \frac{q_{ie}/C_{Oi}}{\sum_{j=1}^{n} q_{je}/C_{Oj}} \approx \frac{q_{im}^{mix}/C_{Oi}}{\sum_{j=1}^{n} q_{jm}^{mix}/C_{Oj}} \tag{4.5}$$

where q_{ie} and C_{Oi} are the amount of adsorbed component i at equilibrium (mg/g) and initial concentration of component i, respectively, q_{je} and C_{Oj} are the amounts of adsorbed component j at equilibrium (mg/g) and initial concentration of component j, respectively, and q_{jm}^{mix} is the maximum amount of adsorbed component j (mg/g). The equilibrium competitive and non-competitive equilibrium adsorption of an ion may be compared using the rate of equilibrium adsorption reduction or the non-competitive equilibrium coefficient introduced in previous work (Liu et al., 2000). In addition, the rate of equilibrium adsorption reduction (ΔY) is the ratio of the difference between non-competitive equilibrium adsorption and competitive equilibrium adsorption to non-competitive adsorption observed at equilibrium. The non-competitive equilibrium coefficient, a_{io}, is the ratio of non-competitive equilibrium adsorption of one component to non-competitive adsorption of all components, at equilibrium:

$$\Delta Y = \frac{q_{im}^{o} - q_{im}^{mix}}{q_{im}^{o}} x100\% \tag{4.6}$$

$$a_{io} = \frac{q_{im}^{o}/C_{Oi}}{\sum_{j=1}^{n} q_{jm}^{o}/C_{Oj}} \tag{4.7}$$

The constants for Cu^{2+} Zn^{2+} and Ni^{2+} in single-component and ternary-component systems based on parameters derived from Langmuir model (Figs. 4.25-4.28) were shown in Table 4.9. The results indicate that total adsorbed amount of non-competitive adsorption is higher than those of ternary component competitive adsorption. It can be explained that adsorption sites of both NB and MB for Cu (II) Zn (II) and Ni (II) are limited. Metals in this study occupied the adsorption sites only

once during non-competitive adsorption; but they co-occupied the same sites once during competitive adsorption.

It can be seen in Table 4.9, the values of q_i^{mix}/q_i^o < 1 shown that there was the competitive effect of Cu (II) Zn (II) and Ni (II) in ternary component system with competitive adoration ratio Cu (II)>Zn (II)>Ni (II). These results are in agreement with several works on clay. Compared to Cu (II) adsorption in single-component system, its rate of adsorption equilibrium reduction (ΔY) was reduced by 41.02% and 35.41% in Cu-Zn-Ni system for NB and MB, respectively. Similarly, ΔY of Zn (II) and Ni (II) in single-component system (ΔY) was decreased in range 43.41-47.41% and 37.17-39.72% in ternary system for NB and MB, respectively. These results show that Cu (II) may suppress both Zn (II) and Ni (II) adsorption significantly. In addition, adsorption capacity ratio of Cu (II) Zn (II) and Ni (II) was 0.526-0.590 and 0.603-0.646 for NB and MB, respectively. This means that Cu (II) has more ability to competitive adsorption.

Table 4.9 Adsorption isotherm of single and ternary system of Cu (II) Zn (II) and Ni (II).

Adsorbents	Metals	Systems	Langmuir model				Competitive constants			
			K (L/mg)	q_{im}^{o}, q_{im}^{mix} (mg/g)	R^2	APE (%)	q_{im}^{mix}/q_{im}^{o} (mg/g)	a_{ie}	a_{io}	Y (%)
NB	Cu (II)	Cu	0.077	19.76	0.987	6.790	1.000	1.000	1.000	0.00
		Cu(Cu-Zn-Ni)	0.058	11.66	0.994	3.663	0.590	0.409	0.391	41.02
	Zn (II)	Zn	0.177	15.46	0.993	6.220	1.000	1.000	1.000	0.00
		Zn(Cu-Zn-Ni)	0.101	8.75	0.958	5.000	0.566	0.307	0.306	43.41
	Ni (II)	Ni	0.048	15.36	0.998	2.350	1.000	1.000	1.000	0.00
		Ni(Cu-Zn-Ni)	0.093	8.08	0.986	4.601	0.526	0.284	0.304	47.41
MB	Cu (II)	Cu	0.037	50.76	0.984	5.410	1.000	1.000	1.000	0.00
		Cu(Cu-Zn-Ni)	0.051	32.79	0.994	8.081	0.646	0.468	0.457	35.41
	Zn (II)	Zn	0.303	35.21	0.962	9.420	1.000	1.000	1.000	0.00
		Zn(Cu-Zn-Ni)	0.127	22.12	0.990	3.248	0.628	0.316	0.317	37.17
	Ni (II)	Ni	0.041	25.06	0.995	5.410	1.000	1.000	1.000	0.00
		Ni(Cu-Zn-Ni)	0.052	15.11	0.998	4.124	0.603	0.216	0.226	39.72

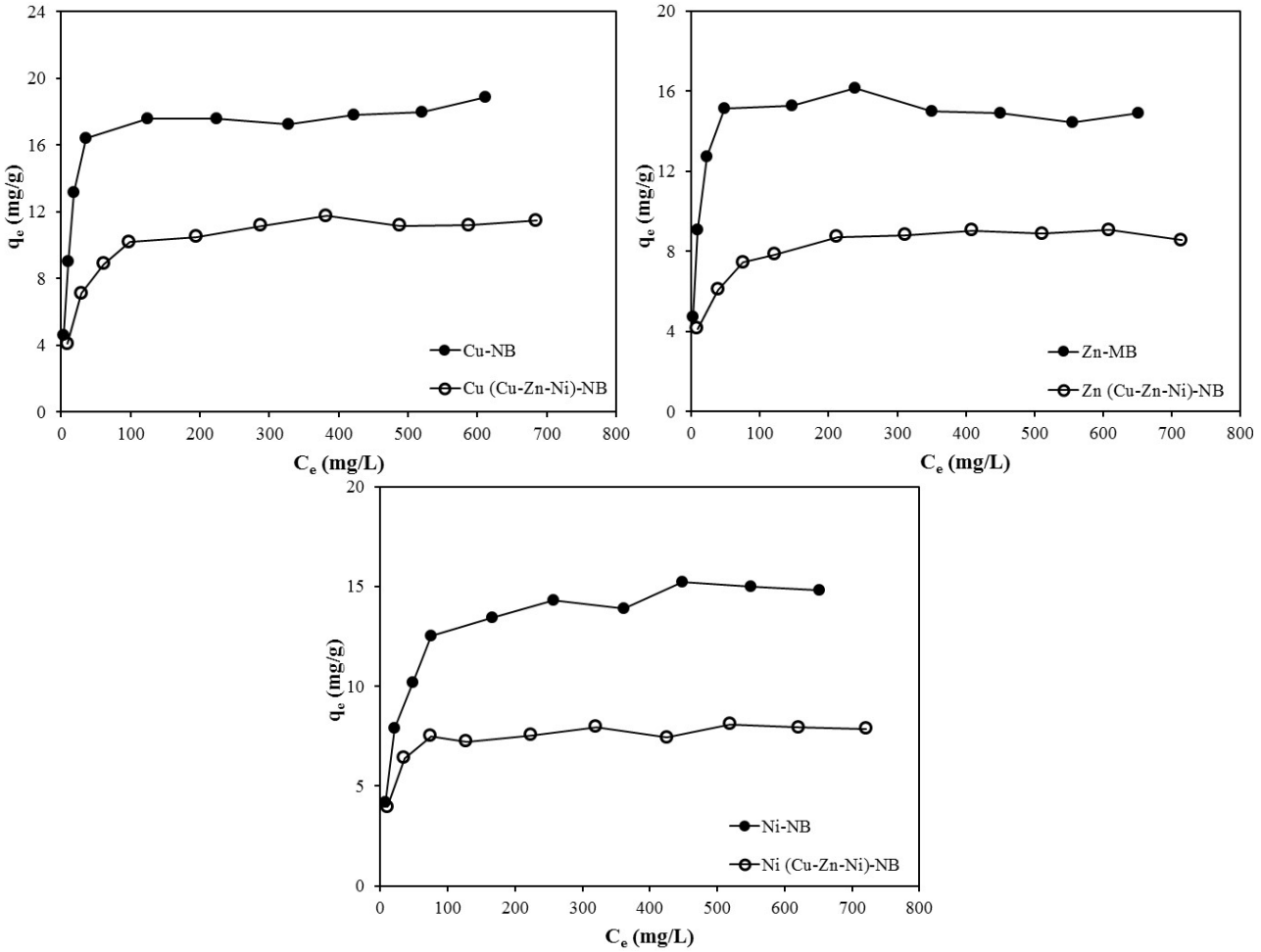

Figure 4.25 Adsorption and competitive adsorption isotherms for Cu (II), Zn (II) and Ni (II) on NB; clay dosage 0.5 g, pH 5 and contact time 80 min, temperature of solution: 298 K.

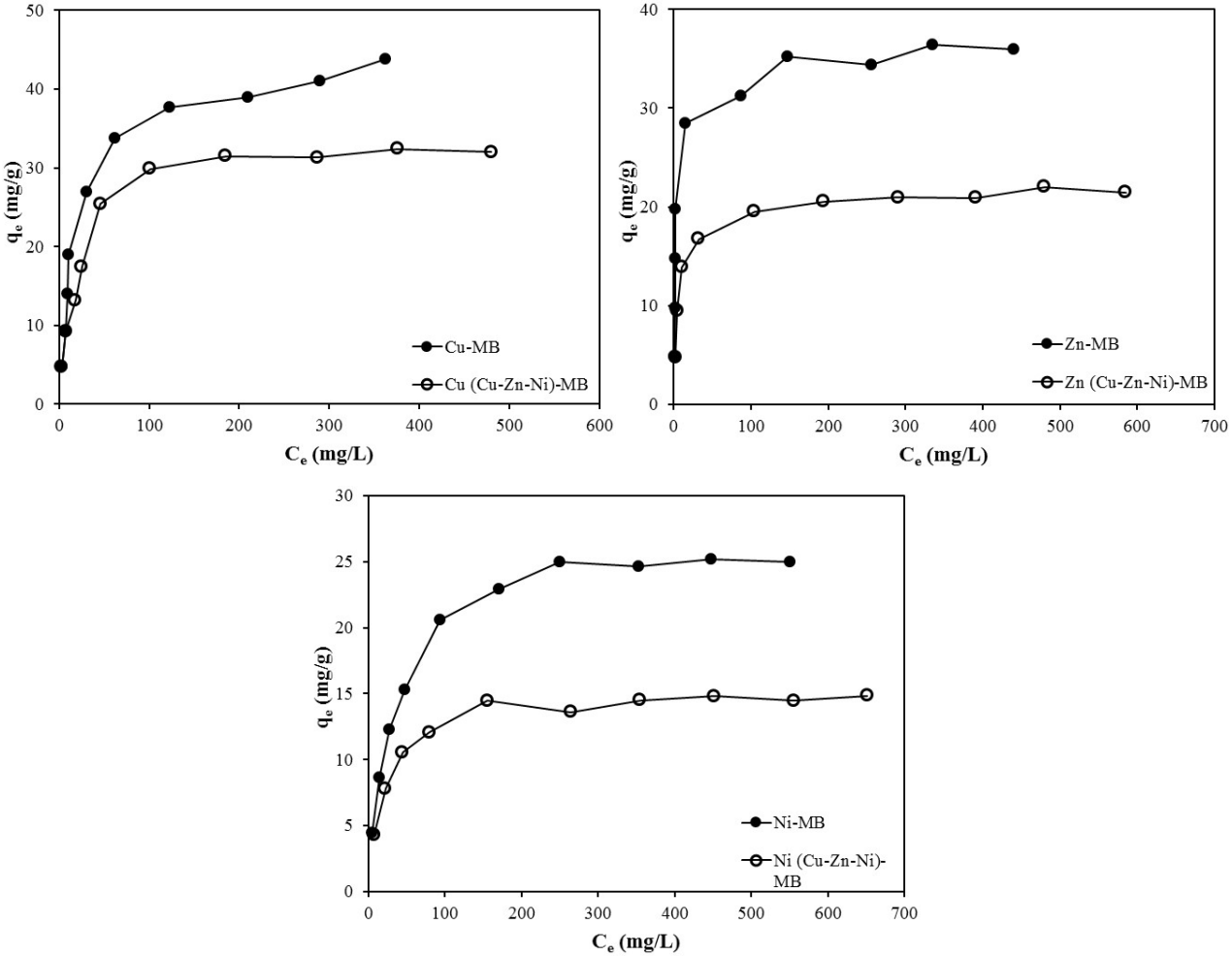

Figure 4.26 Adsorption and competitive adsorption isotherms for Cu (II), Zn (II) and Ni (II) onto MB; clay dosage 0.5 g, pH 5 and contact time 80 min, temperature of solution: 298 K.

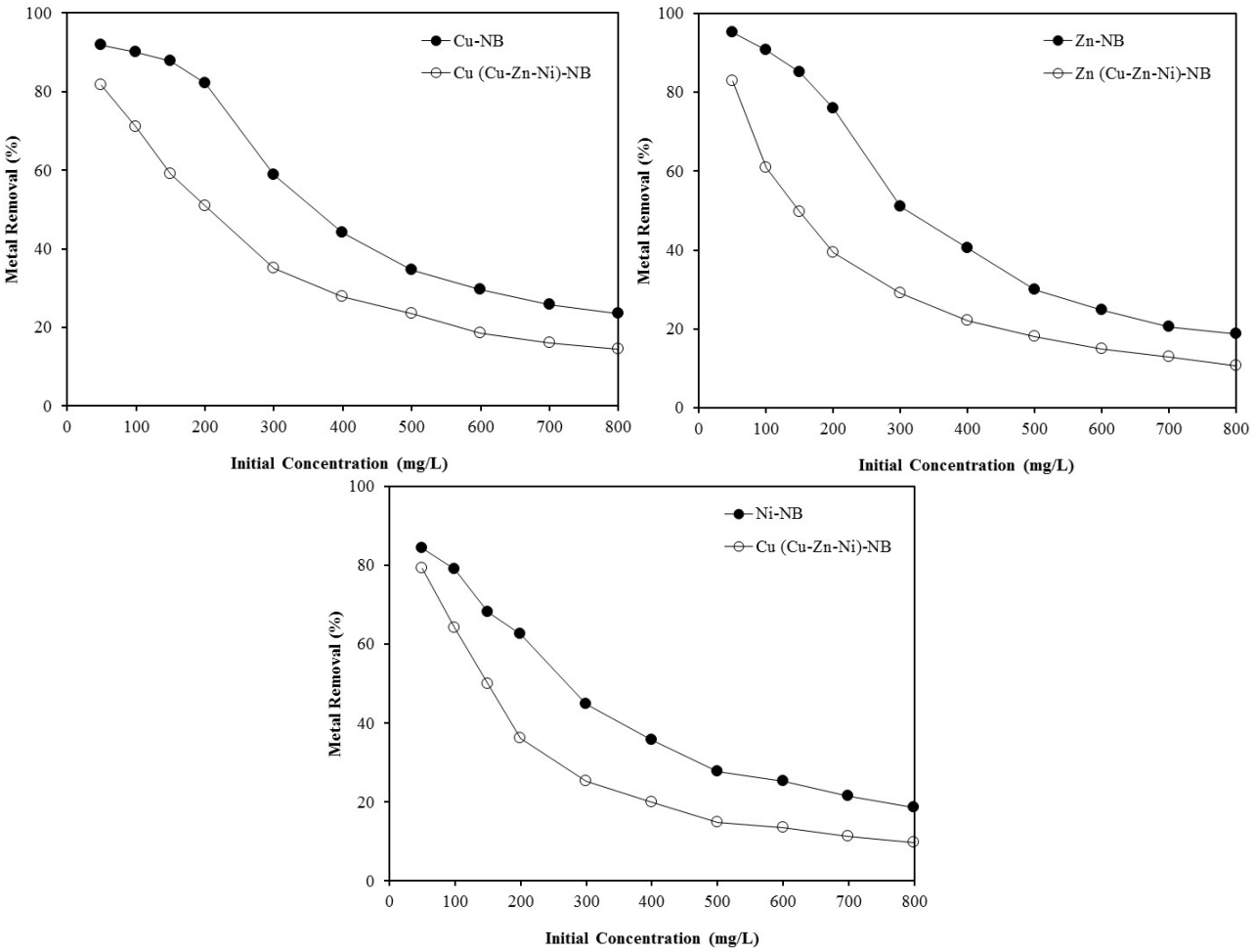

Figure 4.27 Removal of Cu (II), Zn (II) and Ni (II) onto NB under ternary system compared to single system; clay dosage 0.5 g, pH 5 and contact time 80 min, temperature of solution: 298 K.

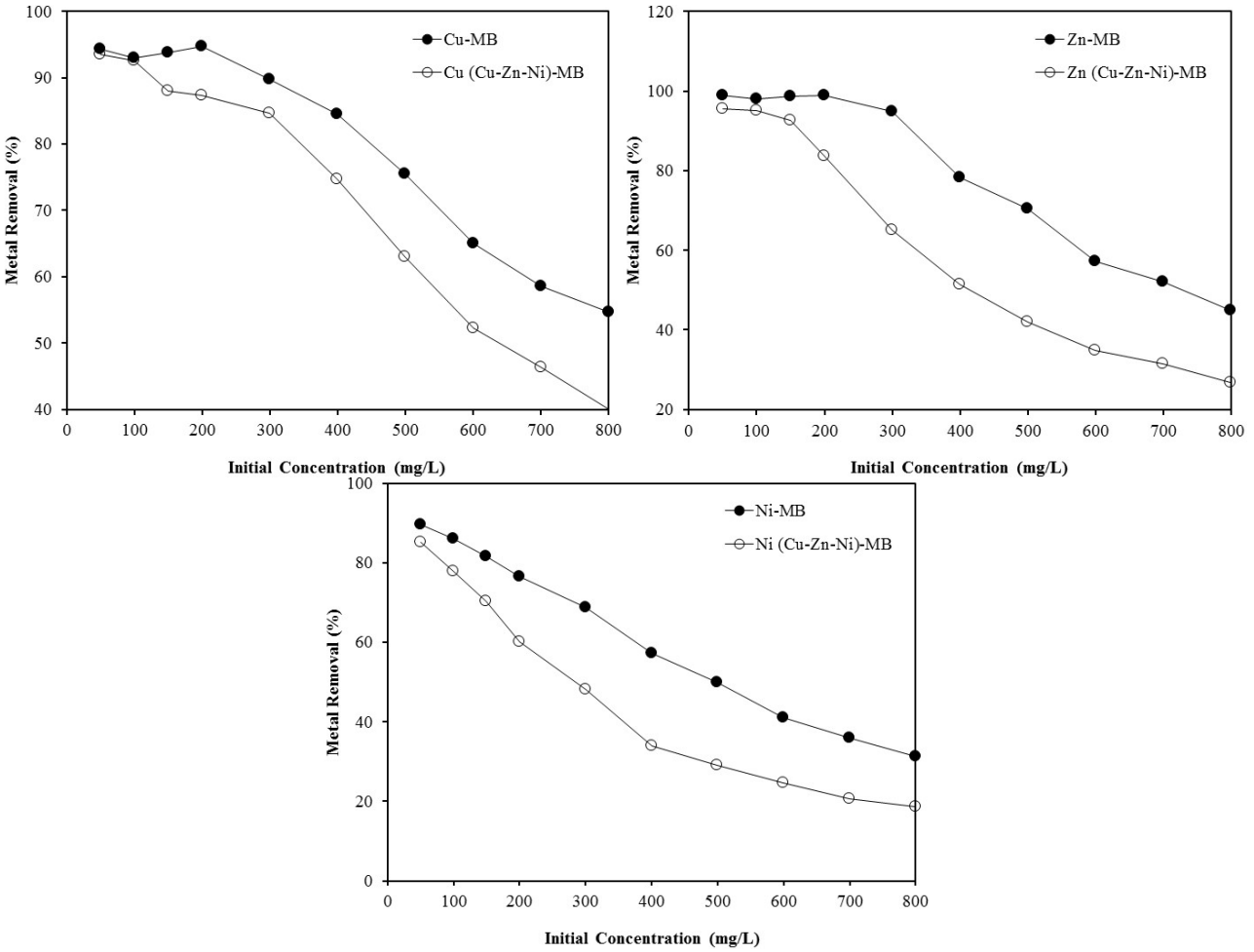

Figure 4.28 Removal of Cu (II), Zn (II) and Ni (II) onto MB under ternary system compared to single system; clay dosage 0.5 g, pH 5 and contact time 80 min, temperature of solution: 298 K.

CHAPTER 5

CONCLUSIONS AND RECOMENDATIONS

5.1 Conclusions

The present study was focused on the enhancement of adsorption capacity by a surface modification technique for removing Cu (II), Zn (II), Ni (II), and humic acid (HA) from aqueous solution. Natural bentonite (clay-based adsorbent) was prepared, and modified using a cationic surfactant (Benzyl hexadecyl dimethyl ammonium chloride, BCDMACl). Both natural bentonite (NB) and modified bentonite (MB) were then characterized their properties, and were used as the adsorbents for studying adsorption of Cu (II), Zn (II), Ni (II), and humic acid (HA) as the model pollutants.

5.1.1 Adsorbents and their characteristics

- The modification of natural bentonite clay (NB) with BCDMACl was successfully performed. The cations of BCDMACl micelles intercalated into the interlayers of bentonite and replaced exchangeable cations. This changed the functional groups of natural bentonite to the cationic surfactant, which dominated heavy metal ion adsorption. The modification also prevented swelling of the bentonite.
- The main chemical compositions of NB were 13.81 and 59.73% of Al_2O_3 and SiO_2, while there were 12.91 and 59.04% of Al_2O_3 and SiO_2 in MB, respectively. The BET result has shown that specific surface area of NB and MB were 44.60 and 15.57 m^2/g, respectively.
- BET surface area of MB was significantly reduced caused by some causes, (1) the alkyl chains screen adsorbent pores, and (2) the surfactant can also adsorb to the micropores.

5.1.2 Adsorption kinetics

- Adsorption kinetics data from NB and MB showed a good agreement with pseudo-second-order model. Thus the kinetics process best describes by this model.
- Adsorption mechanisms of Cu (II), Zn (II), Ni (II), and HA were chemisorption because the fitness of kinetics data with pseudo-second-order was good argument with experimental data.
- The removal of Cu (II), Zn (II), and Ni (II) is sharply increased for about 10 min while it was 40 min for HA, thereafter increasing only slightly or remaining constant over 50.0-200.0 mg/L initial metal concentrations.

5.1.3 Adsorption equilibrium

- The modified bentonite (MB) had about 40.93, 43.88, 25.0 and 34.1 % increases maximally, over unmodified NB, for removal of Cu (II), Zn (II), Ni (II), and HA, respectively.
- Based on two-parameter isotherm, Langmuir model predicted effectively the maximum adsorption capacity ($q_{\max}$) for Cu (II), Zn (II), Ni (II), and HA, with R^2 and APE ranged 0.96-0.998 and 2.35-9.43%, respectively for all cases.
- The maximal adsorption capacities ($q_{\max}$) of MB were 50.76, 35.21, 25.06, and 86.21 mg/ g for Cu (II) , Zn (II) , Ni (II) and HA, respectively, as estimated from the Langmuir fits. These are about 1.7-2.0-fold better than those of NB.
- All the three-parameter models fits supported the two-parameter Langmuir model, regarding these fundamental assumptions underlying it.
- Multi-component system (Cu-Zn-Ni) was assumed in the adsorption modelling caused the presence of several components in the wastewater. Competitive adsorption ratio q_i^{mix} / q_i^o ranged 0.526-0.646,

indicated that the metals were antagonism. Rate of adsorption equilibrium reduction (ΔY) ranged 35.41-47.41 % for all cases.

5.2 Recommendations

In this study, modified bentonite showed enhanced adsorption of heavy metals (Cu (II), Zn (II), and Ni (II)) and humic acid over an unmodified bentonite. This adsorbent can be further used, and modified with another methods for removing heavy metals and/or organic compounds with a real wastewater and contaminated water. The following recommendation can be made for the future study:

- A suitable method of modification for preparing the adsorbent can be considered to maximize the maximum removal of heavy metals.
- This study used sole adsorbent, however, a combination of adsorbents (more than one adsorbent) could be evaluated to remove a pollutant from wastewater.
- The performance of this adsorbent along with several organic compounds can be further evaluated.
- Another contaminant such as a group of electronic waste (e.g. Pb, Sn, Si, Fe and Al) should examine the efficiency of modified bentonite under natural conditions or wastewater from landfill and industry.
- Adapting modified bentonite as an innovation, such as air-filter geomembrane for air-pollutant adsorption related with heavy metals, could be further considered.

REFFERENCES

[1] Abollino, O., Giacomino, A., Malandrino, M., Mentasti E. Interaction of metal ions with montmorillonite and vermiculite. Appl. Clay Sci. 38 (2008) 227-236.

[2] Adebowale, K.O., Unuabonah, E., Owolabi, O., Bamidele, I. The effect of some operating variables on the adsorption of lead and cadmium ions on kaolinite clay. J. Hazard. Mater. B134 (2006) 130-139.

[3] Aiken, G.R., Mcknight, D.M., Wershaw, R.L. (Editors) Humic Substances in Soil, Sediments, and Water. New York : Wiley-Interscience, 1985.

[4] Akpomie, K.G., Dawodu F.A. Acid-modified montmorillonite for sorption of heavy metals from automobile effluent. BJBAS. 5 (2016) 1-12.

[5] Alvarez-Ayuso, E., Garcia-Sanchez, A., Querol, X. Purification of metal electroplating waste waters using zeolites. Water Res. 37 (2003) 4855-4862.

[6] Alvarez-Ayuso, E., Garcia-Sanchez, A. Removal of heavy metals from wastewaters by natural and Na-exchanged bentonites. Clays. Clay. Miner. 51 (2003) 475-480.

[7] Anna, B., Kleopas, M., Constantine, S., Anestis, F., Maria, B. Adsorption of Cd (II), Cu (II), Ni (II) and Pb (II) onto natural bentonite: study in mono and multi-metal systems. Environ. Earth. Sci. 73 (2015) 5435-5444.

[8] Anirudhan, T.S., Ramachandran, M. Surfactant-modified bentonite as adsorbent for the removal of humic acid from wastewaters. Appl. Clay Sci. 35(2007) 276-281.

[9] Arias, F., Sen, T.K. Removal of zinc metal ion (Zn^{2+}) from its aqueous solution by kaolin clay mineral: A kinetic and equilibrium study. Colloids and Surfaces A: Physicochem. Eng. Aspects. 348 (2009) 100-108.

[10] ASTM D5890-06, Standard test method for swell index of clay mineral component of geosynthetic clay liners, ASTM International (2006), West Conshohocken, PA, USA.

[11] Azizian, S. Kinetic models of sorption: a theoretical analysis. J. Colloid Interface Sci. 276 (2004) 47-52.

[12] Bhattacharya, A.K., Mandal, S.N., Das, S.K. Adsorption of Zn (II) from aqueous solution by using different adsorbents. Chem. Eng. J. 123 (1-2) (2006) 43-51.

[13] Blanchard, G., Maunaye, M., Martin, G. Removal of heavy metals from waters by means of natural zeolites. Water Research. 18 (1984) 1501-1507.

[14] Brigatti, M.F, Galan, E. and Theng, B.K.G. Structures and Mineralogy of Clay Minerals. [ed.] F., Theng, B.K.G. and Lagaly, G. Bergaya. Handbook of Clay Science. s.l. : Elsevier, 2006, 2, pp. 19-86.

[15] Bujnova, A., Lesny, J. Sorption characteristics of zinc and cadmium by some natural, modified, and synthetic zeolites. Hung. Electron. J. Sci., Environ. Eng. (2004) 1-10.

[16] Bulgariu D., Bulgariu L. Equilibrium and kinetics studies of heavy metal ions biosorption on green algae waste biomass. Bioresource Technol. 103 (2012) 489-493.

[17] Chang, P.P., Wang, X.K., Yu, S.M., Wu, W.S. Adsorption of Ni (II) on Narectorite from aqueous solution: effect of pH, ionic strength and temperature. Colloid. Surf A. 302 (2008) 75-81.

[18] Chao, H.P., Chen, S.H. Adsorption characteristics of both cationic and oxyanionic metal ions on hexadecyltrimethylammonium bromide-modified NaY zeolite. Chem. Eng. J. 193 (2012) 283-289.

[19] Chen, W.J., Hsiao, L.C., Chen, K.K.Y. Metal desorption from copper (II)/nickel (II)-spiked kaolin as a soil component using plant-derived saponin biosurfactant. Process Biochemistry. 43 (2008) 488-498.

[20] Chen, Y.N., Zhang, D.C., Chen, M., Ding, Y.C. Biosorption properties of cadmium (II) and Zinc (II) from aqueous solution by tea fungus. Desal. Water Treat. 8 (1-3) (2009) 118-123.

[21] Chen, Y., Schnitzer, M. Scanning Electron Microscopy of a Humic Acid and A Fulvic Acid and its Metal and Clay Complexes. Soil. Sci. Soc. Amer. J. 40 (1976) 682-686.

[22] Chervona, Y., Arita, A., Costa, M. Carcinogenic metals and the epigenome: understanding the effect of nickel, arsenic, and chromium. Metallomics. 2012 Jul;4(7):619-27. doi: 10.1039/c2mt20033c. Epub 2012 Apr 3. Review.

[23] Chutia, P., Kato, S., Kojima, T., Satokawa, S. Arsenic adsorption from aqueous solution on synthetic zeolites. J. Hazard. Mater. 162 (2009) 440-447.

[24] Dalida, M.L.P., Mariano, A.F.V., Futalan, C.M., Kan, C.C., Tsai, W.C., Wan. M.W. Adsorptive removal of Cu (II) from aqueous solutions using non-crosslinked and crosslinked chitosan-coated bentonite beads. Desal. 275 (1-3) (2011) 154-159.

[25] Dawodua, F.A., Akpomie, K.G. Simultaneous adsorption of Ni (II) and Mn (II) ions from aqueous solution unto a Nigerian kaolinite clay. J. Mater. Res. Technol. 3 (2014) 129-141.

[26] Diaz-Nava, M.C., Olguin, M.T., Solache-Rios, M. Adsorption of phenol onto surfactants modified bentonite. J. Incl. Phenom. Macrocycl. Chem. 74 (2012) 67-75.

[27] De-Pablo, L., Chavez, M.L., Abatal, M. Adsorption of heavy metals in acid to alkaline environments by montmorillonite and Ca-montmorillonite. Chem. Eng. J. 171 (2011) 1276-1286.

[28] Dubinin, M.M. Modern state of the theory of volume filling of micropore adsorbents during adsorption of gases and steams on carbon adsorbents. Z. Fiz. Khim. 39 (1965) 1305-1317.

[29] Dutta A., Singh N. Surfactant-modified bentonite clays: preparation, characterization, and atrazine removal. Environ. Sci. Pollut. Res. 22 (2015) 3876-3885.

[30] Echeverría, J., Indurain, J., Churio, E., Garrido, J. Simultaneous effect of pH, temperature, ionic strength, and initial concentration on the retention of Ni on illite. Colloids. Surf A. 218 (2003) 175-187.

[31] El-Eswed, B., Khalili, F. Adsorption of Cu (II) and Ni (II) on solid humic acid from Azraq area, Jordan. J. Colloid. Interface Sci. 299 (2006) 497-503.

[32] Erdem, E., Karapinar, N., Donat, R. The removal of heavy metal cations by natural zeolites. J. Colloid Interface Sci. 280 (2) (2004) 309-314.

[33] Farmer, V.C. The layer silicates. In: Farmer VC (ed) The infrared spectra of minerals, Mineralogical Society Monograph 4, London, 1974, pp. 331-363.

[34] Gast, R.G.: in: Minerals in Soil Environments; Dixon, J.B., and Weed, S.B. (Eds.), Soil Sci. Soc, Am., Madison, Wis., 1977; Chap. 2)

[35] Gates, W.P., Teppen, B.J., Bertzsch, P.M., Aiken, S.C. Sorption of aromatics in the interlayer space of organo-clays. Schriftenr. Angew. Geowiss. 1 (1997) 41-48.

[36] Ghomri, F., Lahsini, A., Laajeb, A., Addaou, A. The removal of heavy metal ions (copper, zinc, nickel and cobalt) by natural bentonite. Larhyss J. 12 (2013) 37-54.

[37] Giles C.H., MacEwan T.H., Makhwa S.N., Smith D.J. Studies in Adsorption. Part XI J. Colloid Interf. Sci. 3 (1960) 3973-3993

[38] Giles, C.H., Smith, D., Huitson, A. A general treatment and classification of the solute adsorption isotherm: I Theoretical. J. Colloid Interface Sci. 47 (1974) 755-765.

[39] Gładysz-Płaska, A., Majdan, M., Pikus, S., Sternik, D. Simultaneous adsorption of chromium (VI) and phenol on natural red clay modified by HDTMA. Chem. Eng. J. 179 (2012) 140-150.

[40] Grim, R.E. McGraw-Hill Book Company, Applied Clay Mineralogy. s.l, 1962.

[41] Guan, H.P., Li, P., Imparl-Radosevich, J., Preiss, J., keeling, P. Comparing the properties of Escherichia coli branching enzyme and maize branching enzyme. Arch. Biochem. Biophys. 342 (1997) 92-98.

[42] Gupta, S.S., Bhattacharyya, K.G. Immobilization of Pb (II), Cd (II) and Ni (II) ions on kaolinite and montmorillonite surfaces from aqueous medium. J. Environ. Manage. 87 (2008) 46-58.

[43] Gunatilake, S.K. Methods of removing heavy metals from industrial wastewater. JMESS. 1 (2015) 1309-2912.

[44] Haghseresht, F., Lu, G. Adsorption characteristics of phenolic compounds onto coal-reject-derived adsorbents. Energy Fuels. 12 (1998) 1100-1107.

[45] Hayes, M.H.B., Swift, R.S. The Chemistry of Soil Organic Solids. [ed.] D.J. and Hayes, M.H.B. Greenland. The Chemistry of Soil Constituents. s.l. : John Wiley & Sons, 1978.

[46] Helal, A.A., Murad, G.A., Helal, A.A. Characterization of different humic materials by various analytical techniques, Arab. J. Chem. 4 (2011) 51-54.

[47] Hu, Q.H., Qiao, S.Z., Haghseresht, F., Wilson, M.A., Lu, G.Q. Adsorption study for removal of basic red dye using bentonite. Ind. Eng. Chem. Res. 45 (2006) 733-738.

[48] Hui, K.S., Chao, C.Y.H., Kot, S.C. Removal of mixed heavy metal ions in wastewater by zeolite 4A and residual products from recycled coal fly ash. J. Hazard. Mater. 127 (2005) 89-101.

[49] Igberase, E., Osifo, P. Equilibrium, kinetic, thermodynamic and desorption studies of cadmium and lead by polyaniline grafted cross-linked chitosan beads from aqueous solution. J. Ind. Eng. Chem. 26 (2015) 340-347.

[50] Iskandar, H.M., Casu, R.E., Fletcher, A.T., Schmidt, S., Xu, J., Maclean, D.J., Manners, J.M., Bonnett, G.D. Identification of drought-response genes and a study of their expression during sucrose accumulation and water deficit in sugarcane culms. BMC Plant Biol. 11 (2011) 12.

[51] Jackson, J.B.C., Kirby, M.X. Kirby, Berger W.H., Bjorndal, K.A., Botsford, L.V., Bourque, B.J., Bradbury, R.H., Cooke, R., Erlandson, J., Estes, J.A., Hughes, T.P., Kidwell, S., Lange, C.B., Lenihan, H.S., Pandolfi, J.M., Peterson, C.H., Steneck, R.S., Tegner, M.J., Warner, R.R. Historical overfishing and the recent collapse of coastal ecosystems. Science. 293 (2001) 629-638.

[52] Jin, L., Williamson, A., Banerjee, S., Philipp, I., Rape, M. Mechanism of ubiquitin-chain formation by the human anaphase-promoting complex. Cell. 133 (2008) 653-665.

[53] Karnik, B.S., Davies, S.H., Baumann, M. J., Masten, S.J. The effects of combined ozonation and filtration on disinfection by-product formation. Water Research. 39 (2005) 2839-2850.

[54] Kurniawan, T.A., Chan, G.Y.S., Lo, W., Babel, S. Comparisons of low-cost adsorbents for treating wastewaters laden with heavy metals. Science of the Total Environment. 366 (2006a), 409-426.

[55] Kurniawan, T.A., Chan, G.Y.S., Lo, W.H., Babel, S. Physico-chemical treatment techniques for wastewater laden with heavy metals. Chem. Eng. J. 118 (2006b), 83-98.

[56] Lagergren S. About the theory of so-called adsorption of soluble substances. Kungliga Suensk Vetenskapsakademiens Handlingar, 241 (1898) 1-39.

[57] Langmuir, I. The adsorption of gases on plane surfaces of glass mica and platinum. J. Am. Chem. Soc. 40 (1918) 1361-1403.

[58] Li, P., Abarbanell, L., Gleitman, L., Papafragou, A. Spatial reasoning skills in Tenejapan Mayans. Cognition. 120 (2011) 33-53.

[59] Li, X., Hai, F.I., Nghiem, L.D. Simultaneous activated carbon adsorption within a membrane bioreactor for an enhanced micropollutant removal. Bioresour Technol. 102 (2011) 5319-24.

[60] Li, Z., Gallus, L. Surface configuration of sorbed hexadecyltrimethylammonium on kaolinite as indicated by surfactant and counterion sorption, cation desorption, and FTIR. Colloids and Surfaces A: Physicochem. Eng. Aspects. 264 (2005) 61-67.

[61] Li, Z. Oxyanion sorption and surface anion exchange by surfactant-modified clay minerals. J. Environ. Qual. 28 (1999) 1457-1463.

[62] Li Z. Oxyanion sorption and surface anion exchange by surfactant-modified clay minerals. J. Environ. Qual. 28 (1999) 1457-1463.

[63] Ma, X.K., Lee, N.H., Oh, H.J., Kim, J.W., Rhee, C.K., Park, K.S., Kim, S.J. Surface modification and characterization of highly dispersed silica nanoparticles by a cationic surfactant. Colloid Surf. A 358 (2010) 172-176.

[64] Malek, A., Farooq, S. Comparison of isotherm models for hydrocarbon adsorption on activated carbon. Am. Inst. Chem. Eng. J. 42 (1996) 3191-3201.

[65] Matouq, M., Jildeh, N., Qtaishat, M., Hindiyeh, M., Maha, Q., Syouf, A.l. The adsorption kinetics and modeling for heavy metals removal from wastewater by Moringa pods. J. Environ. Chem. Eng. 3 (2015) 775-784.

[66] McBride, M.B. A critique of diffuse double layer model applied to colloid and surface chemistry. Clays. Clay. Miner. 45 (1997) 598-608.

[67] Mohan, D., Singh, K.P. Single- and multi-component adsorption of cadmium and zinc using activated carbon derived from bagasse-an agricultural waste. Water. Res. 36 (2002) 2304-2318.

[68] Ngah, W.S.W., Hanafiah, M.A.K.M., Yong, S.S. Adsorption of humic acid from aqueous solution on cross-linked chitosan-epichlorohydrin beads: kinetic and isotherm studies. Colloids Surf. B 65 (2008) 18-24.

[69] Olu-Owolabi, B.I., Unuabonah, E.I. Adsorption of Zn^{2+} and Cu^{2+} onto sulphate and phosphate-modified bentonite, Appl. Clay Sci. 51 (2011) 170-173.

[70] Paul Chen, J., Wu, S. Simultaneous adsorption of copper ions and humic acid onto an activated carbon. J. Colloid. Interface. Sci. 280 (2004) 334-342.

[71] Peng, X., Luan, Z., Chen, F., Tian, B., Jia, Z. Adsorption of humic acid onto pillared bentonite. Desalination. 174 (2005) 135-143.

[72] Pinskii, D.L., Minkina, T.M., Mandzhieva, S.S., Fedorov, U.A., Nevidomskaya, D.G., Bauer, T.V. Adsorption features of Cu(II), Pb(II), and Zn(II) by an ordinary

chernozem from nitrate, chloride, acetate, and sulfate solutions. Eurasian. Soil. Sci. 47 (2014) 400-417.

[73] Redlich, O., Peterson, D.L. A useful adsorption isotherm. J. Phys. Chem. 63 (1959) 1024-1026.

[74] Salman, M., El-Eswed, B., Khalili, F. Adsorption of humic acid on bentonite. Appl. Clay Sci. 38 (2007) 51-56.

[75] Sparks, D.L. Environmental soli chemistry. Academic, New York. 2002.

[76] Spark, D.L. Metal and oxyanion sorption on naturally occurring oxide and clay mineral surfaces. In: Grassian VH (ed) Environmental catalysis. Taylor & Francis, Boca Raton. 2005.

[77] Schindler, P.W. and Stumm, W. The Surface Chemistry of Oxides, Hydroxides and Oxide Minerals. [ed.] W. Stumm. Aquatic Surface Chemistry: Chemical Processes at the Particle-Water Interface. s.l. : Wiley, 1987, pp. 83-110.

[78] Schnitzer, M. Binding of Humic Substances by Soil Mineral colloids. [ed.] Schnitzer, P.M., Huang, M. Interactions of Soil Minerals with Natural Organics and Microbes. Madison, Soil. Sci. Soc. Amer. 17 (1986) 77-101.

[79] Schnitzer, M., Khan, S.U. Humic Substances in the Environment. New York : Dekker, 1972.

[80] Schnitzer, M.A., Sparks D.L. A lifetime Perspective on the Chemistry of Soil Organic Matter. Advances in Agronomy. 68, (2000) 1-58.

[81] Schulten, H.R., Schnitzer, M. A State of the Art Structural concept for Humic Substances. Naturwissenschaften, 80 (1993) 29-30.

[82] Schultz, D. An Introduction to Soil Mineralogy. In Minerals in Soil Environments; Dixon, J., Weed, S., Eds.; Soil Science Society of America: Madison, WI, 1989, 1-34.

[83] Seki Y., Yurdakoç, K. Adsorption of Promethazine hydrochloride with KSF Montmorillonite. Adsorption. 12 (2006) 89-100.

[84] Sips, R. On the structure of a catalyst surface. J. Chem. Phys. 16 (1948) 490-495.

[85] Shanmugapriya, A., Hemalatha, M., Scholastica, B., Augustine, T.B. Adsorption studies of lead (II) and nickel (II) ions on chitosan-G-polyacrylonitrile. Der Pharma Chemica. 5 (2013) 141-155.

[86] Sparks, Donald L. Environmental Soil Chemistry (2nd Edition). San Diego : Academic Press, 2002.

[87] Srivastav, V.C., Mall, I.D., Mishra, I.M. Removal of cadmium(II) and zinc(II) metal ions from binary aqueous solution by rice husk ash. Colloid Surf. A312 (2008) 172-184.

[88] Stefanovic, S.C., Logar, N.Z., Margeta, K., Tusar, N.N., Arcon, I., Maver, K., Kovac, J., Kaucic, V. Structural investigation of Zn^{2+} sorption on clinoptilolite tuff from the Vranjska Banja deposit in Serbia. Micropor. Mesopor. Mater. 105 (2007) 251-259.

[89] Stevenson, F.J. Humus Chemistry. New York : Wiley, 1982.

[90] Stumm, W. The Inner-Sphere Surface Complex. [ed.] C.P., O'Melia, C.R. and Morgan, J.M. Huang, Aquatic Chemistry: Interfacial and Interspecies Processes, Washington : Amer. Chem. Soc. (1992) 1-32.

[91] Stumm, W., J.M. Morgan, Aquatic Chemistry: Chemical Equilibria and Rates in Natural Waters. 3. Toronto : John Wiley & Sons, Inc., 1996.

[92] Sun, X.Q., Peng, B., Jing, Y., Chen, J., Li, D.Q. Chitosan(chitin)/cellulose composite biosorbents prepared using ionic liquid for heavy metal ions adsorption. Separations 55 (2009) 2062-2069.

[93] Tahir, S.S., Rauf, N. Removal of a cationic dye from aqueous solutions by adsorption onto bentonite clay. Chemosphere 63 (2006) 1842-1848.

[94] Temkin, M., Pyzhev, V. Kinetics of Ammonia Synthesis on Promoted Iron Catalysts. Acta Physicochimica URSS, 12 (1940) 217-222.

[95] Tohdee, K., Kaewsichan, L., Asadullah. Enhancement of Adsorption Efficiency of Heavy Metal Cu (II) and Zn (II) onto Cationic Surfactant Modified Bentonite. J. Environ. chem Eng. 6 (2) (2018) 2821-2828.

[96] Toth, J. Calculation of the BET-compatible surface area from any type I isotherms measured above the critical temperature. J. Colloid Interf. Sci. 225 (2000) 378-383.

[97] USEPA, United States Environment Protection Agency, National primary drinking water regulations. http://www.epa.gov/safewater/consumer/pdf/mcl.pdf, 2009.

[98] Veli, S., Alyuz, B. Adsorption of copper and zinc from aqueous solutions by using natural clay. J. Hazard. Mater. 149 (1) (2007) 226-233.

[99] Vengris, T., Binkiene, R., Sveikauskaite, A. Nickel, copper and zinc removal from waste water by a modified clay sorbent. Appl. Clay Sci. 18 (2001) 183-190.

[100] Weng, C.H., Tsai, C.Z., Chu, S.H., Sharma, Y.C. Adsorption characteristics of copper (II) onto spent activated clay. Sep. Purif. Technol. 54 (2) (2007) 187-197.

[101] WHO, Health systems: improving performance, World Health Organization, Geneva, Switzerland. 2000.

[102] WHO, Zinc in Drinking-water, Background document for development of WHO Guidelines for Drinking-water Quality. WHO/SDE/WSH/03.04/17, 2003.

[103] WHO, Copper in Drinking-water, Background document for development of WHO Guidelines for Drinking-water Quality. WHO/SDE/WSH/03.04/88, 2004.

[104] Witek-Krowiak, A., Szafran, R.G., Modelski, S.Z. Biosorption of heavy metals from aqueous solutions onto peanut shell as a low-cost biosorbentu. Desalination 265 (2011) 126-134.

[105] Worch, E. Adsorption technology in water treatment: fundamentals, processes, and modeling. Walter de Gruyter, 2012.

[106] Xu, D., Zhou, X., Wang, X.K. Adsorption and desorption of Ni2+ on Namontmorillonite: effect of pH, ionic strength, fulvic acid, humic acid and addition sequences. Appl .Clay Sci. 39 (2008) 133-141.

[107] Yanhui, L., Fuqiang, L., Bing, X., Qiuju, D., Pan, Z., Dechang, W., Zonghua, W., Yanzhi, X. Removal of copper from aqueous solution by carbon nanotube/calcium alginate composites. J. Hazard. Mater. 177 (2010) 876-880.

[108] Yusof A.M., Malek N.A.N.N. Removal of Cr (VI) and As (V) from aqueous solutions by HDTMA-modified zeolite Y. J. Hazard. Mater. 162 (2009) 1019-1024.

[109] Zhan, Y.H., Zhu, Z.L., Lin, J.W., Qiu, Y.L., Zhao, J.F. Removal of humic acid from aqueous solution by cetylpyridinium bromide modified zeolite. J. Environ. Sci. 22 (2010) 1327-1334.

[110] Zhang, Z.Z., Sparks, D.L., Scrivner, N.C. Sorption and desorption of quaternary amine cations on clays. Environ. Sci. Technol. 27 (1993) 1625-1631.

.

APPENDEX

Publication 1:

K. Tohdee, L. Kaewsichan, Asadullah, Enhancement of Adsorption Efficiency of Heavy Metal Cu(II) and Zn(II) onto Cationic Surfactant Modified Bentonite, J. Environ. Chem. Eng. 6 (2018) 2821-2828.

Journal of Environmental Chemical Engineering 6 (2018) 2821–2828

Contents lists available at ScienceDirect

Journal of Environmental Chemical Engineering

journal homepage: www.elsevier.com/locate/jece

Enhancement of adsorption efficiency of heavy metal Cu(II) and Zn(II) onto cationic surfactant modified bentonite

Kanogwan Tohdee*, Lupong Kaewsichan, Asadullah

Department of Chemical Engineering, Faculty of Engineering, Prince of Songkla University, Hat Yai, Songkhla 90112, Thailand

ARTICLE INFO

Keywords:
Langmuir
Cationic surfactant
Modified bentonite
Adsorption
Heavy metal

ABSTRACT

This study sought to enhance the metal adsorption capacity of bentonite by improving its surfaces. Surface modification by the cationic surfactant (Bencylhexadecyldimethyl ammonium chloride, BCDMACl) was successful in this respect, and was characterized by FTIR spectroscopy, XRF, BET, and swelling test. A major characteristic of BCDMACl is forming micelles that can intercalate into interlayers of clay and prevent swelling. The adsorption of Cu (II) and Zn (II) from aqueous solutions was studied in batch experiments, varying both contact time and concentrations of the metal ions. Retention of the metals in solution was detected by Atomic Absorption Spectroscopy (AAS). The adsorption data were fitted with Langmuir, Freundlich, and Dubinin-Radushkevich isotherm models, of which the Langmuir isotherm provided the best fit with experimental data (R^2 range 0.962–0.993). The results also revealed that the modified bentonite had significantly improved adsorption capacities (q_{max} 50.76 and 35.21 mg/g for Cu(II) and Zn(II), respectively); about 2.5 and 2.0 fold improvements over natural bentonite. The pseudo-second-order rate equation provided the best fit to observed adsorption kinetics. This study demonstrated the modified bentonite as an effective adsorbent for the removal of heavy metals from aqueous solutions.

1. Introduction

Water pollution by heavy metals is harmful to most animal species. Most of such pollution is released in the waste streams from chemical industries, including production of electric batteries, mining, and manufacture of glass. According to a listing by the United States Environmental Protection Agency [1], Cu (II) and Zn(II) are heavy metals potentially harmful to human health. Moreover, The World Health Organization (WHO) suggests that maximum allowed concentrations of these metals in drinking water should not exceed 1.0 mg/L and 5.0 mg/L [2,3], respectively. The concerns are particularly serious because these heavy metals can be accumulated by a living organism: even low levels of exposure can be harmful if prolonged.

Numerous methods have been developed to remove heavy metals and organic matter from wastewater and contaminated soil, including physicochemical methods (e.g., chemical precipitation, coagulation and flocculation, electrochemical treatments, ion exchange, membrane filtration, and electrodialysis) and biological methods [4]. Physicochemical adsorption is inexpensive and easy to adapt [5], so it is practiced widely. Adsorbent types can be classified into bio-adsorbents and natural materials [6]. The removal of several heavy metals and organic compounds by bio-adsorbents (chitin, chitosan, biomass etc.) has been studied [7–9]. Recently, clay minerals (a natural material adsorbent) have become alternative adsorbents, having high specific surface area, layer structure and high cation exchange capacity (CEC) as their advantages.

Natural bentonite is a potent adsorbent that has been recently used in several studies to adsorb heavy metal ions and organic matter [10–12]. It is known that, similar to clay, bentonite is important to several technologies due to its physicochemical properties including high CEC. These properties can be considerably modified by acid activation, soda activation, ion exchange, and heat treatments [13–16]. It is noted that swelling can reduce the hydraulic conductivity of natural clay, so that the solution treated cannot seep into the clay easily. It is for this reason that natural clay cannot effectively adsorb metal ions from an aqueous solution.

Modification of natural bentonite is required to improve its adsorption capacity and surfactants are widely used for such modification. Diaz-Nava et al. [17] succeeded in modifying bentonite with Bencylhexadecyldimethyl ammonium chloride (BCDMACl) and hexadecyl trimethyl ammonium bromide (HDTMABr), and tested the surfactant modified bentonite for phenol adsorption. They concluded that the removal of phenol depended on several factors, such as structure of surfactant, phenol species, pH, and initial concentration of solute.

* Corresponding author.
E-mail address: tohdee.k@gmail.com (K. Tohdee).

https://doi.org/10.1016/j.jece.2018.04.030
Received 24 December 2017; Received in revised form 1 March 2018; Accepted 15 April 2018
Available online 17 April 2018

However, the adsorption of heavy metals by BCDMACl modified bentonite is still not well-understood. Therefore, an objective of this study was to study the removal of heavy metals Cu(II) and Zn(II) using a cationic surfactant BCDMACl modified bentonite. Batch adsorption experiments were performed to determine the adsorption capacities of natural and modified bentonite, during removal of Cu(II) and Zn(II) from aqueous solutions.

2. Materials and methods

2.1. Material and chemicals

2.1.1. Chemicals

All chemicals used in this study were analytical grade. Heavy metal salts $CuSO_4{\cdot}5H_2O$ and $Zn(NO_3)_2$, purchased from Ajax Finechem and Loba Chemie, respectively, were used to prepare the stock solutions of Cu(II) and Zn(II). A cationic surfactant (bencylhexadecyldimethyl ammonium chloride, BCDMACl), obtained from Sigma Aldrich, was used to modify bentonite in this study.

2.1.2. Natural and modified bentonite

A commercial grade natural bentonite (clay mineral) was used in this study. The material was passed through a 200 mesh laboratory sieve before use. Modified bentonite (MB) was prepared from natural bentonite (NB) specimens by adding the NB into 1 M sodium acetate buffer solution at pH 5, and allowing to react for 18 h. Potassium chloride solution (1 M at pH 7) was then added and allowed to react for 18 h. After that, the solid phase was separated and left in 0.2 M cesium chloride solution for 6 h. The solid-phase was again separated and left in cesium chloride solution for 10 min [17]. The solids (preprocessed bentonite) were then mixed into 8.40 mmol/L of BCDMACl. The mixture was shaken for 48 h at 303 K. Finally, the clay sample was separated from the solution using a centrifuge at 2500 rpm (770 relative centrifugal force) for 10 min and rinsed with distilled water for various times to eliminate excess surfactant. The solid sample was then dried at 343 K for 24 h.

2.2. Instrumentation

The concentrations of copper(II) and zinc(II) were measured by atomic absorption spectrophotometry (AAS), using AANALYST 100 SPECTROMETER, Perkin-Elmer, Norwalk CT/USA. Natural and modified bentonites were characterized with an X-ray fluorescence spectrometer, PW2400, PHILIPS, Netherlands. The FTIR spectra of the natural and the modified bentonite were recorded from KBr pellets with a Fourier Transform Infrared Spectrometer, VERTEX 70, Bruker, Germany. Surface area and porosity were determined using BET-technique, ASAP2460, Micromeritics, USA. Cation exchange capacities (CEC) of the natural and the modified bentonite were determined by the ammonium acetate method described by Chapman [18].

2.3. Batch adsorption

Batch experiments were performed to find out the capacities of NB and MB to adsorb Cu(II) and Zn(II). Stock solutions (1000 mg/L) of Cu (II) and Zn(II) were prepared by dissolving 3.929 g of $CuSO_4{\cdot}5H_2O$ and 2.896 g of $Zn(NO_3)_2$, each in 1 L distilled water. Standard Cu(II) and Zn (II) solutions in the range 50–200 mg/L were then prepared by diluting appropriately the stock solutions, and 0.1 M NaOH or HCl was used to adjust the final pH of the metal solutions. On testing an aliquot of a prepared solution (50 mL) was placed in a 250 mL conical flask and 0.5 g of adsorbent was added to it before placing in an incubator shaker at 150 rpm and 293 K (controlled temperature). The effects of pH metal solution, contact time, and initial metal concentration were investigated. To obtain adsorption isotherms, higher concentrations from 300 to 800 mg/L with 100 mg/L increments were allowed to equilibrate with the adsorbents.

3. Theory

The amount of heavy metal adsorbed on a solid surface at equilibrium (q_e, in mg of ion/g of adsorbent) can be determined from the following mass-balance equations:

$$q_e = \frac{(C_i - C_e) \times V}{m} \tag{1}$$

$$\%\ \text{Removal} = \frac{(C_i - C_e) \times 100}{C_i} \tag{2}$$

where C_i and C_e are the initial and equilibrium concentrations of heavy metal (mg/L), respectively, V is volume of the aqueous solution (L), and m is mass of the adsorbent (g).

3.1. Adsorption kinetics models

3.1.1. Pseudo-first-order model

The pseudo-first-order model proposed by Lagergren [19] based is expressed as follows:

$$\frac{dq_t}{dt} = k_1(q_e - q_t) \tag{3}$$

where q_t is the heavy metal adsorbed at the given contact time (mg/g), and k_1 is the rate constant of the pseudo-first order (1/min). Integration of Eq. (3) provides linear relationship of $\log(q_e - q_t)$ and t with slope equal to the rate constant k_1.

3.1.2. Pseudo-second-order model

The pseudo-second-order model is commonly used when the adsorption/desorption balance controls the overall sorption kinetics. The model was developed by Blanchard et al. [20] is expressed as follows:

$$\frac{dq_t}{dt} = k_2(q_e - q_t)^2 \tag{4}$$

where k_2 is the rate constant of the pseudo-second order (g/mg/min). Integration of Eq. (4) with suitable boundary conditions gives linearly related t/q_t and t, and the rate constant k_2 can be calculated from the slope.

3.2. Adsorption isotherm models

3.2.1. Langmuir isotherm

Langmuir model assumes adsorption forming a monolayer on the surface, by adsorption at specific mutually homogenous adsorption sites, and that the attraction force between molecules sharply decreases with distance to the adsorption sites [21]. The Langmuir model is given by:

$$q_e = \frac{q_m K C_e}{1 + K C_e} \tag{5}$$

where q_e is the amount of metal adsorbed on the adsorbent surfaces (mg/g), q_m is the maximal amount of metal adsorbed (mg/g), and K is the Langmuir constant (L/mg). C_e is the equilibrium concentration of metal (mg/L). To identify the model parameters from data, Eq. (5) is rearranged to a linear form of $1/q_e$ vs. $1/C_e$. Then the model parameters q_m and K can be calculated from the intercept and the slope of a linear plot, respectively.

3.2.2. Freundlich isotherm

Freundlich model is one of the earliest empirical models. It is used with multilayer adsorption and can deal with both homogeneous and heterogeneous surfaces, and with both physical and chemical adsorption. The Freundlich isotherm is expressed as:

$$q_e = K_f C_e^{1/n} \quad (6)$$

where K_f and n are the model parameters. Eq. (6) implies a linear relationship of $\log q_e$ and $\log C_e$ used to identify the model parameters from data: K_f and n can be calculated form the intercept and the slope of a fitted line.

3.2.3. Dubinin-Radushkevich isotherm

Dubinin-Radushkevich model is more general than the Langmuir model. It does not assume a homogenous adsorbent, and this model is used to assess the nature of adsorption processes [22]. The Dubinin-Radushkevich model is as follows [23]:

$$q_e = q_m \exp(-K_{DR}\varepsilon^2) \quad (7)$$

$$q_e = q_m \exp\left(-K_{DR}\left[RT \ln\left(1 + \frac{1}{C_e}\right)\right]^2\right) \quad (8)$$

where K_{DR} is the Dubinin-Radushkevich constant related to the free energy of adsorption (mol^2/J^2), and ε^2 is a Polanyi potential (J^2/mol^2). Rearranging Eq. (7) gives a linear relationship between $\ln q_e$ and ε^2 and the model parameters can again be calculated from the slope and the intercept. Moreover, the roles of chemisorption and physical adsorption can be assessed from Eq. (9). An E_s value between 8 and 16 kJ/mol indicates chemisorption. On the other hand, the E_s value below that range indicates that physical adsorption is dominant.

$$E_s = \frac{1}{\sqrt{2K_{DR}}} \quad (9)$$

4. Results and discussion

4.1. Characterization of natundral a modified bentonite

4.1.1. FTIR analysis results

The FTIR spectra of natural bentonite (NB) and modified bentonite (MB) are shown in Fig. 1. FTIR spectra of NB and MB were recorded over the range 4000–400 cm^{-1} and are reported in Fig. 1. The broad band at 3452 cm^{-1} was assigned to OH stretching vibrations for NB and MB, whereas water present in the bentonite displayed the peak at 1638 cm^{-1}, which is assigned to OH bending vibrations. The NB shows the Al—Al—OH stretching band at 3620 cm^{-1}. At 917 and 852 cm^{-1} the bands can be assigned to Al—Al—OH and Al—Fe—OH bending vibrations, respectively [24]. The Si—O stretching was observed at band 1042–1045, and the band at 521 cm^{-1} was assigned to Si—O bending vibrations. The doublet at 852 and 797 cm^{-1} indicated the presence of quartz in the bentonite [25]. Generally, all the bands described above are typical in NB spectra. For MB, there was a slight shift of those bands due to modification by cationic surfactants. Appearance of the pair of bands at 2923 and 2852 cm^{-1} confirmed that the cationic surfactant was present in the modified bentonite. These bands were assigned to symmetric and asymmetric C—H stretching vibrations of methyl and methylene groups, which were absent from spectra of NB [25].

4.1.2. Bentonite structure

Bentonite is a clay mineral containing montmorillonite. As shown in Fig. 2, montmorillonite structure has three mineral layers periodically, with two tetrahedral layers (silica sheets) sandwiching a central octahedral layer (alumina sheet). NB shows a net negative charge due to isomorphic replacement of Al^{3+} with Mg^{2+} in the central octahedral layer. The negative charge is balanced by exchangeable cations in the lattice structure, such as Ca^{2+} and Na^+ located in the interlayer, which can enhance the adsorption of cationic pollutants [26,27].

To modify bentonite, a cationic surfactant (BCDMACl) was added to natural bentonite. BCDMACl micelles consists of two main parts (hydrophilic head and hydrophobic tail), with ammonium cation [R′-$(CH_3)_2N^+$R] being the head and a long chain forming the tail (see Fig. 3). The ammonium cation of BCDMACl micelles intercalated into the interlayers and replaced exchangeable cations (Ca^{2+} and Na^+ in interlayer) and Mg^{2+} for Al^{3+} in the central octahedral layer, as shown in Fig. 2 [28].

4.1.3. XRF analysis results

Table 1 shows a comparison of the chemical constituents in NB and MB, from the XRF results. The NB and MB had alumina and silica as the major species, at 13.81% and 59.73%, and at 12.91% and 59.04% by weight, respectively. It was found that Cs and Cl were present in MB at 3.86 and 0.31%, respectively. This implies that the intercalation of BCDMACl was successful by ion exchange. Furthermore, the results indicate obvious decreases in the cations of the interlayer (Ca^{2+} and Na^+) and of the octahedral layer (Mg^{2+} for Al^{3+}), on forming MB from NB. This corroborates cation exchange and replacement as mechanisms acting during the modification [28].

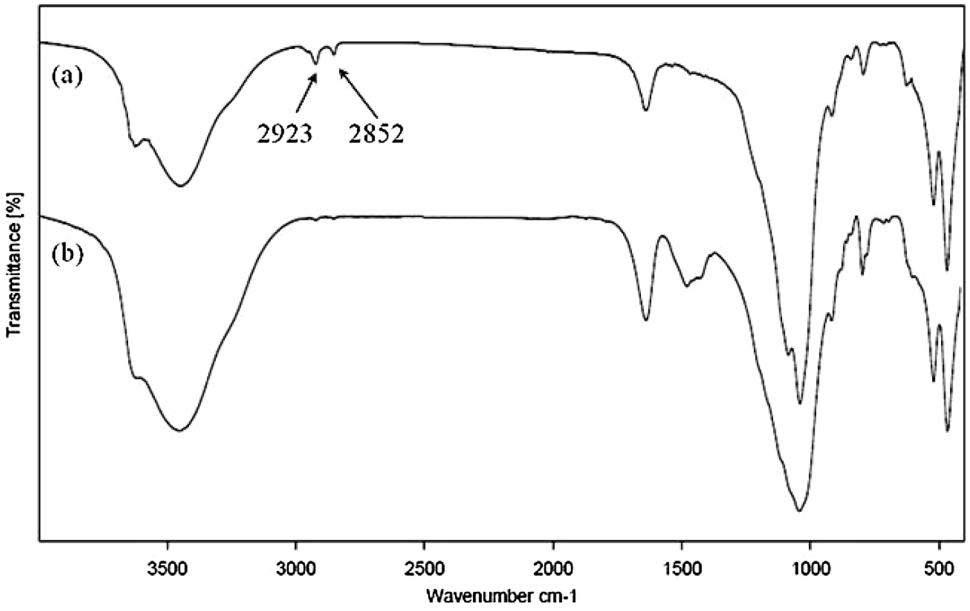

Fig. 1. The FTIR spectra of (a) the modified bentonite (MB) and (b) natural bentonite (NB).

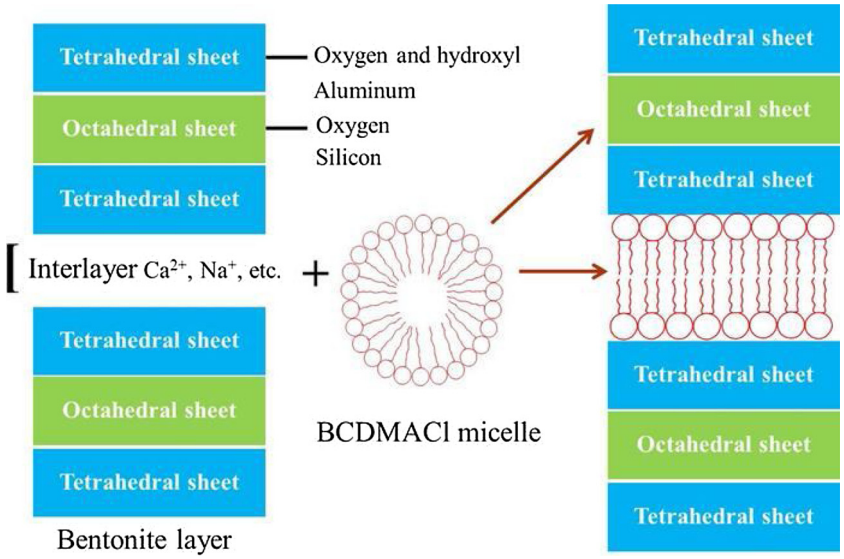

Fig. 2. Schematic illustration of surfactant modified bentonite.

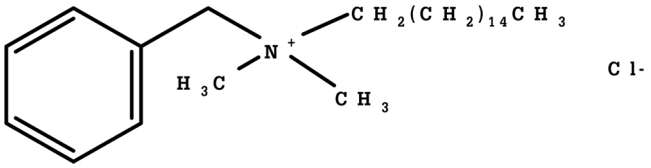

Fig. 3. Chemical structure of cationic surfactant (BCDMACl).

Table 1
Chemical constituents and physical properties of NB and MB.

Constituents	NB	MB
Chemical constituents (% by weight)		
Na_2O	2.72	0.48
MgO	2.38	1.81
Al_2O_3	13.81	12.91
SiO_2	59.73	59.04
P_2O_5	0.10	0.14
SO_3	0.31	0.28
K_2O	1.10	5.22
CaO	3.18	2.18
TiO_2	0.36	0.37
Fe_2O_3	3.00	3.57
SrO	0.06	0.04
ZrO_2	0.03	0.04
BaO	0.15	0.22
Cs_2O	–	3.86
Cl	–	0.31
Structural parameters		
BET surface area (m^2/g)	44.60	15.57
Pore volume (cm^3/g)	0.054	0.035
Pore size (nm)	4.81	9.10
CEC ($cmol_c$/kg)	75.95	68.70
Free swelling[a] (mL/2 g)	10.33	0.00 (no swelling)

[a] Following ASTM D5890-06 [33].

4.1.4. CEC and textural characteristics

As a consequence of the modification, cation exchange capacity (CEC) was reduced from 75.95 (NB) to 68.70 $cmol_c$/kg (MB), as shown in Table 1. The cation from the surfactant was intercalated in the clay and pushed other cations into solution, thereby significantly decreasing CEC [29]. After bentonite was modified by BCDMACl, the BET results indicate significantly reduced specific surface, from 44.60 to 15.57 m^2/g, caused by the alkyl chains screening adsorbent pores [30]. The surfactant could also adsorb to the micropores and the inner surfaces of the particles, decreasing the specific surface of MB [31]. Moreover, the average pore diameter increased from 4.81 to 9.10 nm, which suggests elimination of the smallest pores in the adsorbent [30].

The BET surface area and the pore size are not the only determinants affecting the adsorption of heavy metals. The surface functional groups are key characteristics of an adsorbent which metal ions can be adsorbed by interactions with the surface functional group of the adsorbent [32]. Eventually, swelling tests following ASTM D5890-02 [33] confirmed that no swelling occurred in the cationic surfactant modified bentonite, while the natural bentonite had 10.33 mL/2 g which the swelling is almost completed during preparation process.

4.2. Adsorption results

4.2.1. Adsorption kinetics

In order to study the adsorption kinetics, both pseudo-first and pseudo-second order of kinetic models were fit to the experimental data. Linear fits were used with the transformed models, instead of nonlinear regression. The results revealed that the pseudo-first-order model did not reliably match with the experimental data related to coefficient of determination (R^2) ranges 0.164–0.923. In contrast, the adsorption kinetics of Cu(II) and Zn(II) were well described by the pseudo-second-order model, see Fig. 4, and the identified model parameters are listed in Table 2. Comparison of q_e from the experiment ($q_{e,\exp}$) and from the model ($q_{e,cal}$) revealed the good fit with R^2 better than 0.990. This indicates that the pseudo-second-order model was appropriate for the adsorption kinetics in this study. Fig. 5 shows a plot of the pseudo-second-order model without linearizing transform, while the parameters were obtained with the transform (see Table 2). The equilibrium was practically reached by 10 min. To ensure equilibration, 80 min equilibration time was used when determining the adsorption isotherms of the next section.

4.2.2. Effect of initial solution pH

Solution pH is an important factor which can affect the adsorption process. The removals of metal Cu(II) and Zn(II) were observed by batch experiments at various pH of metal solutions range 3–11. Fig. 6 illustrated the metal removal as a function of solution pH. There were increases in the removals of Cu(II) and Zn(II) with increasing the pH solutions over the range of 3–5. However, it was remarkable that the removals of both ions almost reached a maximal capacity of metal concentration at the solution pH 7–11 (more than 95%). This was due to the reason that a chemical precipitation became a dominant process on metal removal at this range which mainly formed the solid state of

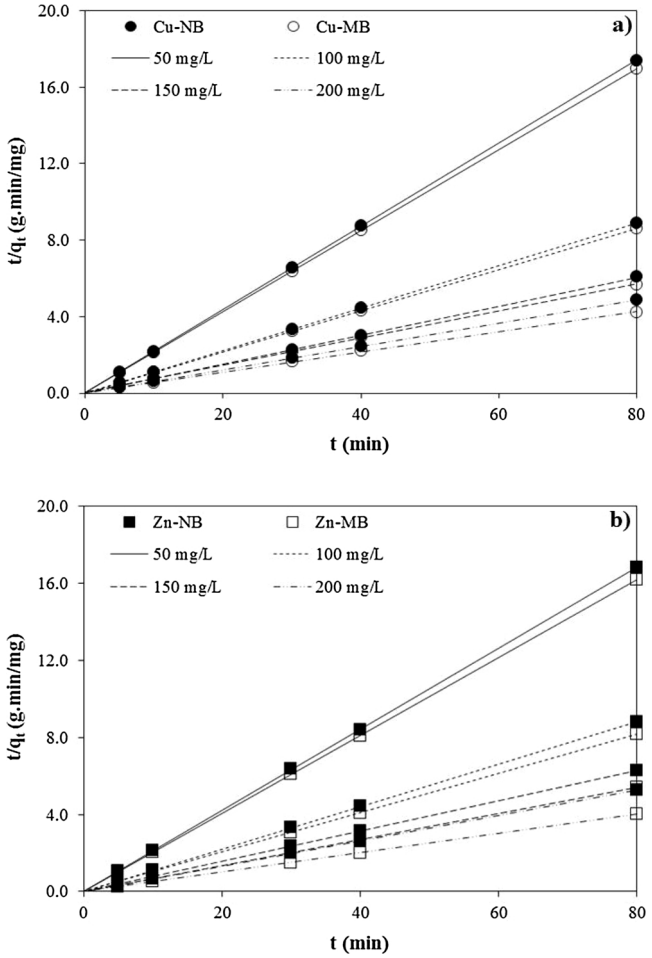

Fig. 4. Pseudo-second-order model of Cu(II) (a) and Zn(II) (b) on to NB and MB, linear plot.

$Cu(OH)_2$ and $Zn(OH)_2$. This condition was not solely considered as the adsorption because the metal precipitation may lead to a misinterpretation of adsorption capacity. This result had a similar trend with adsorption study on several metal ions which has been reported by numerous studies [34–36]. Therefore, the optimum pH in this study should be 5–6 for adsorption study of both Cu(II) and Zn(II).

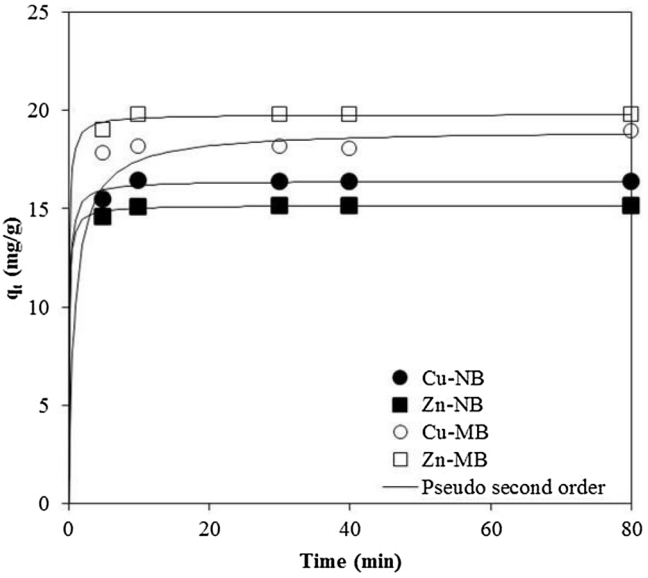

Fig. 5. Pseudo-second-order model of Cu(II) and Zn(II) onto NB and MB, nonlinear plot at initial metal concentration 200 mg/L, NB and MB dosage 0.5 g, and pH 5.

4.2.3. *Effect of contact time*

Contact time is one of the most important factors affecting adsorption efficiency. The adsorption efficiency can be experimentally optimized for optimal pH, adsorbent dose and concentration of adsorbate. Therefore, a series of a batch experiments varying contact time was performed, and the metal ion concentrations were determined by Atomic Absorption Spectrophotometry (AAS).

The adsorption capacities of Cu(II) and Zn(II) by the different adsorbents were determined as the removal percentages of Cu(II) and Zn (II), and are presented as time profiles in Fig. 7. The removal of metal ions by adsorption onto both NB and MB was in the ranges 77.50–94.75% (± 0.50–2.81%) and 72.97–98.93% (± 0.17–1.51%) for Cu(II) and Zn(II), respectively, with initial concentrations varying from 50 to 200 mg/L. NB maximally removed 82.05% and 75.74% of Cu(II) and Zn(II), respectively, from 200 mg/L initial concentration. The maximal removal was higher on using MB, reaching up to 94.75% and 98.90% of Cu(II) and Zn(II), respectively. Generally, the removal rapidly increased initially for about 10 min, and thereafter either increased only slightly or remained constant. The high equilibrium fractions of ions removed indicate that the dosages of NB and MB were

Table 2
Kinetic model parameters of Cu(II) and Zn(II) onto NB and MB.

Adsorbents	Metal	C_i (mg/L)	$q_{e,exp}$ (mg/g)	Pseudo-first-order model			Pseudo-second-order model		
				k_1 (1/min)	$q_{e,cal}$ (mg/g)	R^2	k_2 (g/mg/min)	$q_{e,cal}$ (mg/g)	R^2
NB	Cu(II)	50	4.60	0.016	36.71	0.462	2.94	4.60	1.000
		100	9.01	0.046	20.35	0.888	2.93	9.01	1.000
		150	13.18	0.026	9.79	0.309	1.22	13.19	1.000
		200	16.40	0.050	2.57	0.665	0.43	16.42	1.000
	Zn(II)	50	4.75	0.020	13.78	0.923	2.13	4.76	1.000
		100	9.06	0.026	11.55	0.698	1.13	9.06	1.000
		150	12.75	0.051	17.62	0.861	2.79	12.76	1.000
		200	15.15	0.115	2.92	0.799	0.65	15.17	1.000
MB	Cu(II)	50	4.72	0.039	21.69	0.738	2.72	4.72	1.000
		100	9.30	0.103	16.12	0.468	1.72	9.30	1.000
		150	14.07	0.007	2.79	0.922	0.17	14.08	1.000
		200	18.95	0.004	1.04	0.164	0.06	19.01	0.999
	Zn(II)	50	4.95	0.076	5.82	0.835	1.19	4.96	1.000
		100	9.81	0.064	15.77	0.631	1.01	9.82	1.000
		150	14.79	0.045	31.05	0.315	0.89	14.81	1.000
		200	19.78	0.108	6.22	0.721	0.53	19.80	1.000

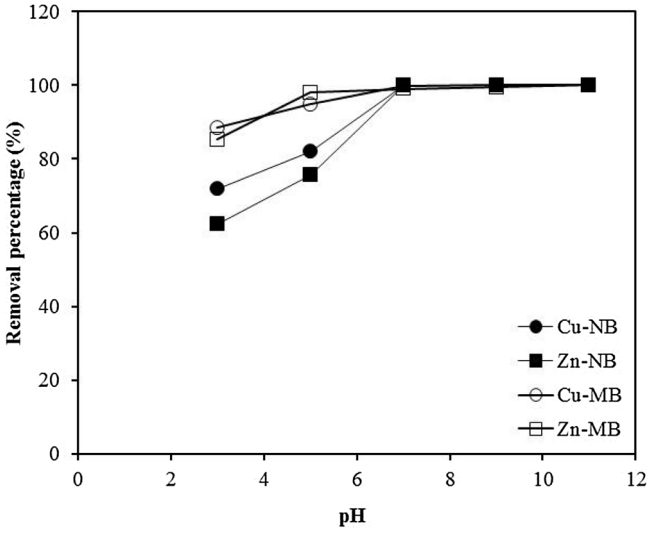

Fig. 6. Effect of solution pH of Cu(II) and Zn(II) onto NB and MB, initial metal concentration 200 mg/L, NB and MB dosage 0.5 g, and contact time 80 min.

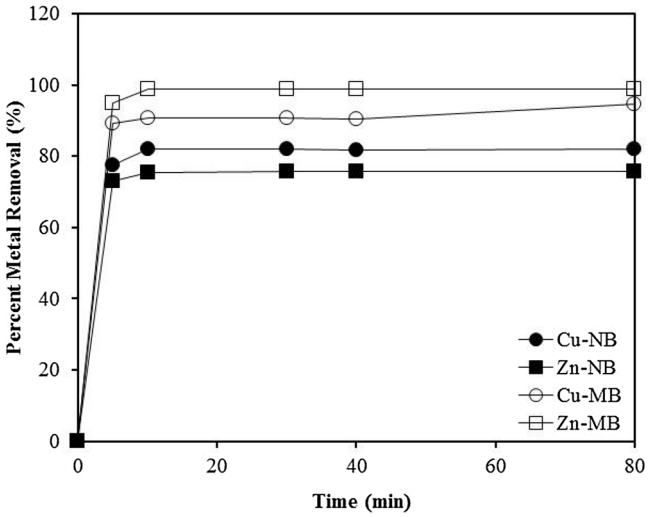

Fig. 7. Effect of contact time on the removal of Cu(II) and Zn(II) by NB and MB, initial metal concentration 200 mg/L, NB and MB dosage 0.5 g, and pH 5.

sufficient for adsorption over the range of initial concentrations tested.

4.2.4. Effects of metal ion concentration

Fig. 8 illustrates the relationship of metal ion concentration to the removals of Cu(II) and Zn(II) at equilibrium. The overall response shapes are similar across all cases, but MB was clearly better adsorbent than NB at high concentration of the heavy metals. The maximal improvement in removal by adsorption on comparing MB to NB was by 40.93 and 43.88% for Cu(II) and Zn(II), respectively.

The experimental results indicate near complete removal or cleanup of 100–150 mg/L concentrations with NB, and the higher 250–300 mg/L range with MB. These are higher concentration ranges than previously reported for natural bentonite by Veli and Alyuz [11]. The results clearly confirm that cationic surfactant treatment enhanced the adsorption capacity of natural clay.

4.2.5. Adsorption isotherms

The adsorption of Cu(II) and Zn(II) onto NB and MB was assessed against various equilibrium isotherm models, namely the Langmuir, Freundlich, and Dubinin-Radushkevich models. The experimental results were applied to those models and the identified parameters are

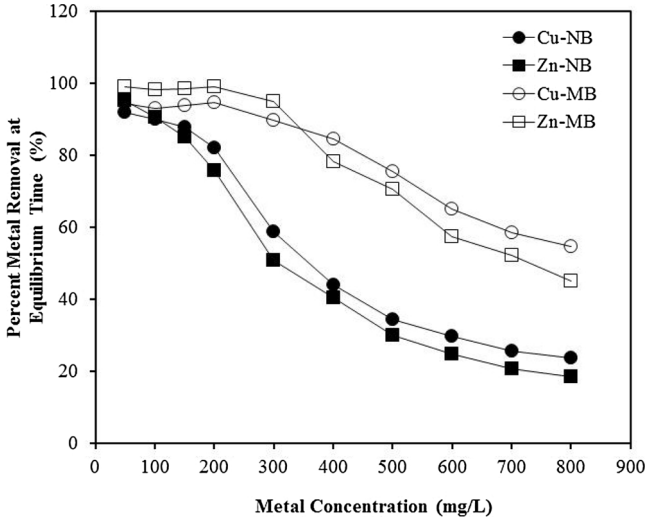

Fig. 8. Effect of initial metal concentration on the removal of Cu(II) and Zn(II) by NB and MB, clay dosage 0.5 g, pH 5 and contact time 80 min.

Table 3
Adsorption isotherm parameters of Cu(II) and Zn onto MB and NB.

Isotherm Parameters	NB		MB	
	Cu	Zn	Cu	Zn
Langmuir isotherm model				
K (L/mg)	0.077	0.177	0.037	0.303
q_{max} (mg/g)	19.76	15.46	50.76	35.21
R^2	0.987	0.993	0.984	0.962
Freundlich isotherm model				
K_f (mg/g)	5.363	5.887	5.026	10.170
n	4.684	5.988	2.486	4.203
R^2	0.741	0.713	0.868	0.799
Dubinin-Radushkevich isotherm model				
K (mol^2/J^2)	5.0E-06	2.0E-06	4.0E-06	3.0E-07
q_{max} (mg/g)	17.66	14.25	29.62	28.11
E_s (kJ/mol)	0.316	0.500	0.354	1.291
R^2	0.896	0.872	0.728	0.762

tabulated in Table 3, along with the coefficient of determination (R^2) to indicate the goodness of fit (larger values are better).

It is found that the experimental data were best fit by the Langmuir isotherm among the models tested, suggesting homogenous adsorption sites on the surfaces and monolayer formation [20,37]. This result indicated that the Langmuir isotherm can be described the adsorption mechanism in this study although the mean free energy of adsorption (E_s) in the Dubinin-Radushkevich model was below 6–18 kJ/mol indicating physical adsorption of Cu(II) and Zn(II).

The model-based responses of q_e to C_e of all the adsorption isotherms are shown in Fig. 9. The Langmuir isotherm model was the best fit over the experiments for all metal and adsorbents compared to other isotherm models. The maximal adsorption q_{max} was estimated from the fitted Langmuir models to be 19.76 and 15.46 mg/g for Cu(II) and Zn(II) on NB, while MB had q_{max} improved by 2.0–2.5 fold with up to 50.76 and 35.21 mg/g adsorptions of Cu(II) and Zn(II), respectively. This is considerable because the cationic surfactant treatment of bentonite in this study modified it to MB by changing the functional groups of natural bentonite and increasing both the anionic adsorptive capacity and the cation affinity of the clay [38,39], thereby improving the adsorption of heavy metals.

It can be seen from Fig. 9 that the experimental adsorption isotherms of this study were L-type [40] in all cases, indicating high affinity of sorbent and solute. Amount of the metal ions adsorbed on the

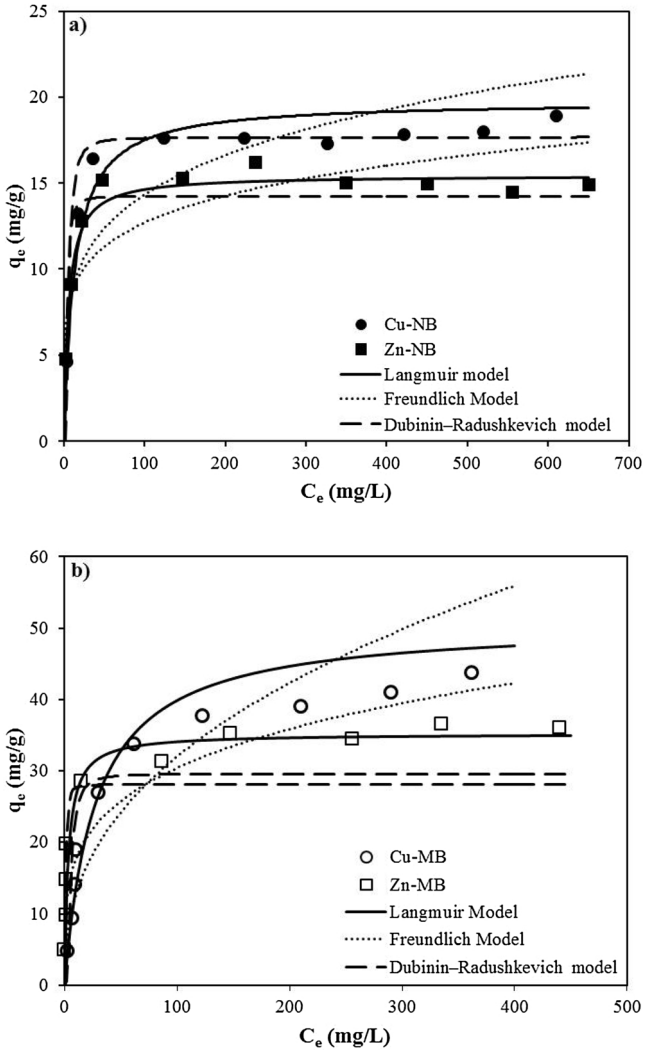

Fig. 9. non-linear curves of various adsorption isotherms with experimental data, a) NB, and b) MB.

adsorbents was increased with increasing an equilibrium concentration (C_e). In addition, there was insignificant difference between NB and MB in q_e at low initial concentrations (C_i50–150 mg/L), while at higher initial metal ion concentrations the NB became saturated earlier than MB. An initial slope of the breakthrough graph, the q_e was suddenly increased with increasing C_i while there was gradually risen when C_i was more than 150 and 200 mg/L for NB and MB, respectively. This result confirmed the fact that, a large number of surface coverage sites can be available for the adsorption at the lower concentration. However, the adsorption at higher initial concentration is difficult to occur due to a repulsive forces between the metal molecules adsorbed on the adsorbent and those in the bulk phase [10,41].

The maximum adsorption capacities (q_{max}) estimated from Langmuir model for modified bentonite are compared to relevant prior studies in Table 4. The middling performance of MB in this study, however, is associated with simple and attractive pre-processing to prepare/modify the adsorbent. This comparison obviously concluded that the modification of natural bentonite using cationic surfactant clearly improved physical and chemical properties of its capacity as an adsorbent which were effectively used to enhance the adsorption efficiency of heavy metals, by over 2-fold relative to untreated bentonite.

5. Conclusions

In this study modified bentonite clay was prepared in order to enhance its adsorption capacity of Cu(II) and Zn(II) ions in aqueous solution. The batch adsorption experiments lead to the following conclusions.

- The modification of bentonite clay (NB) with a cationic surfactant (Bencylhexadecyldimethyl ammonium chloride, BCDMACl) was successfully performed in this study. The cations of BCDMACl micelles intercalated into the interlayers of bentonite and replaced exchangeable cations. This changed the functional groups of natural bentonite to the cationic surfactant, which dominated heavy metal ion adsorption. The modification also prevented swelling of the bentonite.
- Kinetic study demonstrated that adsorption equilibrium was reached in about 10 min for Cu(II) and Zn(II). In addition, the pseudo-second-order model fit the adsorption data well for the heavy metals used in this study.
- The removal of Cu(II) and Zn(II) is sharply increased for about 10 min, thereafter increasing only slightly or remaining constant with 50–200 mg/L initial metal concentrations. The modified bentonite (MB) had about 40.93 and 43.88% increases maximally, over unmodified NB, for removal of Cu(II) and Zn(II), respectively. The adsorption capacity for saturation was about two-fold with MB relative to NB.
- Among the empirical Langmuir, Freundlich, and Dubinin-Radushkevich adsorption models, the Langmuir model fit the experimental equilibrium data the best with coefficient of determination in 0.962–0.993 for all cases. The maximum adsorption capacities (q_{max}) of MB were 50.76 and 35.21 mg/g for Cu(II) and Zn (II), respectively, as estimated from the Langmuir fits. These are about two-fold better than for NB.

In summary, modification of natural bentonite by treatment with a cationic surfactant significantly enhanced its adsorption efficiency for the removal of heavy metal ions from wastewater.

Acknowledgement

The authors would like to acknowledge financial support provided by PSU-Ph.D. Scholarship, Prince of Songkla University, and Dr. Seppo Karrila for reviewing the manuscript.

Table 4
A comparison of maximum adsorption capacity (q_{max}) for Langmuir model of previous studies in literature.

Metal	Adsorbents	q_{max} (mg/g)	Reference	Metal	Adsorbents	q_{max} (mg/g)	Reference
Zn(II)	Zeolite	3.45	Alvarez-Ayuso et al. [42]	Cu(II)	Chitosan/cellulose	26.50	Sun et al. [46]
	Coal fly ash prepared zeolite 4A	30.80	Hui et al. [43]		Carbon nanotubes CNTs/CA	84.88	Yanhui et al. [49]
	Na-modified zeolite	49.69	Stefanovic et al. [44]		Modified clay	83.3	Vengris et al. [50]
	NH_4-zeolon P4A clinoptilolite	111.90	Bujnova et al. [45]		Spent activated clay	13.20	Weng et al. [51]
	Chitosan/cellulose	19.81	Sun et al. [46]		Natural zeolite	8.96	Erdem et al. [52]
	Sugar beet pulp	17.78	Chen et al. [47]		Crosslinked chitosan-coated bentonite beads	9.43	Dalida et al. [53]
	Activated alumina	13.69	Bhattacharya et al. [48]		Sulphate-modified bentonite	158.73	Bamidele et al. [54]
	Modified bentonite	35.21	This study		Modified bentonite	50.76	This study

References

[1] USEPA, United States Environment Protection Agency, National Primary Drinking Water Regulations, (2009) http://www.epa.gov/safewater/consumer/pdf/mcl.pdf.
[2] WHO, Zinc in Drinking-water, Background Document for Development of WHO Guidelines for Drinking-water Quality, (2003) (WHO/SDE/WSH/03.04/17).
[3] WHO, Copper in Drinking-water, Background Document for Development of WHO Guidelines for Drinking-water Quality, (2004) (WHO/SDE/WSH/03.04/88).
[4] S.K. Gunatilake, Methods of removing heavy metals from industrial wastewater, JMESS 1 (1) (2015) 1309–2912.
[5] K.G. Bhattacharyya, S.S. Gupta, Kaolinite, montmorillonite, and their modified derivatives as adsorbents for removal of Cu(II) fromaqueous solution, Sep. Purif. Technol. 50 (3) (2006) 388–397.
[6] M.d. Ahmaruzzaman, Adsorption of phenolic compounds on low-cost adsorbents: a review, Adv. Colloid Interface Sci. 143 (1–2) (2008) 48–67.
[7] H. Tang, C. Chang, L. Zhang, Efficient adsorption of Hg^{2+} ions on chitin/cellulose composite membranes prepared via environmentally friendly pathway, Chem. Eng. J. 173 (2011) 689–697.
[8] M. Matouq, N. Jildeh, M. Qtaishat, M. Hindiyeh, M.Q. Al Syouf, The adsorption kinetics and modeling for heavy metals removal from wastewater by Moringa pods, J. Environ. Chem. Eng. 3 (2015) 775–784.
[9] H.T. Tran, N.D. Vu, M. Matsukawa, M. Okajima, T. Kaneko, K. Ohki, S. Yoshikawa, Heavy metal biosorption from aqueous solutions by algae inhabiting rice paddies in Vietnam, J. Environ. Chem. Eng. 4 (2) (2016) 2529–2535.
[10] B. Anna, M. Kleopas, S. Constantine, F. Anestis, B. Maria, Adsorption of Cd(II), Cu (II), Ni(II) and Pb(II) onto natural bentonite: study in mono and multi-metal systems, Environ. Earth. Sci. 73 (2015) 5435–5444.
[11] S. Veli, B. Alyuz, Adsorption of copper and zinc from aqueous solutions by using natural clay, J. Hazard. Mater. 149 (1) (2007) 226–233.
[12] A.T. Sdiri, T. Higashi, F. Jamoussi, Adsorption of copper and zinc onto natural clay in single and binary systems, Int. J. Environ. Sci. Technol. 11 (2014) 1081–1092.
[13] G.R. Alter, The effect of the exchangeable cations on the physico-chemical properties of Wyoming bentonites, Appl. Clay Sci. 1 (1986) 273–284.
[14] J.M. Adams, Synthetic organic chemistry using pillared cation exchanged and acid treated montmorillonite catalysis: a review, Appl. Clay Sci. 2 (1987) 309–342.
[15] P. Komadel, J. Bujdak, J. Madejava, V. Sucha, F. Elsass, Effect of non-swelling layers on the dissolution of reduced-charge montmorillonite in hydrochloric acid, Clay Miner 31 (1996) 333–345.
[16] G.E. Christidis, Physical and chemical properties of some bentonite deposits of Kimolos Island, Greece, Appl. Clay Sci. 13 (1998) 7998.
[17] M.C. Diaz-Nava, M.T. Olguin, M. Solache-Rios, Adsorption of phenol onto surfactants modified bentonite, J. Incl. Phenom. Macrocycl. Chem. 74 (2012) 67–75.
[18] H.D. Chapman, Part 2. Chemical and microbiological properties, in: C.A. Black (Ed.), Methods of Soil Analysis, Soil Science Society of America, Agronomy Monograph, Madison, 1965, pp. 891–901.
[19] S. Lagergren, About the theory of so-called adsorption of soluble substances, Kungliga Suensk Vetenskapsakademiens Handlingar 241 (1898) 1–39.
[20] G. Blanchard, M. Maunaye, G. Martin, Removal of heavy metals from waters by means of natural zeolites, Water Res. 18 (1984) 1501–1507.
[21] N. Unlu, M. Ersoz, Adsorption characteristics of heavy metal ions onto a low cost biopolymeric sorbent from aqueous, J. Hazard. Mater. 136 (2) (2006) 272–280.
[22] M. Matouq, N. Jildeh, M. Qtaishat, M. Hindiyeh, Q. Maha, Al. Syouf, The adsorption kinetics and modeling for heavy metals removal from wastewater by Moringa pods, J. Environ. Chem. Eng. 3 (2015) 775–784.
[23] M.M. Dubinin, Modern state of the theory of volume filling of micropore adsorbents during adsorption of gases and steams on carbon adsorbents, Z. Fiz. Khim. 39 (1965) 1305–1317.
[24] V.C. Farmer, The layer silicates, in: V.C. Farmer (Ed.), The Infrared Spectra of Minerals, Mineralogical Society Monograph 4, London, 1974, pp. 331–363.
[25] A. Dutta, N. Singh, Surfactant-modified bentonite clays: preparation, characterization, and atrazine removal, Environ. Sci. Pollut. Res. 22 (2015) 3876–3885.
[26] Q.H. Hu, S.Z. Qiao, F. Haghseresht, M.A. Wilson, G.Q. Lu, Adsorption study for removal of basic red dye using bentonite, Ind. Eng. Chem. Res. 45 (2006) 733–738.
[27] S.S. Tahir, N. Rauf, Removal of a cationic dye from aqueous solutions by adsorption onto bentonite clay, Chemosphere 63 (2006) 1842–1848.
[28] Z. Li, Oxyanion sorption and surface anion exchange by surfactant-modified clay minerals, J. Environ. Qual. 28 (1999) 1457–1463.
[29] K.G. Akpomie, F.A. Dawodu, Acid-modified montmorillonite for sorption of heavy metals from automobile effluent, BJBAS 5 (2016) 1–12.
[30] A. Gładysz-Płaska, M. Majdan, S. Pikus, D. Sternik, Simultaneous adsorption of chromium (VI) and phenol on natural red clay modified by HDTMA, Chem. Eng. J. 179 (2012) 140–150.
[31] X.K. Ma, N.H. Lee, H.J. Oh, J.W. Kim, C.K. Rhee, K.S. Park, S.J. Kim, Surface modification and characterization of highly dispersed silica nanoparticles by a cationic surfactant, Colloid Surf. A 358 (2010) 172–176.
[32] E. Worch, Adsorption technology in water treatment: fundamentals, processes, and modeling, Walter de Gruyter (2012).
[33] ASTM D5890-06, Standard Test Method for Swell Index of Clay Mineral Component of Geosynthetic Clay Liners, ASTM International, West Conshohocken, PA, USA, 2006.
[34] O. Abollino, A. Giacomino, M. Malandrino, E. Mentasti, Interaction of metal ions with montmorillonite and vermiculite, Appl. Clay Sci. 38 (2008) 227–236.
[35] W.J. Chen, L.C. Hsiao, K.K.Y. Chen, Metal desorption from copper(II)/nickel(II)-spiked kaolin as a soil component using plant-derived saponin biosurfactant, Process Biochem. 43 (2008) 488–498.
[36] F. Arias, T.K. Sen, Removal of zinc metal ion (Zn^{2+}) from its aqueous solution by kaolin clay mineral: a kinetic and equilibrium study, Colloids Surf. A: Physicochem. Eng. Aspects 348 (2009) 100–108.
[37] I. Langmuir, The adsorption of gases on plane surfaces of glass mica and platinum, J. Am. Chem. Soc. 40 (1918) 1361–1403.
[38] K.O. Adebowale, E. Unuabonah, O. Owolabi, I. Bamidele, The effect of some operating variables on the adsorption of lead and cadmium ions on kaolinite clay, J. Hazard. Mater. B134 (2006) 130–139.
[39] Z. Li, L. Gallus, Surface configuration of sorbed hexadecyltrimethylammonium on kaolinite as indicated by surfactant and counterion sorption, cation desorption, and FTIR, Colloids Surf. A: Physicochem. Eng. Aspect 264 (2005) 61–67.
[40] C.H. Giles, D. Smith, A. Huitson, A general treatment and classification of the solute adsorption isotherm: I Theoretical, J. Colloid Interface Sci. 47 (1974) 755–765.
[41] V.C. Srivastava, I.D. Mall, I.M. Mishra, Removal of cadmium(II) and zinc(II) metal ions from binary aqueous solution by rice husk ash, Colloid Surf. A312 (2008) 172–184.
[42] E. Alvarez-Ayuso, A. Garcia-Sanchez, X. Querol, Purification of metal electroplating waste waters using zeolites, Water Res. 37 (2003) 4855–4862.
[43] K.S. Hui, C.Y.H. Chao, S.C. Kot, Removal of mixed heavy metal ions in wastewater by zeolite 4A and residual products from recycled coal fly ash, J. Hazard. Mater. 127 (2005) 89–101.
[44] S.C. Stefanovic, N.Z. Logar, K. Margeta, N.N. Tusar, I. Arcon, K. Maver, J. Kovac, V. Kaucic, Structural investigation of Zn^{2+} sorption on clinoptilolite tuff from the Vranjska Banja deposit in Serbia, Micropor. Mesopor. Mater. 105 (2007) 251–259.
[45] A. Bujnova, J. Lesny, Sorption characteristics of zinc and cadmium by some natural, modified, and synthetic zeolites, Hung. Electron. J. Sci. Environ. Eng. (2004) 1–10.
[46] X.Q. Sun, B. Peng, Y. Jing, J. Chen, D.Q. Li, Chitosan(chitin)/cellulose composite biosorbents prepared using ionic liquid for heavy metal ions adsorption, Separations 55 (2009) 2062–2069.
[47] Y.N. Chen, D.C. Zhang, M. Chen, Y.C. Ding, Biosorption properties of cadmium(II) and Zinc(II) from aqueous solution by tea fungus, Desal. Water Treat. 8 (1–3) (2009) 118–123.
[48] A.K. Bhattacharya, S.N. Mandal, S.K. Das, Adsorption of Zn(II) from aqueous solution by using different adsorbents, Chem. Eng. J. 123 (1–2) (2006) 43–51.
[49] L. Yanhui, L. Fuqiang, X. Bing, D. Qiuju, Z. Pan, W. Dechang, W. Zonghua, X. Yanzhi, Removal of copper from aqueous solution by carbon nanotube/calcium alginate composites, J. Hazard. Mater. 177 (2010) 876–880.
[50] T. Vengris, R. Binkiene, A. Sveikauskaite, Nickel, copper and zinc removal from waste water by a modified clay sorbent, Appl. Clay Sci. 18 (2001) 183–190.
[51] C.H. Weng, C.Z. Tsai, S.H. Chu, Y.C. Sharma, Adsorption characteristics of copper (II) onto spent activated clay, Sep. Purif. Technol. 54 (2) (2007) 187–197.
[52] E. Erdem, N. Karapinar, R. Donat, The removal of heavy metal cations by natural zeolites, J. Colloid Interface Sci. 280 (2) (2004) 309–314.
[53] M.L.P. Dalida, A.F.V. Mariano, C.M. Futalan, C.C. Kan, W.C. Tsai, M.W. Wan, Adsorptive removal of Cu(II) from aqueous solutions using non-crosslinked and crosslinked chitosan-coated bentonite beads, Desalination 275 (1–3) (2011) 154–159.
[54] B.I. Olu-Owolabi, E.I. Unuabonah, Adsorption of Zn^{2+} and Cu^{2+} onto sulphate and phosphate-modified bentonite, Appl. Clay Sci. 51 (2011) 170–173.

VITAE

Name Miss Kanogwan Tohdee

Student ID 5710130025

Educational Attainment

Degree	Name of Institution	Year of Graduation
Bachelor of Science (Chemistry)	Prince of Songkla University	2008
Master of Science (Chemistry)	Prince of Songkla University	2011

Scholarship Awards during Enrolment

PSU-Ph.D. Scholarship

PSU. GS. for Ph.D. Scholarship for the Graduate Studies Grant

List of Publications

K. Tohdee, L. Kaewsichan, Asadullah, Enhancement of Adsorption Efficiency of Heavy Metal Cu (II) and Zn (II) onto Cationic Surfactant Modified Bentonite, J. Environ. Chem. Eng. 6 (2018) 2821-2828.

K. Tohdee, L. Kaewsichan, Asadullah, Potential of BCDMACl Modified Bentonite in Simultaneous Adsorption of Heavy Metal Ni (II) and Humic Acid, J. Environ. Chem. Eng. 6 (2018) 5616-5624.